The VLA Expansion Project, Phase I: Science with the Ultrasensitive Array

compiled & edited by Michael P. Rupen

August 14, 1999

Contents

Chapter 1

Overview

This document describes the scientific advances which will be made possible by the Ultrasensitive Array, the first phase of the VLA Expansion Project, whose goal is to improve by a factor of ten or more the scientific capabilities of the Very Large Array. The major new elements of the Ultrasensitive Array are:

- A new correlator,
- A new wideband fiber-optics data transmission system,
- A new on-line computing system,
- New or improved receivers to provide continuous frequency coverage from 1.0 to 50 GHz,
- Further study of other aspects of the VLA Expansion Project, including lower frequency prime focus receivers, a more compact antenna configuration, and additional antennas required to improve the spatial resolution by a factor of 10.

These improvements will increase the maximum bandwidth by a factor of 80, the number of channels by a factor of 64, and the frequency coverage by a factor of 3, in addition to reducing or eliminating most known sources of systematic error.

The Ultrasensitive Array will build on the sound basic design and infrastructure of the Very Large Array to produce a revolution in centimeter-wavelength astronomy, using currently-available technology to obtain **speed, sensitivity, and flexibility exceeding the capabilities of any current radio observatory by an order of magnitude or more**. The Ultrasensitive Array will be an instrument to be classed with NASA's Great Observatories, but at a very modest cost: a total of $60.6M. Since the Ultrasensitive Array requires neither new antennas, nor a new site, nor a larger staff, the operational costs of the expanded instrument will remain nearly constant.

1.1 The Very Large Array

The Very Large Array (VLA) is the premier radio telescope in the world. Since its commissioning nearly twenty years ago, it has been used by thousands of astronomers from every continent for research which spans the entire breadth of modern astronomy. Despite its age, it remains heavily subscribed, with over 600 different users receiving observing time for about 500 projects each year.

A short, and far from comprehensive, list of fundamental scientific results from the VLA includes the following:

- Imaging magnetic reconnection events on the Sun
- The discovery of water ice on Mercury
- Imaging dust disks around protostars
- The discovery of the non-thermal coronae of main-sequence stars
- The direct measurement of the motion of the Sun around the Galactic center
- The discovery & imaging of superluminal jet sources associated with X-ray binaries
- The discovery of ram-pressure stripping of gas in spiral galaxies in the Virgo Cluster
- The measurement of the strong magnetic fields which permeate galaxy clusters,
- Detailed polarimetric imaging of extragalactic relativistic jets
- The discovery of the first Einstein ring
- Direct estimates of the sizes and expansion speeds of gamma-ray burst sources

These discoveries span the 20-year history of the VLA; most could not have been anticipated when the VLA was built. That the VLA continues to make important discoveries at the forefront of international radio astronomy is a testimony to its sound design and efficient operation.

The key to the VLA's success has been its unique combination of resolution, sensitivity, and flexibility. The VLA can switch sources and observing frequencies in seconds, make useful images in under a minute, and study objects on scales ranging from 10s of millarcseconds to 10s of arcminutes – anywhere in the northern three-quarters of the sky. No other instrument in the world can match these capabilities. But the VLA has fulfilled only a fraction of its true potential. The antennas, site, array layout, and infrastructure – the most expensive components of any array – are fundamentally sound; but the electronics which sit atop this solid foundation are decades behind modern technology. These technologies would, if implemented on the VLA, **improve its observational capabilities by more than an order of magnitude, without requiring any fundamental changes to the antennas, the array design, or the operational infrastructure.**

Ideally, the VLA's construction would have been followed by incremental upgrades, so that the observational capabilities of the instrument would improve as the enabling technology became available. Unfortunately, while some new high-priority capabilities have been developed (mostly with non-NSF funding), the operating budget has prohibited other, critical improvements. The imbalance between our technical ability to increase the VLA's scientific productivity and our capacity to fund such improvements has grown steadily, to the point that there is now a vast gap between the array's current and potential capabilities. The best way now to address this gap is by funding a major re-capitalization of the VLA's hardware, following a comprehensive, coordinated plan.

1.2 The VLA Expansion Project

The VLA Expansion Project has as its goal **to enhance, by an order of magnitude or more, all the scientific capabilities of the Very Large Array**, at a cost considerably below that already invested in the instrument. A few key parameters are summarized in Table 1.1, while Figure 1.1 illustrates two important aspects, the frequency coverage and angular resolution. The current instruments (VLA and VLBA) show up in the figure as the thin horizontal blue stripes, while the full VLA Expansion Project results in the additional yellow area – an enormous increase, considering that the full cost of the VLA Expansion Project is less than half of the investment in the two existing arrays.

Table 1.1: **The Current and the Expanded VLA.**

	Current VLA	Ultrasensitive Array
Sensitivity	10μJy	0.7μJy
Max. bandwidth	200 MHz	16,000 MHz
No. channels at max. bandwidth	16	1,024
Maximum no. of channels	512	32,768
Frequency coverage, 1–50 GHz	30%	100%
	Current VLA	A+ configuration
Spatial resolution (5 GHz)	0.4 arcsec	0.04 arcsec

The VLA Expansion Project consists of two phases of roughly equal cost: the **Ultrasensitive Array**, which builds entirely on the existing infrastructure to improve all aspects of the VLA *except* its angular resolution; and the **A+ configuration**, which focuses primarily on improving the VLA's resolution by adding new antennas at distances up to $\sim 250\,$km from the center of the current VLA. The Ultrasensitive Array is the subject of this document; we anticipate preparing a similar scientific justification for the A+ configuration later this year.

1.3 Science with the Ultrasensitive Array

The scientific potential of the Ultrasensitive Array is tremendous, with vast improvements in almost every major observational capability of the array. Observations which are difficult now will become routine; projects which are simply inconceivable with current instruments will become practical, and even easy. A short selection of unique experiments made possible by the Ultrasensitive Array includes

- Measuring the three-dimensional structure of the magnetic field on the Sun
- Using the scattering of radio waves to map the changing structure of the dynamic heliosphere
- Measuring the rotation speeds of asteroids
- Observing ambipolar diffusion and thermal jet motions in young stellar objects
- Measuring three-dimensional motions of ionized gas and stars in the center of the Galaxy
- Mapping out the magnetic fields in individual galaxy clusters

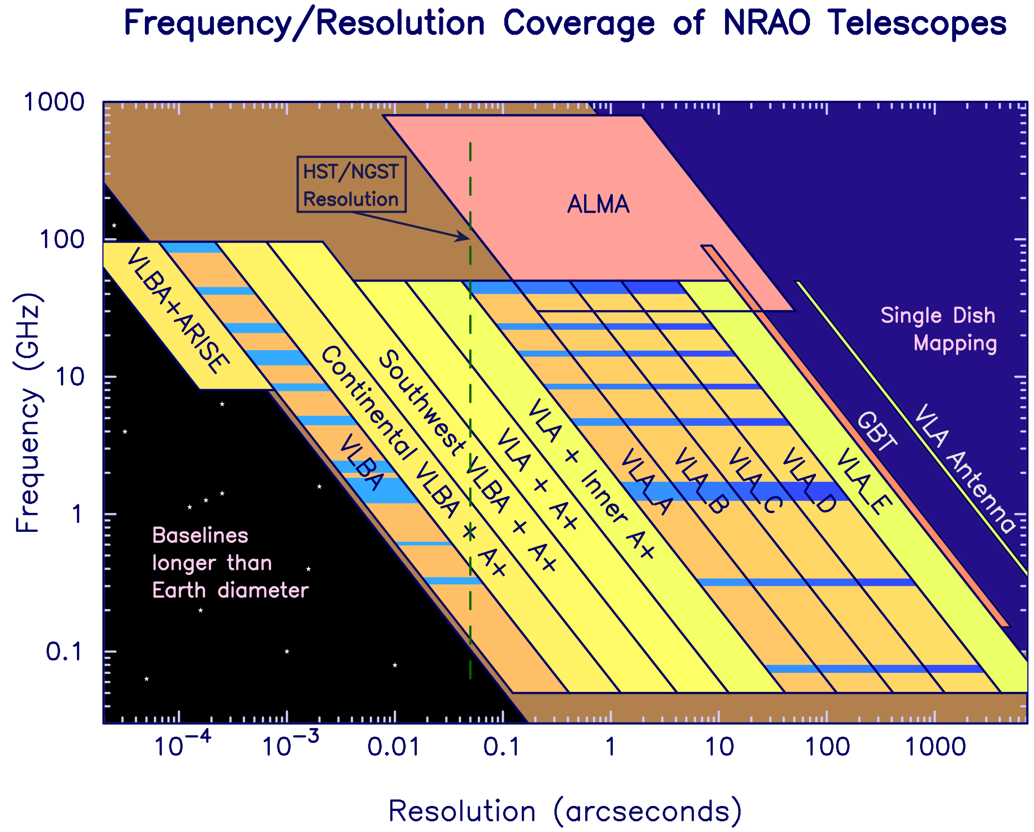

Figure 1.1: The frequency/resolution coverage of current and planned NRAO telescopes. The horizontal blue strips show the capabilities of the current VLA; the yellow shows the improvement after the VLA Expansion Project, with the areas specific to the A+ configuration indicated. Note that the new frequencies below 1 GHz rely on the prime focus system, for which the current proposal requests only development funds. It is not yet clear what the lowest frequency on the ALMA will be, though it will certainly be $\gtrsim 30\,$GHz (as shown in this figure).

- Conducting unbiased searches for redshifted atomic and molecular absorption lines
- Looking through the enshrouding dust to image the formation of high-redshift galaxies
- Disentangling starburst from black hole activity in the early universe
- Providing direct size and expansion estimates for up to 100 gamma-ray bursts every year.

As with the original instrument, the vast area of 'discovery space' opened up by the Ultrasensitive Array makes it likely that the most important discoveries to be made will be those which cannot now be anticipated. Indeed, **an order-of-magnitude improvement of the VLA's fundamental capabilities, when combined with its proven flexibility of design and operational excellence, clearly mark the Ultrasensitive Array as an instrument to be classed with NASA's Great Observatories in all ways except cost.**

1.3.1 Relation to Other Observatories

Just as radio astronomy is not an isolated field, so the VLA is not an isolated instrument. Its discoveries and contributions must be judged against, and with, the full panoply of front-line astronomical telescopes. The capabilities of the Ultrasensitive Array nicely complement those provided by major observatories at other wavelengths.

Two of the main science drivers for NGST, SIRTF, Keck, and ALMA, as well as for instruments such as SCUBA and BOLOCAM, are the twin evolutionary questions of star formation in the Galaxy, and galaxy formation at high redshifts. For star formation, optical and near-infrared observations provide spectacular images and detailed spectroscopy of relatively dust-free regions, while millimeter and submillimeter telescopes map out the molecular gas and thermal dust emission. The Ultrasensitive Array in turn will fill out the picture by imaging the most obscured regions in protostellar disks where planets might form, mapping out the acceleration regions of thermal jets, and providing the complete spectral information needed to disentangle synchrotron, free-free, and dust emission.

Similarly, optical and infrared instruments are essential to measure redshift and emission lines in the most distant galaxies, and to trace the detailed morphology of these sources at the wavelengths most often studied locally. Observations by ALMA, SIRTF, and SOFIA will be sensitive to the bulk of the luminosity of starburst galaxies shrouded in dust, and follow the evolution of the molecular gas out of which stars are formed. The Ultrasensitive Array will contribute valuable parallel data on the evolution of the ground state of hydrogen, as well as the redshifted low-order transitions of such vital molecules as CO. The Ultrasensitive Array will see through the dust to directly image ultraluminous infrared galaxies, showing the relative contributions from active galactic nuclei and star formation, providing an independent dust-free estimate of the star-formation rate, and simultaneously measuring the strength and orientation of the magnetic fields. While single instruments like the Hubble Space Telescope (HST) have clearly had an enormous impact, multi-frequency studies provide much more information than isolated spectral points. The importance of radio data is illustrated by the fact that VLA campaigns are already underway to follow up on distant galaxies detected at submillimeter wavelengths by SCUBA, and high-redhift quasars found optically by the Sloan Digital Sky Survey.

The connection between radio and high-energy observations is even tighter and more direct, since both trace highly energetic phenomena. One of the major results of the Yohkoh mission was the clear positional coincidence between solar X-ray flares and simultaneous radio events imaged by the VLA. Most target-of-opportunity proposals on ASCA and RXTE are now triggered by radio observations, with the VLA providing sensitive and comprehensive monitoring, as well as imaging, of the jets accelerated by X-ray black hole binaries. The X-ray/radio correlation for active stars is as tight, and as mysterious, as the far-infrared/radio correlation for star-forming galaxies, with correspondingly important implications for energy loss mechanisms. On larger scales, ROSAT, Chandra, and XMM provide vital information on the amount and distribution of hot gas in galaxy clusters, while the VLA traces the equally pervasive magnetic fields and relativistic particles. Similarly, the same active galactic nuclei which emit the gamma-rays seen by INTEGRAL are strong radio sources, and the VLA can provide accurate light curves as well as sensitive probes of both continuum and line absorption, giving unique information on the accretion disks and any obscuring material, as well as on the AGNs themselves. Finally, while BATSE and Beppo-SAX find and localize gamma-ray bursts, and the HST and Keck track their optical light curves, find their host galaxies, and measure their redshifts, only the VLA can provide extinction-free statistics on GRB afterglows, follow the bursts from the initial relativistic fireball to the late sub-relativistic stage, and (through interstellar scattering) directly measure source sizes and expansion rates. Full realization of the potential of X-ray and gamma-ray satellites requires the complementary radio observations that only the VLA can provide.

1.3.2 The VLA in Context

There are many excellent radio telescopes operating in the 50 MHz to 50 GHz frequency range of the VLA. However, none of them can compete with the VLA's combination of speed, flexibility, sensitivity, resolution, and operational capabilities. Stated another way, these instruments are either more limited in some key aspects of their capability, or have been designed with a highly specific scientific goal in mind. The most powerful characteristic of the VLA is that it is not restricted by any such limitation. It has been designed to provide the maximum capability and flexibility, with no compromises for specialized scientific return.

The VLA's unique role will continue until a next-generation world-class centimeter telescope is built – something which is not likely to happen for at least another decade. However, precisely *because* of its present and anticipated dominance, we cannot afford simply to maintain the VLA's current scientific capability. Consider building a 10m optical telescope, but neglecting to equip it with a CCD or a modern spectrograph: the idea is absurd. Yet the VLA's is an equivalent case, with the essential difference that **there is no other comparable instrument anywhere in the world**. The scientific potential is obvious, and enormous; the proposed improvements rest on currently-available technology that is well understood and relatively inexpensive. Indeed, much of the development work that would be needed is already underway for the Altacama Large Millimeter Array (ALMA). **Now is the time to allocate the modest resources needed to create an observatory as fully capable at radio wavelengths as are HST, Chandra, SIRTF, and ALMA in their respective wavebands.**

1.4 The Ultrasensitive Array: Timescale and Budget

Implementing the Ultrasensitive Array will take roughly six years, the timescale being set primarily by the need to move antennas through the Antenna Assembly Building for overhaul, which should take on average two months per antenna. The total projected cost of the Ultrasensitive Array is \$60.6M.

Chapter 2

Design Goals for the Ultrasensitive Array

2.1 The Capabilities of the Ultrasensitive Array

This chapter describes the planned technical capabilities of the Ultrasensitive Array. The Very Large Array, after implementation of the improvements described above, will be a vastly more powerful instrument, with the following characteristics:

- **Frequency Accessibility and Bandwidth**
  - The ability to independently tune two different frequency pairs (R and L) anywhere within one, or two, frequency bands, with each pair providing up to 4 GHz bandwidth per polarization – a maximum total of 16 GHz bandwidth.
  - The ability to select, from these broad-band signals, up to 8 individual signals signals with selectable center frequencies and with bandwidths selectable in powers of two from 2 GHz down to 977 kHz, for processing by the correlator.
  - The ability to observe in a hostile RFI environment, through a combination of linear design, and signal processing techniques, including analog/digital filtering, flexible frequency/bandwidth selectability, and post-processing algorithms utilizing multi-channel data.
- **Sensitivity**
  - The Ultrasensitive Array will provide line and continuum sensitivities as shown in Figure 2.1, and listed in Table 2.1.
  - The equivalent surface brightness sensitivities for the **A** and **D** configurations, assuming an object of angular size equal to the synthesized beam, are given in Tables 2.2 and 2.3.

These design goals are taken from the document *Technical Goals of the VLA Expansion Project*, available via the Expansion Project Web site:
`http://www.aoc.nrao.edu/doc/vla/html/Upgrade/Upgrade_home.shtml`.

Table 2.1: **Frequency Coverage and Point Source Sensitivity of the Ultrasensitive Array.** Assumes observation by 27 antennas of a source at declination +30°.

					Continuum			Line (1 km/sec)		
Band	Freq. [GHz]	Freq. Range [GHz]	T_{sys} [K]	η	$\Delta\nu$ [GHz]	rms noise [μJy]		$\Delta\nu$ [kHz]	rms noise [mJy]	
		(dual pol'n)				2 min	12 hr		2 min	12 hr
L	1.5	1.10– 2.00	26	0.50	0.5	36	1.9	5	11	0.58
S	3.0	2.00– 4.00	29	0.62	1.5	21	1.1	10	7.6	0.40
C	6.0	4.00– 8.00	31	0.60	3.0	16	0.82	20	5.7	0.30
X	10.0	8.00–12.00	34	0.56	3.0	18	0.95	33	5.1	0.28
U	15	12.00–18.00	39	0.54	4.0	19	0.98	50	5.1	0.27
K	22	18.00–26.50	54	0.51	6.0	23	1.2	74	6.1	0.32
K_a	33	26.50–40.00	45	0.39	8.0	21	1.1	111	5.3	0.28
Q	45	40.00–50.00	66	0.34	5.0	46	2.4	150	7.6	0.40

Explanation of Table Entries

η: a general efficiency factor, including both aperture efficiency and correlator losses. Assumes a two-bit, four-level correlator.

$\Delta\nu$: the bandwidth used in calculating the noise. The continuum bandwidth accounts for the RFI environment and the opacity; the spectral line bandwidth corresponds to 1 km/sec at the central frequency.

rms noise: the root-mean-square (1σ) thermal noise, assuming dual polarization observations and a data-weighting scheme chosen to give low noise with a reasonably small beam size (Briggs' robustness=0).

Table 2.2: **Surface Brightness Sensitivity: A Configuration.** For the **B** configuration, multiply the beam size by 3.2, and divide the rms noise by 10.

Freq. Range [GHz]	Beam size [arcsec]	Continuum rms noise [K]		Line (1 km/sec) rms noise [K]	
		2 min	12 hr	2 min	12 hr
1.10– 2.00	1.6	11	0.57	3,300	170
2.00– 4.00	0.80	6.3	0.33	2,300	120
4.00– 8.00	0.40	4.8	0.25	1,700	90
8.00–12.00	0.25	5.4	0.30	1,500	84
12.00–18.00	0.17	5.7	0.30	1,500	81
18.00–26.50	0.12	6.9	0.36	1,800	96
26.50–40.00	0.08	6.3	0.33	1,600	84
40.00–50.00	0.06	14	0.72	2,300	120

Assumes the same parameters as in Table 2.1.

Beam size: full-width at half-maximum for the frequency at the center of the band, assuming the same data-weighting as in Table 2.1.

rms noise: the root-mean-square (1σ) thermal noise as in Table 2.1, converted to the surface brightness sensitivity assuming a source whose size is equal to the quoted beam size.

Table 2.3: **Surface Brightness Sensitivity: D Configuration.** For the **C** configuration, divide the beam size by 3.2, and multiply the rms noise by 10.

Freq. Range [GHz]	Beam size [arcsec]	Continuum rms noise [mK]		Line (1 km/sec) rms noise [mK]	
		2 min	12 hr	2 min	12 hr
1.10– 2.00	45	11	0.57	3,200	170
2.00– 4.00	23	6.2	0.33	2,300	120
4.00– 8.00	12	4.8	0.25	1,700	90
8.00–12.00	7.0	5.5	0.29	1,500	84
12.00–18.00	4.8	6.0	0.30	1,500	81
18.00–26.50	3.5	7.0	0.36	1,800	96
26.50–40.00	2.4	6.3	0.33	1,600	84
40.00–50.00	1.9	14	0.72	2,300	120

Assumes the same parameters as in Table 2.1.
Beam size: full-width at half-maximum for the frequency at the center of the band, assuming the same data-weighting as in Table 2.1.
rms noise: the root-mean-square (1σ) thermal noise as in Table 2.1, converted to the surface brightness sensitivity assuming a source whose size is equal to the quoted beam size.

- **Correlator** The new correlator will be designed to provide the following capabilities:
  - Ability to process 8 signals from 40 stations, with up to 16 GHz total maximum bandwidth, and up to 8192 spectral channels per polarization product per baseline. The maximum number of channels, per baseline, in a single-polarization mode, would be 32768.
  - Ability to correlate signals from stations separated up to 250 km from the VLA.
  - Support for ten subarrays, and three simultaneously operating observing modes.
  - Minimum frequency resolution of 1 Hz.
  - Full polarization capability.
  - Sustained dump times as short as 10 msec for specified subsets of the integrators.
  - Pulsar gating mode offering at least 32 phase bins.
  - A burst mode, permitting extra-rapid accumulation of data for a short period of time.
  - Careful design for RFI suppression and very high linearity in the presence of strong narrow-band signals.

  These correlator design goals are a close match to the capabilities of the ALMA correlator. To demonstrate the remarkable capabilities that such a correlator will provide, we show in Table 2.4 the number of channels and frequency resolution that the ALMA correlator would provide, for three different modes of operation: a single-IF mode, a two-IF mode, and a full-polarization mode. It is important to note that this table demonstrates only one quarter of the full ALMA correlator capability. The other three quarters (quadrants) can be linked to provide extra spectral resolution, in return for processing fewer frequency inputs.

  For example,

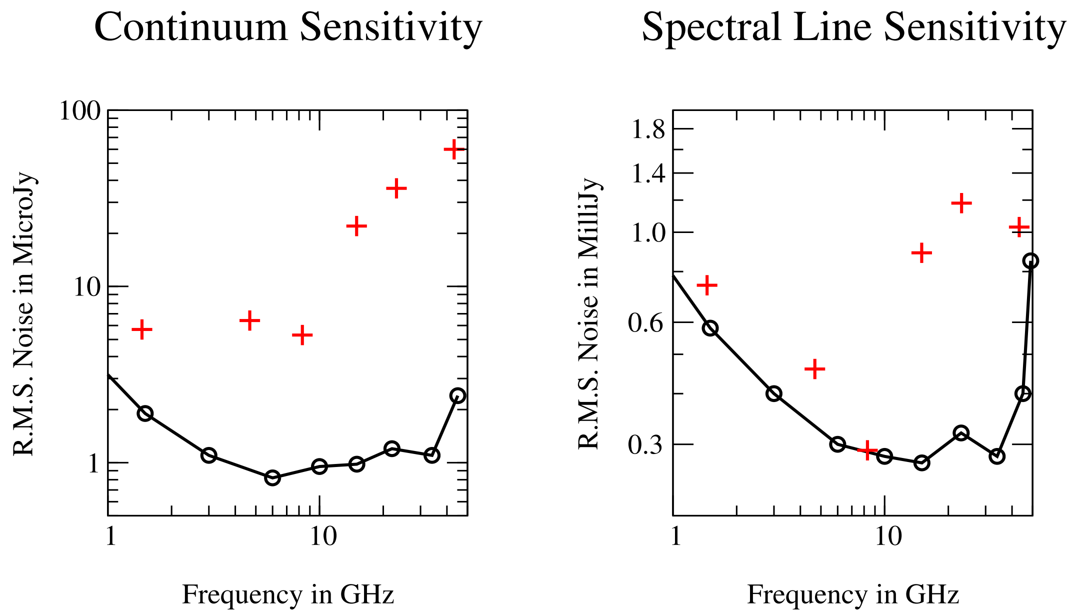

Figure 2.1: The current (+), and projected (o) continuum (left) and spectral line (right) sensitivity (1σ in 12 hours) of the VLA after the Ultrasensitive Array is completed. For the continuum case, a bandwidth of about half the total width of the band is assumed. For the spectral line case, the bandwidth corresponds to a velocity width of 1 km/sec. The width of the '+' symbols demonstrates the approximate range of tuning with the current VLA.

1. If four (R,L) pairs of samplers are used to drive the correlator, each IF pair would provide spectral channels as shown in Table 2.4 for the various possible analog input bandwidths. Each pair of samplers would drive one quadrant of the correlator.
2. If a pair of samplers is used to drive two quadrants of the correlator, this IF pair would have double the number of spectral channels (and thus half the channel separation) shown in Table 2.4. For example, the maximum number of spectral channels would be 16,384 when only one polarization product is calculated. In a like manner, the remaining two quadrants of the correlator could be driven by a single pair of samplers, or each quadrant could be driven by a separate sampler pair as in case (1) above.
3. For the highest spectral resolution, all four correlator quadrants would be connected to a single sampler pair. The number of channels would be increased by a factor of four over the values listed in Table 2.4, up to a maximum of 32,768 channels, and the frequency resolution would be improved by a factor of four over the values listed in the table.

---

[1] Single polarization product, *e.g.*, RR or LL.

[2] Two polarization products, *e.g.*, RR and LL.

[3] All four polarization products, RR RL LR LL.

[4] Channel counts and separations are before smoothing.

Table 2.4: Bandwidths, number of channels, and frequency resolution for a single correlator quadrant for the proposed VLA Expansion Project correlator.

	One Product/Baseline[1]		Two Products/Baseline[2]		Four Products/Baseline[3]	
Bandwidth (MHz)	Number of Channels[4]	Frequency Separation (kHz)	Number of Channels	Frequency Separation (kHz)	Number of Channels	Frequency Separation (kHz)
2000	256	7812.5	128	15625	64	31250
1000	512	1953.1	256	3906	128	5812.5
500	1024	488.28	512	976.56	256	1953.1
250	2048	122.07	1024	244.14	512	488.28
125	4096	30.52	2048	61.04	1204	122.07
62.5	8192	7.629	4096	15.259	2048	30.518
31.25	8192	3.815	4096	7.629	2048	15.259
15.625	8192	1.907	4096	3.815	2048	7.629
7.813	8192	0.954	4096	1.907	2048	3.815
3.906	8192	0.477	4096	0.954	2048	1.907
1.953	8192	0.238	4096	0.477	2048	0.954
0.977	8192	0.119	4096	0.238	2048	0.477

- **Operations**
  - To provide a flexible, real-time interface between the array and the operations staff, and between the array and the users. This will permit users to react quickly to changing observing conditions, and give them the ability to modify their observing goals in response to information already obtained.
  - To provide the operations staff a more powerful and flexible environment, thus permitting simpler and more efficient development of new observing modes.
  - To enable real-time distribution of correlator data to users with access to suitable bandwidth.
- **Antenna Drive/Control**
  - Stop-and-shoot imaging on ten second timescales for mosaicing, with on-source integration of at least 7 seconds for offset movements less than 30 arcminutes.
  - Continuous raster-scan interferometric observing with r.m.s. pointing accuracy of ≤ 10 arcseconds for drive rates of ≤ 2.5 deg/min.
  - Blind pointing accuracy (1σ, calm night conditions) of 6 arcseconds.
  - Reference pointing accuracy (best conditions) of 2 arcseconds.
  - Antenna efficiency exceeding 40% at all Cassegrain frequencies.

2.2 Implications of These Improvements for Quality Science

A telescope with the capabilities described above will revolutionize centimeter-wave radio astronomy, since the speed, sensitivity, and flexibility will exceed current capabilities by an order of magnitude or more. In this section, we discuss in broad terms some implications for science of this new instrument.

2.2.1 Sensitivity

The major gains in sensitivity come from the increased bandwidth at all frequencies, and the improved gain and system temperature at high frequencies. The Ultrasensitive Array will be at least a factor 10 faster than the current VLA for every continuum observation, and almost a factor 1000 faster at high frequencies. What implications does this have for the resulting astronomy?

- *Studying more sources*
  Experiments which are difficult now will be routine with the Ultrasensitive Array, leading to much better, more complete, and less biased source samples. This implies a deeper and more reliable luminosity function for every type of source; just as optical observations turned up important populations when pushed to low flux densities (*e.g.*, faint blue galaxies) and surface brightnesses (*e.g.*, low surface brightness galaxies), so the Ultrasensitive Array may reveal new types of sources, currently unknown. Studies now restricted to the 'best' exemplars of a given class (*e.g.*, polarization mapping of galaxies, imaging of thermal jets in YSOs) will be extended to more typical and more distant members, showing which characteristics are truly general and which are simply high-luminosity eccentricities. In addition, the sheer number of detectable sources will permit experiments that cannot be done at all now. The number of background sources in a random field will go up by a factor of 3 at low frequencies, and a factor 10 or more at high frequencies, giving for the first time significant numbers of background probes for rotation measure and absorption studies, and allowing many fainter sources to be used for phase-referencing – an important point at high frequencies, where atmospheric phase instabilities often limit the sensitivity of the images.

- *Studying sources in more detail*

  Improved sensitivity leads directly to higher-resolution imaging, both because surface brightness sensitivity goes as θ^{-2}, and because one can observe at higher frequencies, with correspondingly smaller beams. The first is important for sensitivity-starved projects like polarization mapping, while the second is vital for intrinsically small sources, such as accetion disks around proto-stars. Greater sensitivity will also allow imaging of large structures which currently 'fade off' into the noise; examples include thermal jets in star-formation regions, and synchrotron haloes in spiral galaxies.

  Similarly, greater instantaneous sensitivity implies finer temporal resolution: the Ultrasensitive Array will detect a 1 mJy source (5σ) in one second, from 2 to 40 GHz. This is more than a parlor trick; aside from the potential for large-scale surveys, many very interesting sources exhibit flux and spectral index variations on these time scales, including the Sun and the radio counterparts to X-ray transients and gamma-ray bursts. The ability to make useful observations in very short time, combined with the advent of true dynamic scheduling, will allow variable sources to be observed more immediately, more consistently, and over a wider range in frequencies; the greater sensitivity will also permit these sources to be followed for longer times.

  Finally, the improved sensitivity combined with the new correlator will ensure that every continuum observation gives sensitive spectral and polarization information, without losing bandwidth or requiring additional observing time.

- *Detecting new types of sources*
  Improving the sensitivity of the VLA will allow many sources to be detected which are simply too faint to be seen with the current instrument. Obvious examples include cometary nuclei, Kuiper belt objects, and spiral galaxies as luminous as the Milky Way at $z \sim 0.5$. More speculative but potentially even more interesting are those objects which currently have no known radio counterparts, like type Ia supernovae – an order-of-magnitude increase in sensitivity, over such a wide frequency range, will undoubtedly start detecting sources we currently think of as radio-quiet.

2.2.2 Flexibility & Efficiency

The second major advance provided by the Ultrasensitive Array is an enormous improvement in flexibility and efficiency. The current system requires working around instrumental limitations to approach the science: frequencies must be chosen to match the available bands and the restrictions of the LO chain; bandwidths and spectral resolution must be juggled to fit in a line or get the minimum acceptable (sometimes not even that!) frequency coverage; observers working at 10s of GHz have to rely on luck for a near enough phase calibrator and good enough weather to give useful data. The Ultrasensitive Array will create an instrument which is infinitely more capable. By tripling the range of available frequencies, and giving roughly equal sensitivity over much of that range, the Ultrasensitive Array will permit astronomers to choose the frequency appropriate to a particular source and scientific problem. By providing much wider bandwidths, allowing two fully-independent frequency settings, (each giving both polarizations) and providing thousands of spectral points across the band, the Ultrasensitive Array will give observers full and flexible access to the entire spectrum received at the telescope. High-fidelity imaging will also be assured at the high frequencies, by making dynamic scheduling a reality, and by providing sensitivity enough to use at least ten times as many sources as calibrators.

The impact on scientific programs will be enormous. Retaining spectral resolution over wide bandwidths will make every spectral line experiment a continuum experiment as well, and *vice versa.* Since at low frequencies the improvement is in bandwidth rather than system temperature or gain, observations of spectral lines like the 1.4 GHz transition of H I will still require long integrations. But with broad bandwidths each pointed observation will also become a search for both emission and absorption over a huge redshift range, as well as providing deeper continuum images than *any* now available. Continuum observations will automatically measure the shape of the spectrum rather than just a single flux density; spectral line observations will be able to target multiple lines within a single band, *e.g.* to measure all of the hyperfine lines of ammonia, or to 'stack' radio recombination lines for sensitivity. Continuous and equally sensitive observations from 1 to 50 GHz will allow the routine measurement of the full spectral energy distribution, from low frequencies dominated by synchrotron emission to high frequencies dominated by dust. Effective spectral line surveys will become possible for the first time, thanks to simultaneous wide bandwidths and high spectral resolution. One will be able to 'tune' the VLA to the proper frequencies for a particular experiment and a particular object, checking for instance for the transition from an optically-thick to an optically-thin spectrum, or choosing the most likely frequency for refractive scintillation. A particular special case is the availability of the new S-band system, allowing the VLA to be used for the first time in 2.3 GHz radar experiments.

2.2.3 Addressing or Eliminating Systematic Errors

Without a conmprehsive plan to neutralize or avoid systematic errors, the Ultrasensitive Array would simply hit the noise floor faster and harder than the current instrument. Although it is unlikely that we will eliminate all such errors, the VLA Expansion Project does directly address the problems we know about, and provides considerably more flexibility for tackling any newly-discovered systematic errors in the future. Some of these improvements include:

- **Spectral improvements**
  - *Better filters:* The bandpasses will probably be defined by digital (FIR) filters, rather than analog devices, offering better, and much more stable bandpass shapes.
  - *Better bandpasses:* The new correlator will provide much higher spectral resolution, even over the widest bandwidths, greatly reducing bandpass closure errors and limiting the spectral 'ringing' due to continuum sources and sharp spectral features (*e.g.*, radio frequency interference or masers). Retaining the full frequency spectrum (instead of throwing away the first channel, as is currently done) will allow re-sampling the spectrum and applying any desired smoothing function after the observations, reducing these effects even further.
  - *Better signal tranmission* Replacing the waveguide with a fiber optics system, and employing a digital data transmission should eliminate the so-called '3 MHz' ripple, which currently dominates the time-dependent part of the frequency response of the instrument, and should eliminate cross-coupling between signal channels, permitting more stable and accurate instrumental polarization.
  - *Better continuum subtraction:* The new correlator will provide much larger bandwidths for spectral line experiments, ensuring ample line-free channels for continuum subtraction. As well as reducing the noise on the estimated continuum, this will allow more accurate subtraction of very distant or extended sources (*e.g.*, the Sun), where the assumption of a linear variation of the visibility with frequency breaks down.
  - *Direct comparisons of the noise statistics:* The combination of wide bandwidths and narrow channels will allow the most direct check possible on the true statistics of the noise, using the large number of line-free channels. This is absolutely essential for deep searches for faint emission or absorption lines, where non-Gaussian statistics could easily lead to spurious detections.
  - *More accurate deconvolutions:* High spectral resolution at high sensitivity across wide bandwidths both enables multi-frequency synthesis, and allows the removal of deconvolution errors due to changes in source structure (or simply flux density) across the band. With typical bandwidth ratios of 1.5:1 the uv-coverage will be improved enormously. Such data should also allow much more accurate calibration (and removal) of the change in the primary beam with frequency, which leads to a frequency-dependent antenna gain which varies with distance from the pointing center.
  - *Unbiased rotation measures:* Rotation measure studies rely on the spectral dependence of the Faraday rotation, which goes as ν^{-2}. In addition to the sensitivity (which determines the accuracy with which the polarization angle can be measured), the maximum detectable RM is set by the channel width, while the minimum is set by the total bandwidth. The new correlator, providing narrow channels over very wide bandwidths, will

  be ideal for these observations, and open the door to sophisticated spectropolarimetry as a standard observing mode at the VLA.

  - *RFI removal:* One of the major advances of the VLA Expansion Project will be to build up an effective, layered approach to finding and removing radio frequency interference (see Section ??). This is essential for utilization of the full bandwidth brought down from the antennas, and for avoidance of the non-linearities which will otherwise drive the system into saturation.

  Quite sophisticated software will be required to take advantage of all these possibilities. Many of the extensions and algorithms mentioned above are already built into AIPS++, and both that project and the ALMA are continuing this development.

- **Improvements in calibration**

  - *Avoiding decorrelation at high frequencies:* Observations at high frequencies are vulnerable to atmospheric phase instabilities especially in the larger configurations, requiring frequent calibration using nearby point sources. The improved sensitivity of the Ultrasensitive Array will allow the use of much weaker and more plentiful calibrators, as well as extending self-calibration to fainter target sources. This last will be particularly useful given the flexibility of the correlator and LO system; one can tune a single IF pair to a strong, narrow maser line, and use that to calibrate simultaneous observations of fainter line and/or continuum emission. The use of dynamic scheduling will also help avoid observations at high frequencies during unsuitable periods, while the high time resolution afforded by the correlator and made useful by the improved sensitivity may help recover those data which are nevertheless taken under adverse circumstances.
  - *Improved pointing:* By improving the 'blind' pointing to 6 arcsec rms and allowing the use of fainter calibrators for referenced pointing, the VLA Expansion Project will greatly improve the sensitivity at high frequencies, and eliminate a major source of uncertainty at all frequencies. More accurate and more consistent pointing gives more consistent relative antenna gains across and beyond the primary beam, leading to easier removal of the sidelobes of distant sources.
  - *Measuring time-dependent effects:* The improved sensitivity will allow self-calibration on shorter time-scales, as well as offering the prospect of pointing self-calibration based on the apparent flux variations of background sources. Time-dependent polarization leakages terms will similarly be easier to measure and remove.
  - *More background sources:* In addition to pointing self-calibration, the availability of many more background sources will allow more accurate relative astrometry and flux calibration. This is a dominant source of error in monitoring observations of gravitational lenses, and in general will allow much more accurate variability and proper motion studies.

- **New monitor & control system**

  - *Easier to extend and debug:* The new on-line system, re-written in a modern language and taking advantage of modern coding practices and hardware, will be much easier both to debug and to extend. The addition of many more 'monitor points' throughout the system will make it much easier to track down and eliminate the sources of systematic errors, both in software and in hardware. The use of modern computers, programming languages, and coding practices will make the entire system more responsive, both in the day-to-day running of the instrument, and in installing and testing new capabilities.

- *Restore interaction to observations:* The new on-line system will provide easy and rapid access to the data as it comes in, and allow correspondingly quick reponses. This can be as important and as trivial as getting an excellent continuum image in a few minutes, and noticing that the telescopes were pointing towards the wrong place – a simple check that optical observers take for granted, but which is at best difficult with the current system at the VLA. More sophisticated responses might include steering around interference, choosing a better calibrator, updating the pointing as necessary rather than at set intervals, and so forth. The Ultrasensitive Array will allow observers to react in real-time, rather than waiting fatalistically for the data to appear on their desks.
- *Monitor data:* Currently VLA data come packaged with uncalibrated system temperatures, a few undocumented on-line flags, and not much else. In large part this is because of the programming effort required to add anything new. The new monitor and control system of the Expansion Project will make this much easier; current plans call for wind speed, barometric pressure, pointing results, the measured atmospheric water content from the K-band receiver, and the ionospheric corrections to be attached directly to the data. This sounds trivial but will make a huge difference in understanding exactly how and under what conditions one's data were taken, a fundamental requirement for their intelligent reduction.

The improvements listed above may seem less exciting than enhanced sensitivity or new frequency bands, but they will affect every observation made with the VLA, producing higher fidelity images, and ensuring that the gains we claim in sensitivity and bandwidth can actually be realized. In the end the reduction of systematic errors will make the difference between an instrument devoted to short snapshots, and one capable of delicate experiments requiring deep integrations and sophisticated data analysis.

Chapter 3

Science with the Ultrasensitive Array

The VLA's astronomical contributions have run the gamut from mapping the magnetic fields of Jupiter, to imaging high-redshift galaxies; indeed, the breadth of the VLA has always been its strongest feature, allowing it to make important discoveries in fields which did not even exist at the time it was built (*e.g.*, gamma-ray burst afterglows). The Ultrasensitive Array may confidently be expected to be similarly productive, becoming the instrument of choice for radio observations of almost any type. This chapter is devoted to describing a few of the more interesting and obvious observations. The list is by no means exhaustive, but concentrates on those areas where radio data provide important information which is complementary to that available at other wavelengths. These unique radio contributions may conveniently be gathered into four major groupings:

- *The Magnetic Universe*
  Magnetic fields are thought to be important in virtually all astrophysical contexts, but they are very difficult to observe. Radio observations offer some of the few direct probes of the strength, structure, and topology of magnetic fields, including synchrotron emission, Zeeman splitting, and Faraday rotation. The sensitivity, frequency agility, and spectral capacity of the Ultrasensitive Array will allow astronomers to map out the three-dimensional structure of magnetic fields on the Sun, image the polarized emission in thousands of spiral galaxies, and (through the use of faint background source as Faraday rotation probes) trace the magnetic fields in the halos of individual galaxy clusters.

- *The Obscured Universe*
  Many interesting phenomena, including star formation and accretion onto massive black holes, occur preferentially behind dense screens of gas and dust which make optical and even infrared observations difficult or impossible. Radio waves by contrast are very difficult to obscure, and hence can be used to look directly through these dust screens. Examples of experiments made possible by the Ultrasensitive Array include probing the depths of the atmospheres of the giant planets, measuring ambipolar diffusion and the proper motions of thermal jets in young stellar objects, imaging the densest regions of nearby starburst galaxies, and conducting unbiased searches for quasar absorption lines.

- *The Transient Universe*
  Astronomical transients tend to be compact objects which emit high-energy photons and

accelerate high-energy particles; the latter are observable primarily through synchrotron emission, which in turn is most easily seen at radio wavelengths. Radio observations are therefore very important to studies of variable sources, particularly because of a number of practical advantages, including high angular resolution, the lack of confusing sources, and the ability to observe both day and night under most weather conditions. The Ultrasensitive Array will be the ideal instrument for these studies, providing accurate mass estimates and three-dimensional images of galactic novae, imaging every relativistic jet in the Milky Way, and measuring the sizes of up to a hundred gamma-ray burst sources every year.

- *The Evolving Universe*
  The formation of stars and galaxies, and the evolution of the gas content of the universe, are among the most important questions in modern astronomy. Radio data are useful both in measuring the evolution of H I and (especially redshifted) molecular gas, and in providing extinction-free measurements of three of the most important emission processes in both young stars and high-redshift galaxies (synchrotron, thermal free-free, and dust emission). Among other experiments, the Ultrasensitive Array will allow astronomers to distinguish dust from free-free emission, and image disks and jets, in local star forming regions; to measure the star formation rate, irrespective of dust extinction, in high-redshift galaxies; and to search for H I emission out to $z \sim 1$ or beyond.

The remaining sections of this chapter summarize the Ultrasensitive Array's contributions in each of these four areas, with special emphasis on the new capabilities provided by the instrument, and the new and unique science which will result.

3.1 The Magnetic Universe

Magnetic fields are known or suspected to be important in every astrophysical context, from solar flares to the dynamics of galaxy clusters. They are also very difficult to measure, with very few direct, observational probes. Almost all of these are associated with emission at centimeter wavelengths. Radio observations thus provide the most direct measurements available of the magnetic field distribution, orientation, and strength, based on synchrotron emission and polarization; Faraday rotation; Zeeman splitting; gyrosynchrotron emission; cyclotron masers; maser polarization; and more esoteric processes like synchrotron self-Compton emission, the Razin-Tsytovich effect, and anisotropic scattering. The VLA has been at the forefront of this work, particularly synchrotron observations, for many years, but even for the VLA these measurements are very demanding. For instance, synchrotron measurements require high sensitivity, to detect low polarization fractions (a few tenths to 10s of per cent) with high enough signal-to-noise ratios to determine accurate polarization angles; they also require wide bandwidths (to measure the spectral index, and to probe small Faraday rotations) and high spectral and spatial resolutions (to avoid depolarization within a frequency channel or a beam, and to ensure sensitivity to high Faraday rotations). Such *desiderata* stretch the abilities of the current instrument to its limits.

The VLA Expansion Project, and particularly the Ultrasensitive Array, offers several important advances:

- *Improved sensitivity*
  With at least a factor 10 increase in speed over the current VLA, the Ultrasensitive Array will measure magnetic fields in larger samples of weaker sources, extending current observations of 'the best and the brightest' to more typical objects. The improved surface brightness sensitivity will also allow observations at much higher spatial resolution (factor 3 to 10), yielding more detailed information on the distribution of the magnetic field, and avoiding beam depolarization. Finally, by significantly increasing the number of background sources suitable for rotation measure studies, the Ultrasensitive Array will probe the magnetic field even where there is no emission, allowing 'blind' searches that are simply not possible today.

- *Higher spectral resolution, over wider bandwidths*
  With 31 MHz resolution over 8 GHz with full polarization information, the new correlator will revolutionize continuum studies, retaining full sensitivity while providing accurate spectral information and unambiguous rotation measures in a single frequency setting, and simultaneously avoiding Faraday depolarization. In place of the careful tradeoffs of sensitivity, frequency coverage, and spectral resolution required currently, *every* experiment will provide more accurate and more complete polarization information than has yet been obtained for any source. Similarly, wide bandwidths will for the first time be available with high enough spectral resolution for maser and Zeeman splitting measurements, yielding a huge increase in efficiency when multiple sources are present in the beam, and permitting high-sensitivity searches to be performed at the same time as delicate Zeeman measurements. The amazing flexibility of the new system will also give excellent continuum measurements during spectral line observations. Since the latter do not benefit (except at the high frequency bands) from the improved bandwidth, one will still have to integrate for many hours to obtain (for instance) good H I sensitivity; with the new correlator one can at the same time obtain more sensitive rotation measure maps than any now existing.

- *Continuous frequency coverage from 1–50 GHz*
  Many broad-band probes of magnetic fields are strongly frequency dependent; for instance,

> both Faraday rotation and the strength of interstellar scattering vary as ν^{-2}, while the Razin-Tsytovich effect leads to a sharp cutoff at the frequency where the phase velocity exceeds the speed of light. Clearly it is advantageous to observe these processes over a broad range of frequencies, and to be able to tune an experiment to match the physical conditions of a particular source. More generally, few sources emit via only one physical process, and covering a wide range of frequencies allows these processes to be distinguished by their spectral shapes. For instance, the intensity of synchrotron emission gives a direct constraint on the magnetic field strength, but one needs some information on the particle energy distribution, and some idea of what fraction of the measured (total) intensity is indeed synchrotron emission. The Ultrasensitive Array combines the flexibility to select the appropriate frequency for an experiment, with the wide frequency coverage essential for an accurate decomposition of the observed spectrum.

The Ultrasensitive Array will thus have a major impact on the study of magnetic fields in astronomy. The remainder of this section details a few specific experiments illustrating the possibilities; the intention is to give some feeling for the expected advances, rather than to provide an exhaustive survey. The improvements provided by the VLA Expansion Project are so dramatic that one may confidently predict that the selection below represents the small tip of a very large iceberg.

3.1.1 Coronal Magnetography in Solar Active Regions

Solar active regions are localized areas on the Sun where magnetic flux has erupted through the photosphere into the chromosphere and corona. As their name implies, solar active regions are the sites of various kinds of solar activity: solar flares, radio bursts, enhanced coronal heating, and mass ejections. A key goal in solar physics is to understand their birth, evolution, and decay, the role of electric currents, and the origin of transient, energetic activity. Addressing this goal requires detailed measurements of the coronal magnetic field. The Ultrasensitive Array offers the unique capability of obtaining such detailed measurements, through rapid imaging observations over a wide range of frequencies.

When the magnetic field is sufficiently large ($\gtrsim$ 100 G) gyroresonance opacity is the dominant source of opacity in solar active regions. Radio waves with frequencies which are low integer multiples of the the electron gyrofrequency ν_B (i.e., $\nu = s\nu_B; s = 1, 2, 3...$) may be resonantly absorbed and emitted by electrons gyrating in the local magnetic field. For example, the electron gyrofrequency in a 600 G magnetic field is $\nu_B = 1.7$ GHz, the third harmonic of which lies in the 5 GHz band. Given sufficient spectral and spatial resolution, one can exploit gyroresonance absorption to place unique constraints on the magnetic field at the base of the corona; that is, to perform *coronal magnetography*. There are no other techniques available to measure strong fields in the Sun's corona.

This works as follows: consider a given frequency ν which is optically thick to gyroresonance absorption in the solar corona at $s = 3$. It therefore yields a brightness temperature which is similar to the effective temperature of the corona ($\mathrm{T_B}(\nu) \approx 3 \times 10^6$ K). Now let ν increase – as ν increases, the resonance condition is matched at higher magnetic field strengths, which occur at lower heights in the corona. At some critical frequency ν_c, the resonance condition is matched at the base of the corona. For $\nu > \nu_c$, $T_B(\nu)$ drops precipitously as the resonance layer traverses the transition region and chromosphere where the effective temperature is much lower. A high resolution map of ν_c may therefore be converted into a map of $|B|$ at the base of the corona. With care, the field vector may also be constrained. Coronal magnetography provides the most direct means available of estimating the magnetic field at these heights. It would provide an invaluable

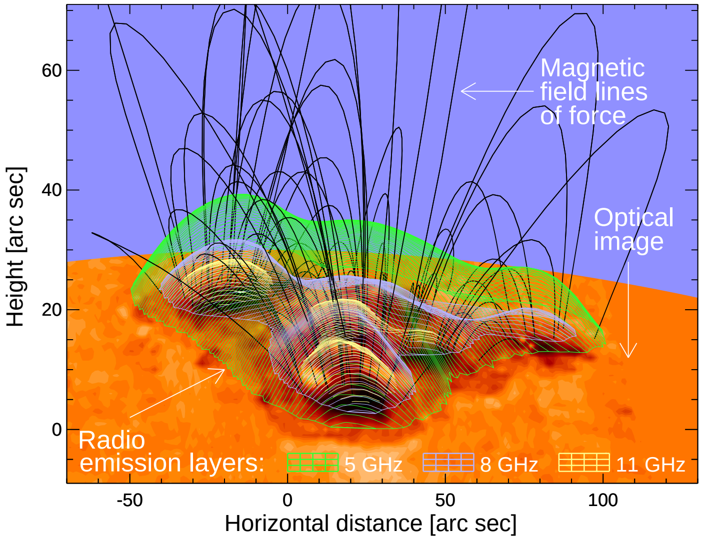

Figure 3.1: A perspective view of a complex sunspot group (7 May 1991) in optical continuum, with field lines extrapolated into the corona using a nonlinear force-free extrapolation by Z. Mikić. The three surfaces are the calculated gyroresonant surfaces in the corona that will dominate the radio opacity at each of three radio frequencies: 5 GHz (B = 600 G), 8 GHz (B = 950 G) and 11 GHz (B = 1300 G). (Produced by Jeongwoo Lee/NJIT.)

tool for assessing departures of the field from potential configurations in active regions, and for assessing the role of electric currents.

A more ambitious goal is to infer the *three-dimensional* distribution of magnetic fields (and currents). At a given frequency, the gyroresonance emission originates from an isogauss surface. Tuning across a broad range of frequencies "peels the magnetic onion", and provides a three-dimensional map of the brightness temperature as a function of magnetic field strength. Such measurements, when coupled with vector magnetic field measurements at photospheric and chromospheric heights, will impose powerful new constraints on field extrapolations.

High resolution imaging observations at many frequencies over a broad bandwidth are needed to exploit the techniques outlined above. While the VLA currently provides sufficient angular resolution, the continuous frequency coverage and the large bandwidth ratios of the Ultrasensitive Array are essential to mapping out the detailed magnetic field structure of the corona.

3.1.2 Imaging the Dynamic Heliosphere

The solar wind inflates a cavity around the Sun, extending to perhaps ~ 100 AU, called the heliosphere; this is filled with a tenuous, magnetized plasma, known as the interplanetary medium (IPM). Radio interferometers like the VLA are ideally suited for measuring the angular broadening and intensity scintillations of background sources viewed through the IPM; these data can be used to deduce the solar wind speed and acceleration profile, to measure properties of the turbulence, and to map large-scale structures in the solar wind. These studies exploit observations of sidereal background sources which, in the absence of the IPM, are either unresolved by the array or have known source structure. Phenomena such as angular broadening, scintillation, Faraday fluctuations, etc., are due solely to the intervening turbulent medium. Currently such studies are limited by sensitivity to occasional determinations of solar wind properties using a handful of bright sources at various elongations and position angles.

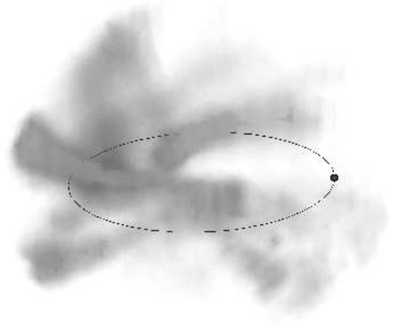

Figure 3.2: An example of a tomographic reconstruction of the inner heliosphere, to a distance of 1.5 AU, which was derived from a combination of IPS intensity level data and velocity data obtained over one solar rotation period (23 June 1994 to 20 July 1994, Carrington Rotation 1884). Earth's orbit is as indicated. The technique is described in detail by Jackson *et al.* (1998).

The greatly improved continuum sensitivity provided by the Ultrasensitive Array is critical for this sort of work. Access to large numbers of background sources will enable determinations of the properties of the solar wind turbulence along many lines of sight over the course of a single observing run; such simultaneous measurements are essential for such a time-variable phenomenon, and will characterize the IPM in the inner heliosphere in a more global fashion. More exciting still is the prospect of mapping the large scale transient disturbances in the IPM (*e.g.*, coronal mass ejections). Here one would like $\sim 10\,\mathrm{min}$ integrations, to sample many instances of the scattering screen while mapping as large an area as possible; with the Ultrasensitive Array this will give on average 5–20 100σ sources per primary beam at 1.5–3.0 GHz, while greater numbers still will be available in the UHF bands.

3.1.3 Galactic Center Magnetic Fields

A strong and highly ordered magnetic field pervades the central region of the Galaxy. This field is oriented vertical to the Galactic plane and is two to three orders of magnitude stronger than the field in the Galactic disk. The primary evidence for the vertical magnetic field comes from VLA observations which reveal a system of long ($\sim$10's of pc) and narrow ($<$0.5 pc) non-thermal filaments and thread-like structures oriented perpendicular to the Galactic plane (Figures 3.3, 3.4; Yusef-Zadeh, Morris, & Chance 1984; Morris & Yusef-Zadeh 1985; Anantharamaiah *et al.* 1991; Liszt & Spiker 1995; Gray *et al.* 1995; Yusuf-Zadeh, Wardle, & Parastaran 1997; Lang *et al.* 1999).

These synchrotron-emitting filaments are strongly linearly polarized with their intrinsic magnetic fields remarkably well aligned along their length. However, their generation remains an enigma.

The Ultrasensitive Array will make a number of major contributions to our understanding of the role of magnetic fields in the Galactic center region, and hence near the nuclei of other spiral galaxies as well. Spectral indices and linear polarizations will be obtained easily for even the faintest known filaments; rotation measure studies will reveal the magnetic field configuration within individual filaments, and in the entire central region, several degrees across. Zeeman measurements will be extended to many more masers and absorption lines, and even to the radio recombination lines which trace the ionized gas as a whole. The result will be a far clearer and more complete picture, on both large and small scales, of the strength and topology of the magnetic fields in the Galactic center region.

Continuum Imaging

Current high-resolution VLA images (*e.g.*, Figure 3.4) suggest that the entire 1−2° region surrounding Sgr A is permeated by these magnetic filamentary structures, many of which are barely detectable. All the known filaments appear to have unresolved sub-structure along their lengths. The Ultrasensitive Array will allow a factor ≥ 4 more sensitive imaging with complete polarization and spectral information over the entire region. This will provide a far superior characterization of the distribution, structure, spectral index, and polarization properties of the filaments on sub-arcsecond scales, and may confirm the ubiquity of these features, as well as revealing the overall field configuration in the central regions of the Galaxy. Spectral indices in particular have never been measured accurately over a large field-of-view. Such measurements are essential to study the details of the interactions between magnetic filaments and associated ionized gas, which are currently thought to provide a mechanism for acceleration of particles and the subsequent synchrotron radiation (Serabyn & Morris 1994).

Differential Faraday Rotation

The magneto-ionic medium in the Galactic center region causes large ($> 10^3$ rad m^{-2}) differential Faraday rotation of the plane of polarization. Multi-frequency, narrow-bandwidth observations are necessary to correct for this Faraday rotation and thus to determine the intrinsic orientation of the magnetic field in Galactic center sources. The rotation measures (RMs), which are determined in the process, give valuable information on the combination of the strength of the parallel component of the magnetic field and the electron density along the line-of-sight ($\int n_e B_{\|} \, dl$). Given the high observed RMs, the spectral resolution of the current VLA correlator limits the total frequency coverage for polarization observations towards the Galactic center to < 25 MHz for frequencies below 5 GHz. This makes 5 GHz the most sensitive frequency for such observations with the current VLA; since this limits the field-of-view to $\lesssim 9$ arcmin, and since the non-thermal filaments are weaker at higher frequencies, only a few selected regions have been studied. The simultaneous broad bandwidth and high spectral resolution of the new correlator will allow unambiguous determination of rotation measures and polarization over a 0.5° field of view in a single pointing at ν=1.5 GHz. One could thus determine for the first time the rotation measures and the magnetic field configuration over a large region of interest (several degrees) around the Galactic center. The improved sensitivity of the Ultrasensitive Array will also allow efficient polarization imaging at higher (sub-arcsecond) resolutions of the stronger filaments; observations of a few selected regions have already shown rotation measure changes from 100s to 1000s of radians/m^2 on scales of several arcseconds (Yusef-Zadeh, Wardle, & Parastaran 1997).

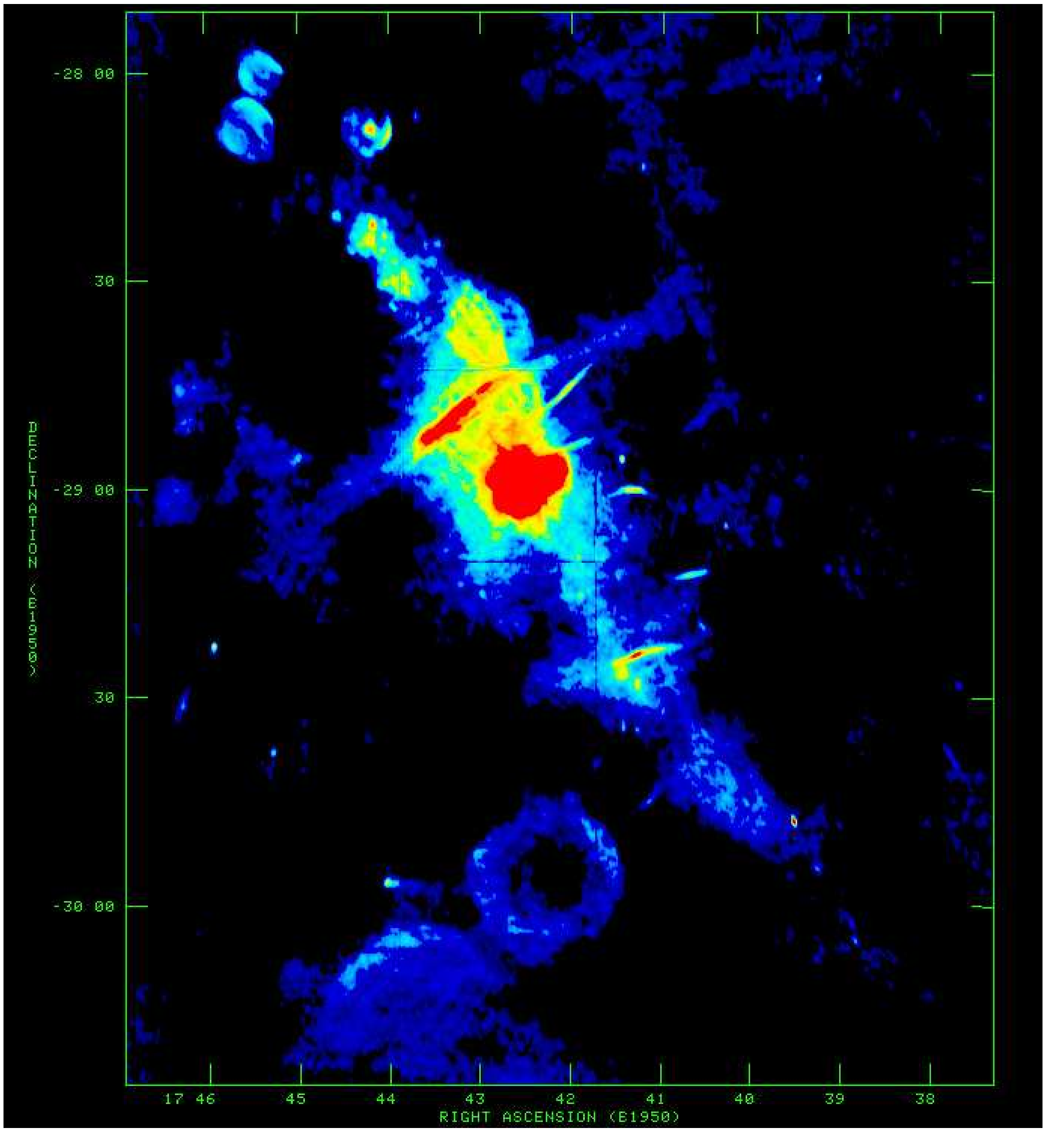

Figure 3.3: 330 MHz VLA image of the central 4° × 4° of the Galaxy, at 48 arcsec resolution. Courtesy Kassim, LaRosa, Lazio, & Hyman (1999).

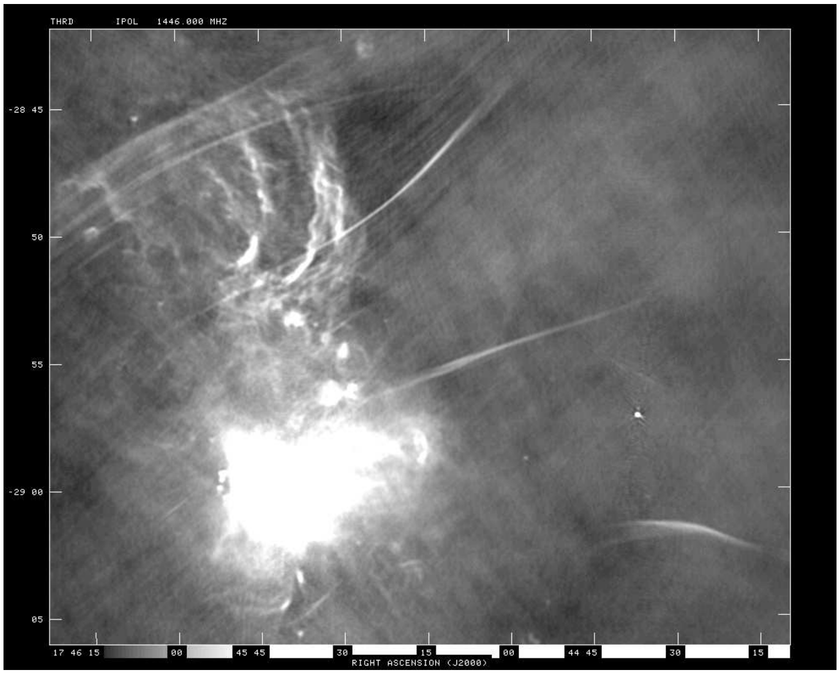

Figure 3.4: Unique radio structures within 30 arcminutes (75 pc) of the Galactic center, as seen with the VLA at 1400 MHz (Lang *et al.* 1999). Similar filaments are observed up to 1.5° from the Galactic center.

Zeeman Splitting

VLA observations of the Zeeman splitting in spectral lines of H I and OH in absorption (Killeen, Lo, & Crutcher 1992; Plante, Lo, & Crutcher 1995) and more recently in the 1720 MHz OH maser line (Yusef-Zadeh *et al.* 1999) have given direct measurements of very strong magnetic fields ($B_{\|} \sim 1-5\,\mathrm{mG}$) in the Galactic center region. Fields this strong may dominate the dynamics, and thus control the fueling of the central engine; the conversion of the substantial magnetic field energy may also dominate cloud heating near the Galactic center. Further, OH Zeeman splitting provides a much-needed probe of the magnetic field *inside* clouds, which seems to differ quite a bit from the field outside (cf. Serabyn & Morris 1996); this may provide a clue to the magnetohydrodynamic interactions in this region.

Currently the absorption measurements are at the limit of the VLA's sensitivity, while only a few 1720 MHz masers are known in this region. The Ultrasensitive Array will improve the current measurements and increase the number of detections substantially, both by allowing higher spectral resolution, and by lowering the system temperature by reducing the ground pickup (the Galactic center is a low elevation source for the VLA). The much-increased bandwidth will also allow simultaneous searches for, and measurement of Zeeman splitting in, a large number of masers. Finally, the Ultrasensitive Array will for the first time allow the detection of the Zeeman effect in radio recombination lines. This is a difficult experiment, requiring multiple transitions to be averaged together to increase the sensitivity, while retaining high spectral resolution; high spatial resolution is also critical, to avoid kinematic broadening of the lines. The best observations so far give a 3σ limit of 8 mG towards the northern arm (Roberts & Goss 1993); the Ultrasensitive Array will give a factor 5−10 improvement, by allowing observations at 15 GHz, stacking four radio recombination lines together, and giving a factor five higher velocity resolution (2 vs. 10 km/sec) over a 2000 km/sec bandwidth, allowing much-improved continuum subtraction. The potential rewards are enormous. Zeeman splitting measures the *local* field, and there is always the worry that the conditions in the absorbing or masing gas may not be representative of the region as a whole. Radio recombination lines by contrast arise from ionized gas which is spread throughout the Galactic center region, including pockets which are known to be present close to the central black hole. Since the magnetic fields observed at larger distances are of order a few milliGauss, the ability to measure 1 mG fields from RRLs should make it possible to measure (or set very interesting limits on) the field strength within a few tenths of a parsec of the black hole itself.

Anisotropic Scattering

Point-like radio sources (generally, OH masers) observed through the turbulent medium near the Galactic center are scatter-broadened, with measured sizes of more than an arcsecond at 1.6. GHz; the scattering region covers at least 25 arcminutes (Frail *et al.* 1994). The scattering disks themselves are elongated due to anisotropies in the ionized scattering medium, which in turn presumably reflect the orientation of an ordered magnetic field. Frail *et al.* observed five masers per day, each requiring a separate tuning of the array. The new correlator of the Ultrasensitive Array will allow the entire inner 30 arcminutes to be searched simultaneously for OH masers, with sub-km/sec channels, over a huge velocity range (±3000 km/sec). This would map the sizes and orientations of the scattering disks across the entire region in one go, yielding direct information both on the magnetic field structure, and on the scattering material itself.

3.1.4 Large-scale Magnetic Field Structures in Normal Galaxies

Synchrotron Emission: Polarization

The past decade has seen something of a revolution in our understanding of the strength, orientation, and orderliness of magnetic fields in spiral galaxies (e.g., Beck *et al.* 1996), thanks in large part to high-resolution polarization observations of synchrotron emission by the VLA (Figure 3.5). However, only the nearest and the (radio) brightest galaxies have been imaged, and then only with rather poor spatial resolution (a few hundred to a few thousand parsecs). This leaves many major questions unanswered:

- How are magnetic fields created? Does the standard dynamo model for generating magnetic fields work?
- What is the relationship between magnetic fields and turbulence and shocks? Are interstellar fields deformed by star-formation processes, and do they influence star formation?
- Do all galaxies show regular magnetic fields? How do these vary with Hubble type? Several edge-on galaxies show magnetic fields perpendicular to the disk in the center; how does this component vary with bulge luminosity?
- How are magnetic fields related to spiral arms? Is the pitch angle determined by the dynamo (as theory would have it) or by the density wave? Why is the inter-arm magnetic field often stronger and more ordered than that along the arms?

- How do gravitational interactions affect the magnetic field?
- What is the diffusivity of interstellar fields? Under what conditions is the field frozen into a gas flow?
- Which component of the ISM gas (molecular, Warm/Cold Neutral Medium, . . .) is mainly responsible for anchoring the field lines?

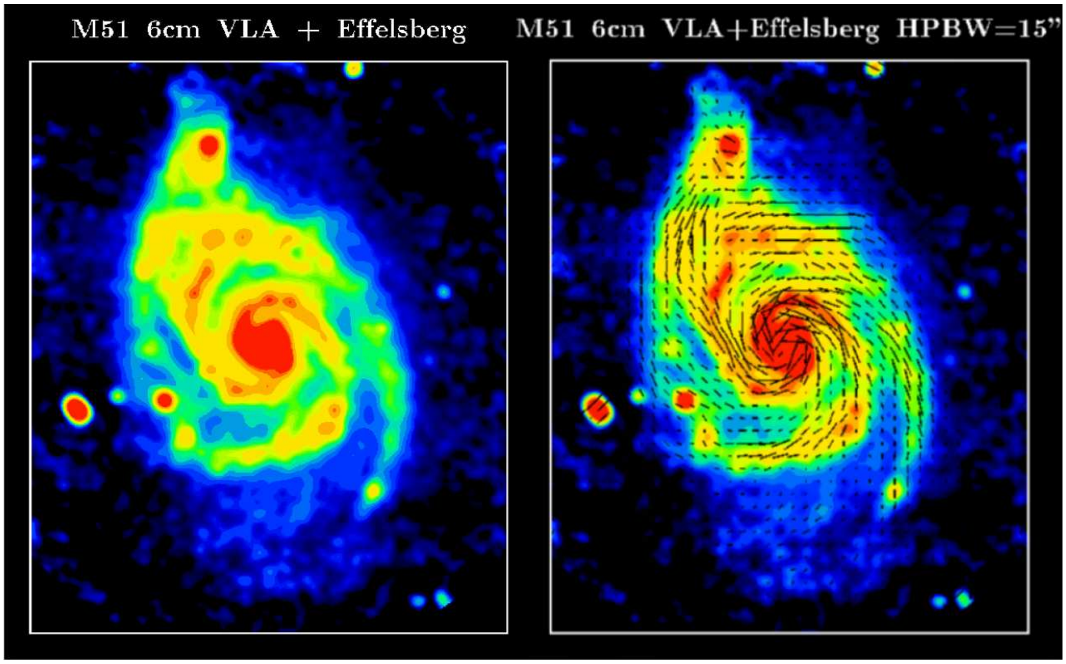

Figure 3.5: Combined VLA+Effelsberg image of M51 radio continuum total (*left*) and polarized (*right*) intensity at 5 GHz, at a resolution of 15 arcsec. The vectors show the magnetic field orientation, and their lengths are proportional to the polarized intensity. Courtesy R. Beck (1999).

Answering these questions requires polarization imaging of many galaxies at high ($\lesssim 100\,\mathrm{pc}$) resolutions. Large samples are necessary to understand how magnetic fields relate to the Hubble type and the galaxy environment; high resolution is essential in studying the relationship between magnetic fields and spiral structure, star formation, and the other components of the ISM. Current observations are limited by several effects. Synchrotron emission is strongest at low frequencies ($S_\nu \propto \nu^\alpha$, with $\alpha \sim -0.6$ to -1.0), but Faraday rotation ($\propto \nu^{-2}$) depolarizes the signal unless one observes at high spectral and spatial resolution. Currently the VLA correlator forces one to choose between spectral resolution and sensitivity (bandwidth), and this pushes observations up to fairly high frequencies (usually 8.3 GHz) where the emission is relatively weak. This then prevents observations at high resolution, since the surface brightness sensitivity of the array goes as θ^2. The result is that only about a dozen galaxies have so far been observed, requiring long (8–12 hour) observations, and achieving rather poor (15–60 arcsec) angular resolution.

The Ultrasensitive Array will dramatically improve the situation, due to a number of interlocking advances. The new correlator will provide high spectral resolution over huge bandwidths, allowing the measurement of Faraday rotation at even the lowest frequencies, while avoiding the effects of spectral depolarization. The improved sensitivity will allow observations with a factor 9 smaller beam, avoiding spatial depolarization and allowing a much more detailed comparison between magnetic fields and other features. Finally, the continuous frequency coverage will allow the choice of an observing frequency suited to each particular galaxy. For instance, there are indications that some spiral galaxies are optically thick to polarized emission at $\sim 1\,\mathrm{GHz}$ (see below), and those would be observed with the new 3 GHz system to maximize both sensitivity and resolution.

To make this more concrete, consider a typical spiral galaxy, which has a mean disk brightness temperature of $\sim 0.75\,\mathrm{K}$ at 1.4 GHz (Hummel 1981). This corresponds to $T_B \sim 0.4\,\mathrm{K}$ at 3 GHz (assuming $\alpha \sim -0.8$). The Ultrasensitive Array could detect $\sim$ 10% polarizations in such a galaxy, at higher resolution than any previous study (7 arcsec), in under 2 hours. This resolution corresponds to physical sizes below 100pc for all galaxies in the Local Group. The UGC lists over 13,000 galaxies with diameters over an arcminute – the polarization could be mapped in *any* of these systems. The Expansion Project would allow us for the first time to study magnetic fields in detail in unbiased samples of ordinary spiral galaxies.

Mapping the Three-Dimensional Structure of the Magnetic Fields

Horrelou *et al.* (1992; see also Buczilowski & Beck 1991) showed that M51 becomes more and more depolarized with decreasing frequency, the effect turning on at about 1–2 GHz. They interpreted this in terms of a Faraday 'optical depth', as one sees further and further into the disk as the frequency increases[1]. That group is now working on turning these multi-frequency data into a three-dimensional map of the magnetic field distribution. Unfortunately, with only two spectral points at $\sim 1\,\mathrm{GHz}$ available with the current VLA, and no information at all from 1.7 to 4.5 GHz, it is impossible either to check this mapping, or to obtain more than a very crude model. The new correlator and continuous frequency coverage provided by the Ultrasensitive Array would provide some *thousands* of spectral points, spread over the full interesting range from 1 to 3 GHz, with only a modest increase in observing time.

Faraday Rotation Towards Background Sources

One of the classic probes of magnetic fields (and ionized particles) in the Milky Way is Faraday rotation towards polarized background radio sources, giving the electron density-weighted integral of the line-of-sight magnetic field. The Ultrasensitive Array will be able to perform similar experiments towards nearby galaxies, opening a new window on their magnetic fields. Assuming an average 2% polarization for random background sources and following Condon's (1984) source counts, more than 10 background sources could be seen through each of more than 40 UGC galaxies. M31 is of course the best case; here we should obtain more than 1100 independent rotation measures scattered throughout the disk and halo.

3.1.5 Galaxy Clusters

Clusters of galaxies are filled with turbulent hot gas, relativistic particles, and magnetic fields. While X-ray observations offer the best probe of the hot gas in this intra-cluster medium (ICM), the magnetic and relativistic components are most readily observed at radio frequencies. The

---

[1] This effect is sometimes referred to as *internal depolarization*.

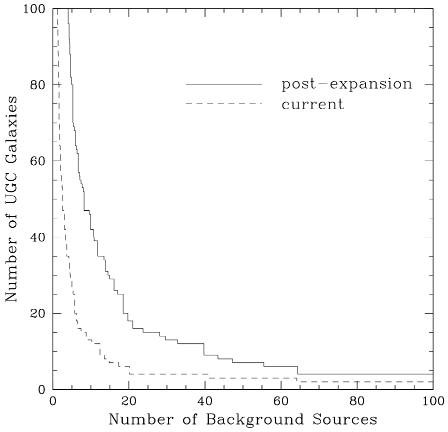

Figure 3.6: The number of UGC galaxies with a given number of background sources suitable for rotation measure studies ($S_\nu > 150\sigma$) with the current VLA (dashed line) and with the Ultrasensitive Array (solid line). For instance, ~ 50 UGC galaxies should have more than 10 such background sources. A few galaxies (*e.g.*, M31, M33) are expected to have many more than 100 suitable background sources. Calculations assume 12-hour integrations at 1.5 GHz for the current VLA, and at either 1.5 or 3.0 GHz for the Ultrasensitive Array (the two frequencies give virtually identical source counts). Based on Condon's (1984) source counts. Note that the Ultrasensitive Array will be sensitive to a far greater range of RM as well, due to the vastly-improved frequency coverage and spectral resolution.

magnetic fields in particular are of great interest, as they may play an important role in galaxy and cluster evolution, and even in cluster dynamics; in addition, even relatively weak fields can have profound effects on energy transport within galaxies/clusters.

Radio observations provide the only means of directly measuring cluster magnetic fields. The detection of smooth, large-scale radio 'halos' shows that both particles and fields are present in several clusters (Feretti & Giovannini 1996). These data are consistent with the interpretation of recent hard X-ray measurements (Fusco-Femiano *et al.* 1999) as inverse Compton emission from lower-energy photons scattered off of relativistic particles; together, the radio and X-ray observations give much more accurate estimates of the division in energy between particles and fields. In addition, Faraday rotation measurements (*e.g.*, Clarke 1999, Feretti *et al.* 1999, Taylor & Perley 1993) provide independent evidence that the ICM is magnetized, possibly at dynamically significant levels.

Current instruments can only hint at the true potential of these observations. We know that some clusters have significant magnetic fields, and (from rotation measure studies) have some idea of their distribution and topology in a few key sources. But the details are far from clear. Do all clusters have large-scale magnetic fields, at some level, or is this confined to the known (bright) halo clusters? At what redshift do such fields 'turn on', and how do they evolve? Rotation measure studies currently are based almost entirely on sources embedded within the clusters; are the magnetic fields thus observed created or heavily influenced by the sources themselves? What is the magnetic field topology *away* from such powerful radio sources, and are there strong fields without relativistic particles to 'light them up' via synchrotron radiation?

The Ultrasensitive Array will be ideally suited to answering these questions. It will allow accurate, high-resolution imaging of radio halos in dozens of clusters, showing whether cluster-wide magnetic fields are present in every cluster, and giving detailed information on cosmic ray acceleration in the cluster environment. The improved sensitivity will also vastly increase the number of rotation measure probes, giving unique information on the magnetic field strength and topology, independent of any relativistic particle population. And by providing sensitive rotation measure images of high-redshift radio galaxies, the Ultrasensitive Array may provide a very effective way to find high-redshift X-ray clusters, with important implications for cluster formation and evolution.

Diffuse Synchrotron Emission

Current studies of radio halos are restricted to low-resolution maps of a handful of the brightest sources, although theories of cluster formation predict diffuse relativistic particles and magnetic fields should exist in many or all clusters. Even the brightest halos can now just be detected above the noise level (Figure 3.7; Giovannini *et al.* 1993); except for their general shape little detail is available, and spectral information is particularly sparse. Studies of sources like the M87 halo (Figure 3.8; Owen, Eilek, & Kassim, *in prep.*) suggest that the picture will turn out to be much more complex, and that we may be looking at unfilled structures. The Ultrasensitive Array will allow many hundreds of fainter halos to be detected, studied as a function of frequency and redshift, and imaged with high fidelity and at high (few arcsecond) resolution. The larger sample will show directly whether cluster-wide fields are the rule or the exception, thus testing current models of cluster formation and early evolution; the more detailed studies will also measure the spectral and spatial distribution of the relativistic particles, thus constraining cosmic ray acceleration (primary or *in situ*) in the cluster environment.

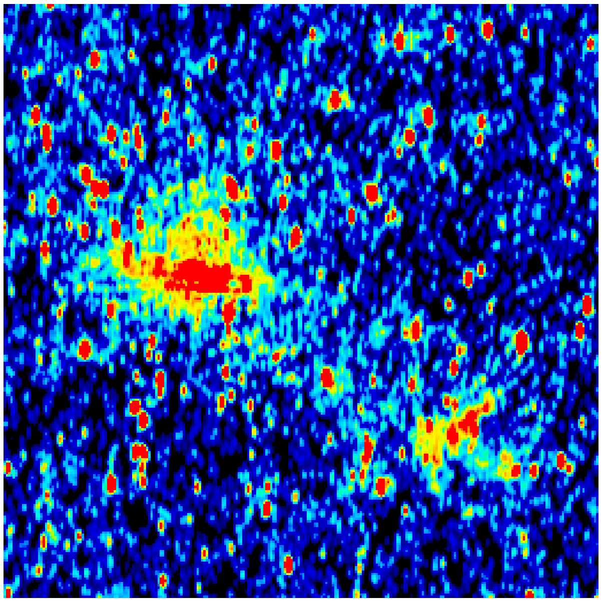

Figure 3.7: WSRT image of Coma at 327 MHz (Giovannini *et al.* 1993), showing diffuse synchrotron emission on a Mpc scale. This is the prototype of the radio halos expected to be common in galaxy clusters; note also the 'relic' source to the southwest. Both provide direct evidence for a cluster-wide distribution of relativistic particles and magnetic fields. There are six undisputed radio halos known (Feretti *et al.* 1999); the Ultrasensitive Array will expand this to several hundred.

Faraday Rotation Studies

Faraday rotation gives an independent measure of the magnetic field and ionized medium along the line-of-sight, and also has the advantage of depending on the strength of the background source rather than the intrinsic radio emission. Two such probes are available in clusters: true background and cluster member sources. The number of useful sources is limited by the sensitivity (requiring reasonable detections of the *polarized* emission, at high enough resolutions to avoid beam depolarization) and the spectral resolution (to avoid polarization angle wraps within a channel, while maintaining broad enough bandwidths to detect even low RMs). With major advances in both areas, the Ultrasensitive Array will bring about a revolution in these studies.

At the moment, RMs can be measured towards one or two background sources in a given cluster. Combining these for many galaxy clusters shows clearly that a magnetic field is present (Figure 3.9: Kim, Kronberg, & Tribble 1991; Clarke 1999), but cannot yet determine whether the fields detected are caused by strong radio galaxies in the cluster, or are intrinsic to all clusters. By contrast, the Ultrasensitive Array will give rotation measures towards more than 20 background sources within 0.2 Abell radii of *each* of more than 80 Abell clusters.

The Ultrasensitive Array will similarly advance RM imaging of embedded sources, which provides the only observational measurement of the detailed magnetic field topology (strength and structure) within individual clusters. Virtually every source that can now be imaged in total in-

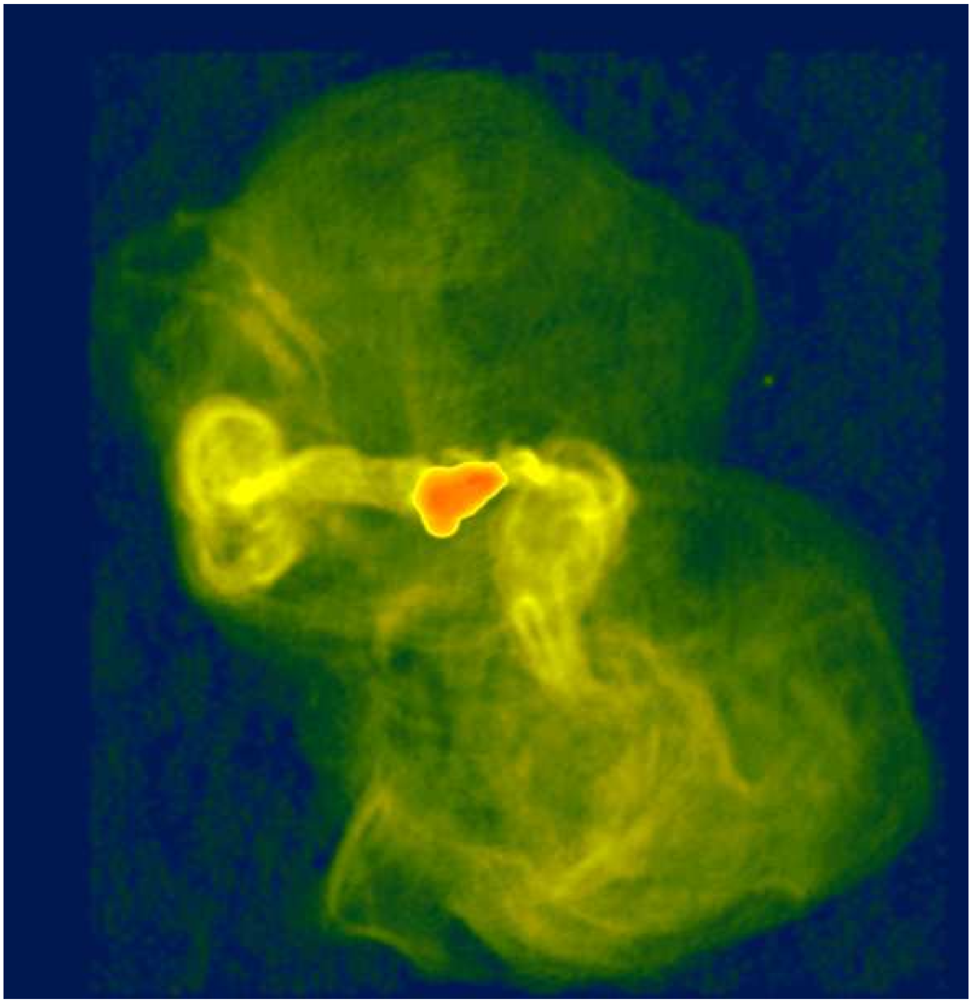

Figure 3.8: 327 MHz VLA image of M87, the central radio source in the Virgo Cluster (D $\sim$ 17 Mpc; Owen, Eilek, & Kassim, *in prep.*). This 80-kpc radio source coexists with the X-ray cluster gas, and is dumping at least as much energy into that gas as is being lost to X-ray emission. The radio source is thus playing an important role in the central dynamics of the cluster gas.

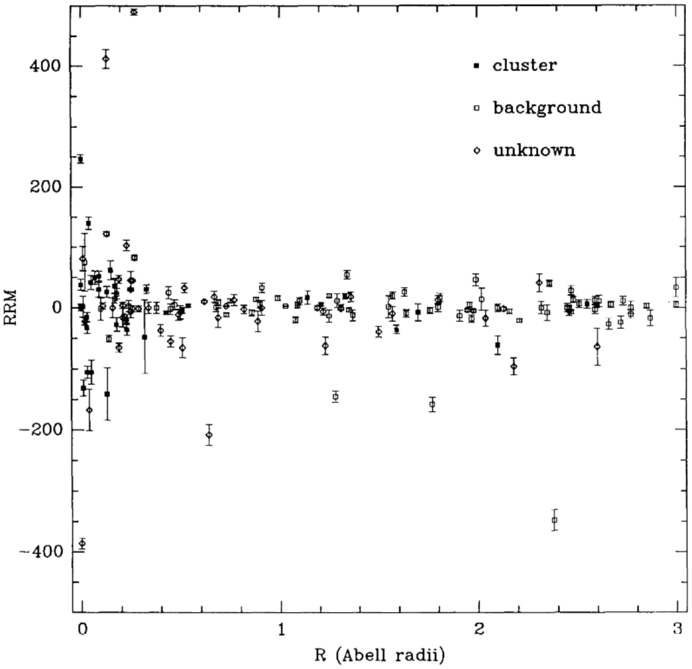

Figure 3.9: The rotation measure vs. impact parameter for radio sources near, within, and behind Abell clusters (Kim, Tribble, & Kromberg 1991). Note the clear increase in the width of the RM distribution at small radii. This plot can only be made currently by combining data from *all* clusters; the Ultrasensitive Array will provide higher-quality measurements, towards more sources, in *individual* galaxy clusters.

tensity will give extended RM maps with the Ultrasensitive Array (cf. Figure 3.10). By combining significant background studies with improved imaging of the cluster sources themselves, the Ultrasensitive Array will finally answer the question of whether magnetic fields exist in all clusters, and if so at what level, and with what spatial topology.

Extreme Rotation Measure Radio Galaxies

Over the past decade, extreme Faraday rotation has been seen toward a number of extended extragalactic radio sources (Dreher, Carilli, & Perley 1987; Taylor, Barton, & Ge 1994; Carilli *et al.* 1997). Rotation measures as high as 20000 rad m^{-2} have been detected, as well as gradients in RM $\geq$1000 rad m^{-2} $arcsec^{-1}$. Observations of the closer radio galaxies have shown a clear correlation between extreme rotation measures and cluster environment: all sources located at the centers of dense, X-ray emitting cluster atmospheres show large amounts of Faraday rotation (Taylor, Barton, & Ge 1994). Since this correlation holds regardless of radio source luminosity and morphological class, the high rotation measures are probably associated with the clusters themselves, rather than with the individual radio sources.

High rotation measures are not confined to nearby galaxies; radio observations have already found 11 galaxies with source-frame RM> 1000 rad m^{-2}, at redshifts between 2 and 3.8 (*e.g.*,

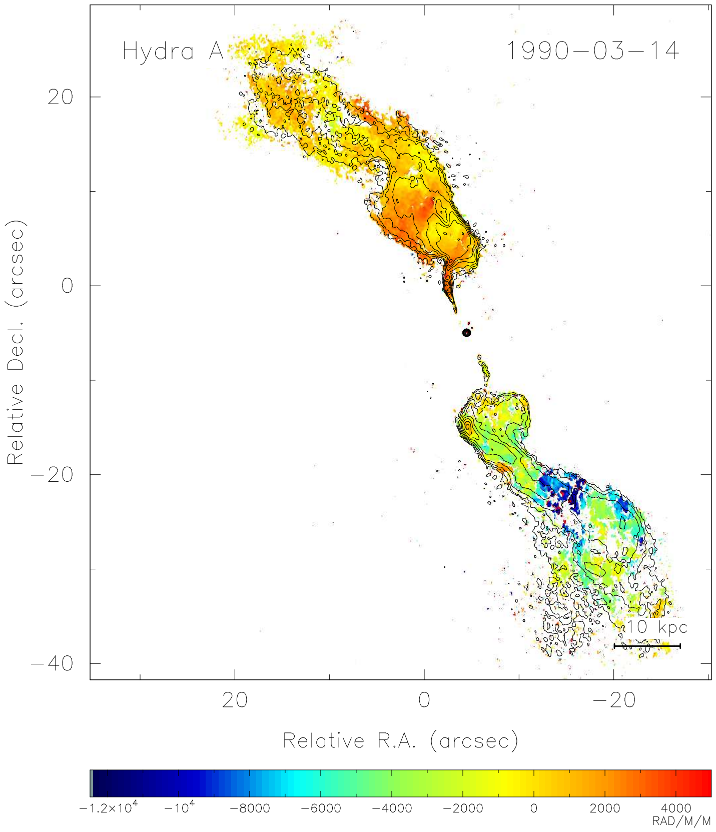

Figure 3.10: The rotation measure structure of Hydra A at 0.3 arcsec resolution (Taylor & Perley 1993). The colors indicate RM from −12,000 to 4000 radians/m^2; the contours represent the 8.4 GHz radio continuum. The Ultrasensitive Array will allow similar RM mapping of sources which are an order-of-magnitude fainter — basically every radio galaxy which can currently be imaged.

Figure 3.11; also Carilli *et al.* 1996; Athreya *et al.* 1998; Carilli, Owen, & Harris 1994). Such high RMs imply that we are looking through some sort of external magnetic field/density distribution; the analogy with low-redshift sources suggests that these are galaxy clusters, but they could also be smaller, higher-density cocoons associated with the radio sources themselves. The problem with the cluster hypothesis is that it requires gathering together both the total mass and the hot gas seen in local clusters, at a much earlier epoch. The 'individual source' model on the other hand implies that young galaxies (quite unlike the ones we see nearby) are surrounded by impressive magnetic fields and quite dense gaseous halos. Both possible explanations are very interesting, but one needs more detailed studies of a much larger sample both to determine which (if either) is correct, and to understand the differences between high and low rotation measure systems at these redshifts.

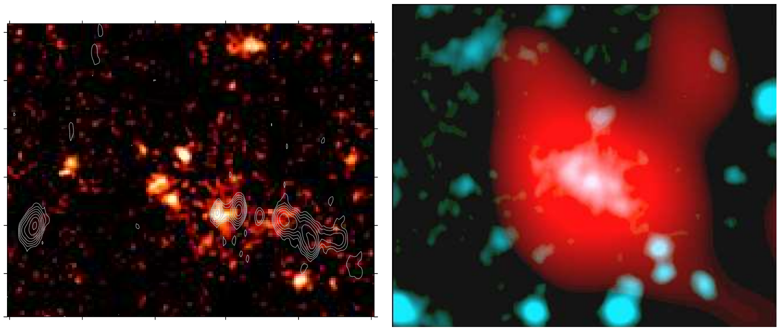

Figure 3.11: Two views of the z=2.156 extreme rotation measure radio galaxy 1138−262. *Left:* VLA 5 GHz contours overlaid on an HST image (grayscale) (Carilli *et al* 1997; Pentericci *et al.* 1997, 1998). The field size in RA is 13 arcsec. The optical and radio morphologies, together with optical velocities and velocity dispersions, all point to a dense local environment. *Right:* ROSAT HRI (X-ray) image in red, overlaid on an optical image in blue (Carilli *et al.* 1998). The field size is 40 arcsec. The X-ray emission can be explained either as thermal emission from an enormous amount of hot gas ($> 10^{13}\,M_\odot$), or as nonthermal radiation from a hidden active galactic nucleus.

The increased sensitivity of the Ultrasensitive Array, combined with the availability of the 2−4 GHz band, will dramatically improve our ability to search for, and study, such extreme RM high-z radio galaxies. Resolved images of these systems (typically smaller than a few arcseconds) are required, to properly determine the RM distributions across the radio lobes. Current searches have been limited to the largest sources, and to frequencies of $\gtrsim$ 5 GHz. Since the radio flux density drops sharply with frequency, especially for these high-z objects, such searches delineate, for the most part, the high surface brightness radio hot spots and core. Furthermore, the high radio frequency in the rest frame of the sources implies that only extremely large RMs can be detected ($\geq$1000 rad m^{-2}). The improved sensitivity of the Ultrasensitive Array will allow imaging the RM distribution across the radio lobes at sub-arcsecond resolutions 1−4 GHz, discovering many new extreme RM radio galaxies, and providing much more reliable rotation measure estimates, especially for relatively low RMs ($\leq$ a few hundred rad m^{-2}). These sources can then be studied using modern X-ray and optical telescopes, to determine whether they are in fact the signposts of massive clusters at high redshift.

3.2 The Obscured Universe

Much interesting astrophysics goes on behind curtains of dust and gas which hide the most important processes from our direct view; two obvious examples are the formation of stars in dense molecular clouds, and the shielding of massive black holes by the material they themselves accrete. Apart from preventing direct observation at optical, infrared, and in many cases even longer wavelengths, such opacity effects introduce subtle systematic biases, for instance, selecting against dusty sources or obscured lines-of-sight in optical samples. Radio observations by contrast are unaffected by dust extinction, and cover such a wide range in frequency (three orders of magnitude, at the VLA) that no single opacity source is likely to remain dominant in any case. Straddling the transition between synchrotron (cosmic ray), free-free, and dust emission, radio data probe three physical processes common to almost every source in the Universe. Superb spatial and spectral resolution complete the picture, making radio synthesis telescopes ideal for high-resolution imaging and dynamical studies of obscured regions.

The Ultrasensitive Array will make this promise a reality. Continuous frequency coverage will allow imaging the depths of the giant planets, and help disentangle the complex superposition of dust emission, H II regions, and thermal jets in star-formation regions. The improved continuum sensitivity will result in rapid and reliable astrometry and proper motions, probing the dynamics and measuring the gas accretion rate in the Galactic center, and determining the speed of young stellar outflows as near as possible to their acceleration regions. With the new correlator and a more flexible LO system astronomers will be able to directly observe ambipolar diffusion, and to determine the redshift evolution of the neutral baryon density without any uncertainties due to dust obscuration. The remainder of this section describes these and other experiments, which are either completely impossible or (for the very brightest sources) just barely do-able with the current instrument. The intent is rather to illustrate the range of the telescope than to exhaust its possibilities: the proper domain of the Ultrasensitive Array includes virtually every region where opacity is important, ranging from the densest to the most distant parts of the Universe.

3.2.1 Bistatic Planetary Radar

Bistatic radar observations offer a unique probe of material beneath the solid surfaces of planets, moons, and asteroids. The Ultrasensitive Array offers two major advances for these studies: the ability to observe at 13cm (2.3 GHz), allowing the VLA to take advantage of powerful 13cm transmitters at Arecibo and Goldstone; and high enough frequency resolution to make Doppler images of even the smallest bodies in the solar system.

Radar observations of planetary surfaces yield important and unique information on their surface and near-surface structure and composition. Currently the VLA, in combination with the Goldstone 70m antenna, is one of the two most powerful 3.6cm (8.4 GHz) radar instruments in the world (the other being Arecibo). With this combined instrument, it is possible to unambiguously image the surfaces of Venus, Mercury, and Mars with resolutions as good as 100 km, and to probe the surfaces of the Galilean satellites and Titan. Such experiments have led to some of the most exciting results in planetary science in recent years, including the discovery of ice deposits in the polar regions of Mercury (Butler, Muhleman, & Slade 1993); the discovery that significant differences between the ice caps of Mars extend to large depths (Muhleman, Grossman, & Butler 1995); the discovery of a huge region near the equator of Mars which reflects no detectable energy (dubbed "Stealth") (Muhleman , Grossman, & Butler 1995); and the discovery that Titan has no deep global ethane/methane ocean, contrary to theoretical predictions (Muhleman *et al.* 1990).

Figure 3.12 shows maps of the surface reflectivity of Mars and Mercury as made with this combined radar setup. This setup has also been used to image several near-earth asteroids (see *e.g.*, de Pater *et al.* 1994), and an experiment on a comet is planned for the future. The Ultrasensitive Array will extend these impressive results to the other major radar frequency (2.3 GHz) and allow Doppler imaging of sources as small as the asteroids.

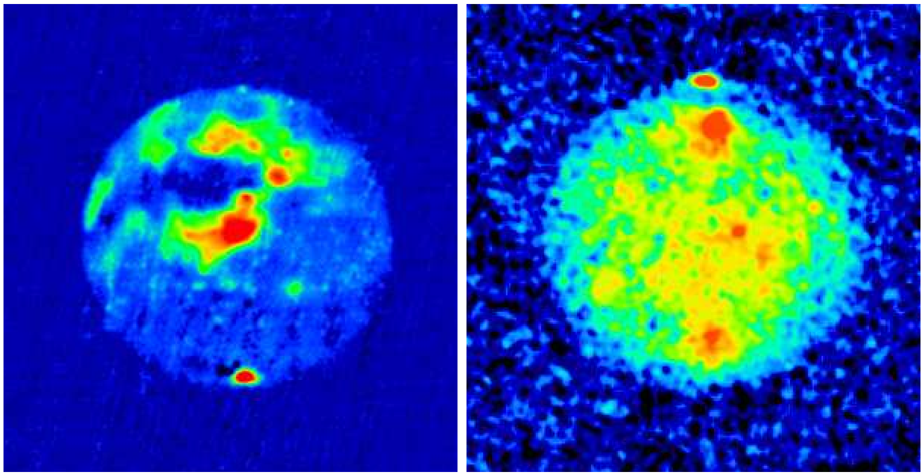

Figure 3.12: Radar reflectivity images of Mars (*left*) and Mercury (*right*) made with the combined Goldstone/VLA radar. Courtesy of B.J. Butler, D.O. Muhleman, & M.A. Slade (1999).

13cm (2.3 GHz) Radar: Surface Textures

When an electromagnetic wave is transmitted toward a surface, the amount of energy scattered toward the transmitter is most heavily dependent upon the "roughness" (or "texture") of the surface on size scales of the order of the wavelength of the e-m wave. Measurement of the reflected power yields information about the radar reflectivity – and therefore the composition – of the surface. Comparison of the scattering seen in the sense of circular polarization opposite to that transmitted (flat-facet reflections from a dielectric) to that seen in the same sense (caused by multiple reflections or by certain types of ices) yields additional information about surface roughness on scales comparable to the wavelength. So, at 3.6cm (8.4 GHz), surface structures from slightly sub-cm to some 10's of cm are most important, and dictate the amount of received flux. Going to longer wavelengths (such as 13cm) provides information on surface roughness at larger scales, approaching 1 m. This is very important additional information regarding the state of the surface.

Both the Goldstone 70m and the Arecibo antennas are equipped with very powerful 13cm (2.3 GHz) transmitters, and could be used in combination with the VLA. While the upgraded Arecibo system will have more power (on the order of 1 MW through a 300m dish), the Goldstone transmitter (∼ 420 kW) is still very important due to its full-sky coverage, which is particularly important for comets and asteroids. The lack of a 13cm (2.3 GHz) system at the VLA is the only bottleneck preventing very fruitful collaborations with both Arecibo and Goldstone in this area.

From 13cm radar observations, in combination with 3.6cm measurements already made, constraints on the depth of the very peculiar "Stealth" region of Mars and on the thickness of polar ices on Mars and Mercury could be obtained. Such observations will also provide the first good polarization measurements of Venus, greatly enhancing the usefulness of radar data from the Magellan mission (which provided only single-polarization radar); 3.6cm observations are severely compromised by attenuation by the Venusian atmosphere.

High-resolution Doppler Imaging

Because different portions of a rotating planetary surface are approaching the radar line-of-sight at different velocities, the received radar power is spread in frequency by some amount. At 8.4 GHz, $\Delta\nu$ varies from about 27 kHz for Mars to about 50 Hz for Venus. Typical bandwidths for asteroids are on the order of 100 Hz. The frequency spreads scale linearly with frequency, so 2.3 GHz widths are about a factor of 4 smaller. With the current VLA correlator, the smallest channel width available is 380 Hz for a single IF: only the largest of the asteroids are resolved, and only if data from only one polarization is recorded. For a typical Goldstone-VLA radar experiment, unless one is willing to give up the polarization information, the minimum channel width is 760 Hz. Unfortunately, this is wider than all of the returned signals except for Mars and barely comparable to those from the icy satellites. Because of inadequate resolution, Doppler information is lost; in addition, a penalty is paid in signal-to-noise ratio, since in those frequencies where there is no radar echo power, there is still noise power. In fact, in order to maximize the signal-to-noise on a particular surface feature, a channel width equal to the equivalent frequency spread of that feature is desirable. Again, this is currently obtainable for Mars, but not for any other body.

The new correlator provided by the Ultrasensitive Array will remove these restrictions, giving frequency resolutions of a few Hz over bandwidths of many kHz. In the case of Titan, such data could be used to calculate the position of the rotational pole, about which almost nothing is known. Determination of the rotational parameters of asteroids could also be done throughout the main belt, in association with the upgraded Arecibo at 13cm (2.3 GHz).

Higher Angular Resolution

Ideally one would like spatial resolution at 13cm which matches the 3.6cm results, requiring baselines which are about a factor of 4 longer than the longest available in A configuration. With these long baselines one could also do interesting work at 3.6cm, resolving for instance the polar caps of Mars. There is still plenty of flux to be imaged; the problem is simply one of missing antennas. While A+ configuration would be ideal for this work, the Pie Town-VLA link (already well under way) will certainly help, effectively doubling the resolution of the current VLA; note that the VLBA antenna at Pie Town already has a 13cm system in place.

3.2.2 The Giant Planets

Ammonia (NH_3) is the major opacity source at centimeter wavelengths on all giant planets; thermal radiation from depths with pressures greater than 1 or 2 bars can only be observed at frequencies below the broad NH_3 absorption band near 24 GHz. In effect, the gaseous planets have an "ammonia lid" on them which is nearly impenetrable in the frequency range from about 5 to 300 GHz. The VLA's gap in frequency coverage between 1.4 and 5 GHz greatly limits our ability to map the deep atmospheres of the giant planets, *e.g.*, at the levels of the expected water clouds. A striking example of this limitation is the interpretation of observations of the Comet Shoemaker-Levy 9 impact with Jupiter: quantitative analysis of the event depends on the existence or non-existence of the presently-unseen deep water clouds. VLA observations at 1.4 GHz may be sensing emission

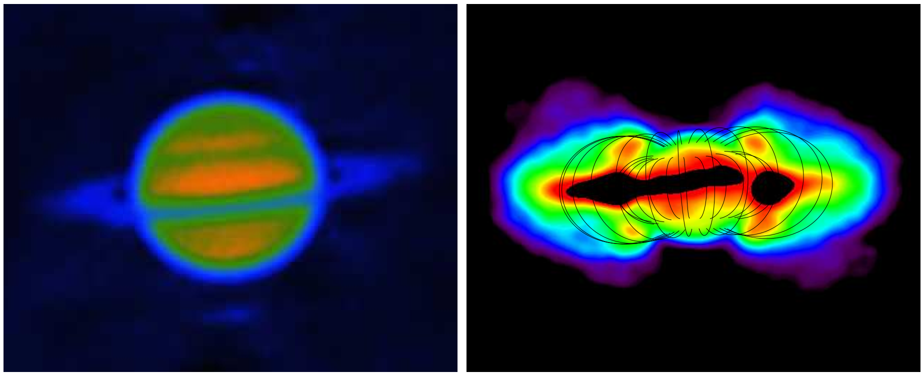

Figure 3.13: VLA images of Saturn at 15 GHz (*left*) and Jupiter at 1.4 GHz (*right*). Lines on Jupiter image are theoretical magnetic field lines. Courtesy of I. de Pater & F. van der Tak (1999).

at the level of the water clouds but the maximum spatial resolution (about 1.2 arcseconds) limits the quality of the maps, severely for Saturn, Uranus, and Neptune (which has a maximum diameter of 2.5 arcsec). The water vapor below the putative water clouds is another major opacity source that can't be penetrated at centimeter wavelengths.

By providing new 2-4 GHz receivers, the Ultrasensitive Array will significantly improve our ability to study the deep atmospheres of Saturn and Uranus, in particular. Jupiter is a very important special case since radio maps of that planet at 1.4 GHz and lower frequencies are completely dominated by non-thermal emission from the radiation belts. The ~ 3 GHz window is ideal for escaping the effects of the ammonia clouds, without being completely dominated by the non-thermal emission. Uranus and Neptune will also benefit from the new frequency band, but here the addition of at least one VLBA antenna into the A configuration is vital for real progress; fortunately the Pie Town link is just now beginning scientific operations, and in a few years should be fully connected to the array.

3.2.3 Young and Proto-Stellar Objects

Continuum Observations: Disks, Cores, & Jets

One of the major results of star formation studies has been the clear association between accretion disks and jets (outflows). This makes the spectral energy distributions (SEDs) of young stellar objects (YSOs) a confusing superposition of several components, any or all of which may be present in an individual case: thermal emission from dust in the accretion disk, free-free emission from the Strömgren sphere and/or a thermal outflow, and even synchrotron emission from shocks and/or non-thermal jets (cf. Wilner, Reid, & Menten 1999). The situation is further complicated by optical depth effects: the dust may be optically thick even down to 10s of GHz, while on the low-frequency side the free-free emission may just become optically thin at around the same frequencies. Disentangling all this requires accurate, high-resolution data over a wide range of frequencies, from a few to a few hundred GHz (cf. Figure 3.14). The ALMA will be the premiere instrument for dust and molecular studies; the Ultrasensitive Array will provide complementary information on the densest dust, the ionized gas, and the relativistic particles. In particular, VLA observations are needed to address a number of key questions, such as:

- Are jets always accompanied by accretion disks, and vice versa? Present models argue for a symbiotic relationship: the rotational energy of disks powers and accelerates the jets, while these take away angular momentum that would otherwise prevent further accretion.
- Are jets and disks as coupled in high-mass as they are in low-mass young stars?
- How are jets accelerated and collimated?
- How do binaries differ from isolated stars? In particular, how frequent are binary disk/jet systems like L1551? Are compact ($r \lesssim 10\,\mathrm{AU}$) protoplanetary disks restricted to binary stars (again like L1551, Figure 3.14), where tidal truncation provides a natural explanation?
- How do planets form? Would compact protoplanetary disks support gravitational instabilities, which could form planets in a few hundred years (*e.g.* Boss 1997), or must they rely on the conventional million-year core accretion paradigm?

The fundamental data needed to address these questions are (1) SEDs for a large number of YSOs, covering the frequency range from several to 100s of GHz; (2) high-resolution imaging of both jet and disk emission; and (3) AU-scale imaging of protoplanetary disks, at frequencies where the dust is optically thin enough to permit seeing so deep into the accretion disk. The Ultrasensitive Array will supply crucial information for these studies:

- *1–50 GHz SEDs:* Currently the VLA can laboriously detect some 10s of sources, and image a handful of those. The Ultrasensitive Array will permit the detection of up to 10,000 YSO disks/jet systems with masses larger than $0.01\,\mathrm{M}_\odot$ within 1 kpc of the Sun, with continuous frequency coverage from a few to several 10s of GHz, at resolutions sufficient to resolve proto-planetary disks for nearby systems (50 mas $\sim 7\,\mathrm{AU}$ at 150pc, somewhat smaller than Saturn's orbit).
- *Deep imaging of known jets:* Radio images typically show a thermal jet extending perhaps an arcsecond from the star, only re-appearing in the near-IR several arcseconds out (Figure 3.15). Since the jet brightness drops roughly as the inverse square of the distance along the jet, the $\sim$ 30-fold increase in sensitivity given by the Ultrasensitive Array should extend the inner radio jets by a factor five. This will link the radio to the near-IR/optical jet, and allow us to follow the jet all the way from its origin to the working surface (the Herbig-Haro object – also a radio source). By having information on the weaker parts of the radio jet we can address questions such as:
  - What is the recent history of the outflow? A few arcseconds from the star corresponds to the last few decades of the outflow, while the near-IR, optical, and molecular data record the history of the last hundreds and thousands of years.
  - Is the radio outflow already clumpy (as the near-IR is) a few arcseconds from the source?
  - How important is nature (time variations in the flow) compared to nurture (interaction with the surrounding medium)?
- *Temporal variations in outflows:* Measuring changes in time – variations in flow rate and possibly direction – requires the Ultrasensitive Array, even for relatively bright jets. Moving knots have been detected a few hundred AU from the exciting star in the HH 80-81 jet (Martí, Rodríguez, & Reipurth 1998); this required multi-epoch observations, separated by several years, of one of the brightest outflows in the sky. Are these enhancements in the flow

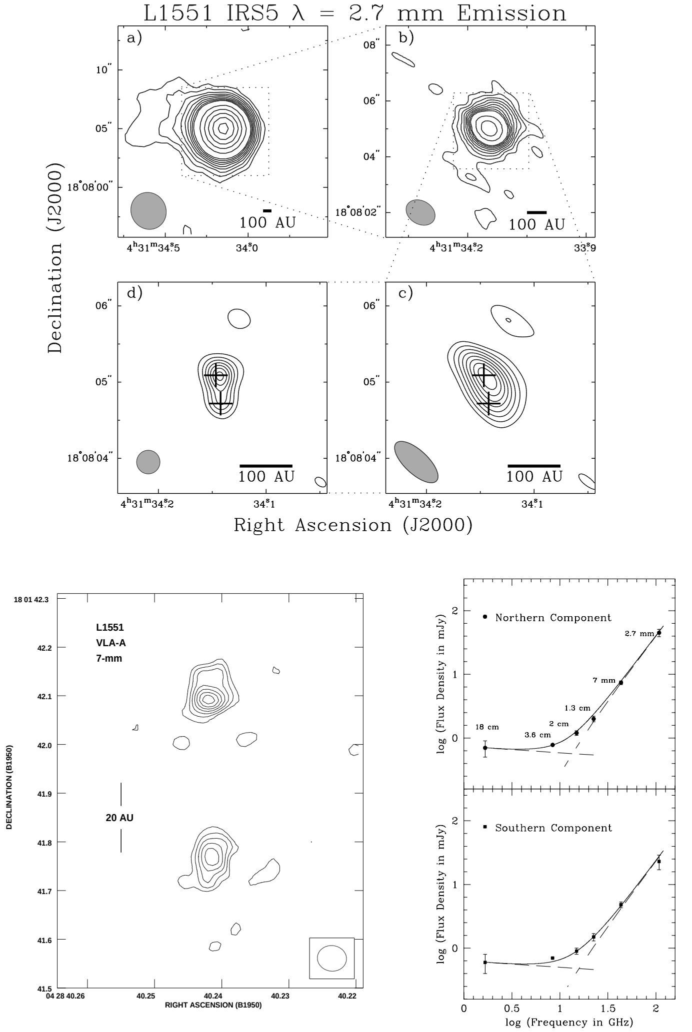

Figure 3.14: Dust emission from L1551 IRS5. (*upper*) BIMA images at 110 GHz with increasing angular resolution (Looney *et al.* 1997), showing that L1551 is composed of two circumstellar disks located within a flattened circumbinary structure embedded in an approximately spherical large-scale envelope. (*lower*) VLA images at 45 GHz with 50 mas (7 AU) resolution (Rodríguez *et al.* 1998) clearly resolve the individual dust disks surrounding the members of the proto-binary system. The spectral decomposition shows that the dust dominates the emission – and is optically thick – down to $\sim 22\,\mathrm{GHz}$, below which optically-thin free-free emission takes over.

periodic? Are these variations the rule or the exception? The Ultrasensitive Array could provide the answers, detecting proper motions of 300 km/sec at kpc distances with only a month between the observations.

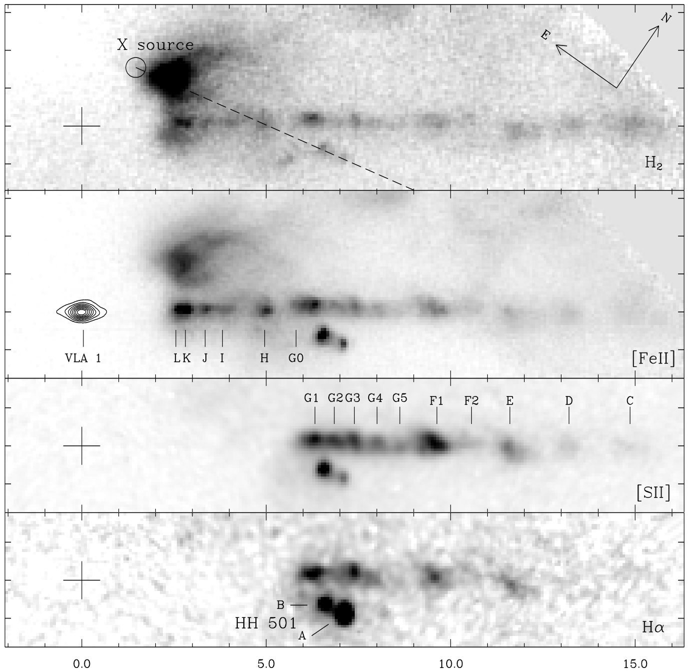

Figure 3.15: The thermal jet in HH 1–2, combining VLA 8.4 GHz (*contours*) with HST $\sim 2\,\mu$m (*grayscale*) data. The [Fe II] panel in particular shows the thermal jet (VLA 1) extending about an arcsecond, while the [Fe II] picks up several arcseconds out and extends to $\sim$ 10 arcsec. The Ultrasensitive Array would give higher resolution and fill in the missing emission, allowing us to follow the jet continuously from the origin to the working surface (the Herbig-Haro objects). Courtesy L. Rodríguez, S. Heathcote, & B. Reipurth (1999).

Ambipolar Diffusion: NH_3 vs. N_2H^+ Kinematics

Although the details of pre-stellar and proto-stellar infall and collapse are still poorly understood, it is clear that the fundamental physics involves gravitational and magnetic interactions. In particular, ambipolar diffusion is often invoked to separate the ions from the neutrals, allowing gravitational collapse in the presence of significant magnetic fields. Typical ion/neutral velocity differences are $\sim$ 0.1 km/sec, so ideally one would like observations with spectral resolutions of $\sim$ 0.02 km/s on scales from $\sim$ 0.1 to $\sim 10^4$ AU, of spectral lines which preferentially trace the cold, thermally-dominated gas in a dense core. Most molecular lines seen by the ALMA will not be suitable for this sort of work, because (i) their linewidths are dominated by much higher-velocity bulk motions in the gas; (ii) they are optically thick; (iii) they are often high-J transitions, which trace warmer gas; (iv) many molecules freeze out onto grains in pre-stellar cores and only appear again once the proto-star begins to heat the interior. Transitions at centimeter wavelengths – especially NH_3 ($\sim$ 24 GHz) – are ideal (*e.g.*, Myers & Benson 1983; Wiseman & Ho 1998). The hyperfine structure of ammonia also allows the easy derivation of temperatures which, together with the kinematics, gives a clear physical picture of the dense core. NH_3 observations with the Ultrasensitive Array will be particularly efficient because the hyperfine components can be observed simultaneously within a single frequency band. Currently these observations are limited both by sensitivity and narrow bandwidths to a handful of star forming regions. The Ultrasensitive Array will provide unprecedented observations that can track the neutral gas at $\lesssim$ 0.1 km/sec velocity resolution, in hundreds of nearby and more distant star forming regions.

Of course, the real question is the interaction between the gravitational potential and the magnetic pressure at the critical radius where the proto-star first forms; one needs a direct comparison between the neutral and the ionized gas. N_2H^+ (at $\sim$ 80 GHz) shares many of the attractive characteristics of NH_3 (including hyperfine structure). The major difference is that it is ionized, and hence responds directly to the magnetic field. Comparisons of the kinematics of NH_3 as seen by the VLA with ALMA observations of N_2H^+, both at $\sim$ 0.1 km/sec resolution, would thus give direct observational constraints on the magnitude and effectiveness of ambipolar diffusion (Benson, Caselli, & Myers 1998).

Measuring Densities with H_2CO

The extended frequency coverage of the Ultrasensitive Array will allow observations of two important transitions of formaldehyde, the 4(1,3)-4(1,4) line at 48.3 GHz (available now only at reduced sensitivity) and the 3(1,2)-3(1,3) line at 29 GHz. These are observed in a number of dense molecular cloud cores believed to harbor extremely young stars; and they act as extremely useful densitometers. As Mangum noted in his dissertation (1990), these K-doublet transitions have a 'spatial density filter' built into their excitation: for densities below $10^5\,\mathrm{cm}^{-3}$ the formaldehyde lines are in absorption for $J \leq 4$, while for higher densities all are in emission. At $J \geq 5$, all lines will always be in emission for reasonable temperatures. Thus an observation of the J=4 line, for instance, gives an immediate indication of the local density, with no complicated modeling required (*e.g.*, Mangum & Wootten 1993). Furthermore, the K-doublet lines have intrinsically lower optical depths than the millimeter and submillimeter lines, and hence allow the astronomer to explore deeper into the core of a star-forming molecular cloud. As a final benefit, formaldehyde is less susceptible than many other molecules (notably ammonia) to abundance peculiarities which can render interpretation difficult. Formaldehyde observations at a few 10s of GHz will provide astronomers with an excellent densitometer, free from the complex cloud-envelope effects that plague the interpretation of formaldehyde lines at lower frequencies.

The Formation of Massive Stars

Although great advances have been made in establishing the paradigm of low-mass star formation, the formation of more massive stars remains poorly understood. In particular, for stars above $20\,M_\odot$, the radiation pressure on dust grains is strong enough to prevent further accretion. Several models have been proposed to circumvent this, *e.g.* coalescence of existing proto-stars and accretion through very massive disks (Stahler, Palla, & Ho 2000). The Ultrasensitive Array will make a fundamental contribution to these studies, by allowing simultaneous multi-transition ammonia studies of the hot, dense cores which are the suspected sites of massive star formation. The ammonia molecule is an ideal tracer of temperature gradients from 20 to several hundred Kelvins; since the hyperfine transitions involved all occur at about the same frequency, they can be observed simultaneously and with almost identical angular resolutions, avoiding major sources of systematic error. In combination with ALMA and SIRTF studies of the heated dust at various physical scales, such observations will provide a detailed picture of the distribution, density, and temperature of the gas and dust and of the location and luminosity of the embedded heating sources. The goal is to learn the amount and kinematics of the material, measuring the velocity dispersion among the clumps, and showing whether there are indeed very massive disks around these stars.

Phase-referenced Imaging at High Frequencies

Most, if not all, young stellar objects (YSOs), both high- and low-mass, go through a phase where conditions are conducive to the formation of water masers. These masers have very high brightness temperatures, and thus are excellent probes of the kinematics and dynamics of the gas near the central objects. The rest frequency of the maser line is 22.235 GHz. At this frequency the troposphere of the Earth (also due to this water line) has quite variable opacity, which introduces rapid interferometric phase variations which are difficult to calibrate out. At nearby frequencies (23–24 GHz) there are also several transitions of the ammonia molecule (see above), which are often too weak to detect in the presence of these phase variations; similarly the broad-band continuum here is often smeared out by residual phase errors. With the large bandwidths and simultaneous excellent spectral resolution of the Ultrasensitive Array's correlator, the water masers and several ammonia transitions can be imaged simultaneously. The masers, a collection of point sources, can be used to measure the tropospheric phase, and these measurements can then be used to provide nearly perfect phase calibration for both the ammonia lines and the continuum emission. Apart from excellent images of all three components, the ammonia and continuum positions would be automatically referenced to the masers, giving excellent (easily milliarcsecond) relative astrometry. Measuring several transitions of the ammonia molecule provides an excellent thermometer for the emitting ($\sim 10^5\,\mathrm{cm}^{-3}$) gas, as well as giving kinematic information which can be directly compared to the water masers from much denser ($\sim 10^9\,\mathrm{cm}^{-3}$) gas.

In a similar vein, the Ultrasensitive Array will permit the simultaneous measurement of the sizes, relative positions, and temperatures of the radio photospheres of asymptotic giant branch (AGB) stars. Many of these stars have thick circumstellar envelopes with molecular masers (OH [1.7 GHz], H_2O [22 GHz], and SiO [43 GHz]). Using the strong masers as phase reference sources, continuum observations at nearby frequencies can be made with essentially perfect phase calibration. Absolute positions of the radio photospheres can then be determined since the absolute positions of the masers are readily measured. In addition the excitation and kinematics of the masers can be refined based on the relative position of the star.

3.2.4 The Galactic Center

Sgr A^* is the closest example of a super-massive black hole, and offers unique opportunities to study the interaction between such a massive compact object and its environment. The Ultrasensitive Array will lead to substantial progress in two areas of particular interest, the dynamics (through observations of the three-dimensional motions of ionized gas and masers) and the gas accretion rate (by measuring stellar outflows and ionized gas masses and motions).

Three-Dimensional Gas Dynamics

Recent infrared studies of stellar proper motions within the central 0.25pc (Eckart & Genzel 1997; Ghez *et al.* 1998) have shown that the stars are moving with large velocities, up to 1400 km/s, implying a mass for the central object of $2.6 \times 10^6\,M_\odot$. Proper motions have recently been reported for the ionized gas as well (Roberts, Yusef-Zadeh, & Goss 1996; Yusef-Zadeh, Wardle, & Parastaran 1997; Zhao & Goss 1998), using VLA observations of free-free emission to measure motions of up to 30 mas/year (1200 km/s) (Figure 3.16). While the bulk motion of the gas is consistent with the gravitational influence of the black hole, the motions of individual features imply in addition hydrodynamic accelerations, presumably from stellar winds, outflows, or explosive events. These data further suggest that the orbiting ionized gas clouds lose angular momentum and accrete onto the central black hole, with some evidence even of tidal disruption.

Although these initial studies are intriguing, they are limited (by sensitivity) to measuring relatively large proper motions of only the brighter regions. The area within a few tenths of a parsec of Sgr A* is full of long, narrow (< 0.1 arcsec) filaments as well as H II regions; the Ultrasensitive Array's enormous increase in sensitivity will allow proper motion studies of all of these sources. The best measurements so far give proper motions for about a dozen sources with error bars between 35 and 180 km/s over an eight year baseline, depending on signal-to-noise ratio. With a factor ~ 30 increase in sensitivity, and working at 45 rather than 22 GHz, one can do a factor ~ 8 better in a single year, raising the possibility of measuring accelerations (on 10-year time-scales) as well as simple velocities. The number of targets will go up by a similar factor.

In addition to the motions in the plane of the sky, radio observations can probe the line-of-sight velocities through radio recombination lines. Here the wide bandwidths and high spectral resolution of the Ultrasensitive Array help in a different way, by allowing the observer to 'stack' multiple lines in a single observation (up to 17 in the 1.5 GHz band), while retaining sufficient velocity resolution to measure interesting Doppler shifts.

The same characteristics will make the Ultrasensitive Array the perfect instrument for stellar OH, H_2O, and SiO maser searches and proper motion/velocity studies. While the gas dynamics probes hydrodynamical and gravitational effects in local regions like the central parsec, the stellar dynamics are set by the Galactic mass distribution on scales out to hundreds of parsecs. Currently one has to use wide-band single dish telescopes to find roughly where a maser is, then 'zoom in' on the appropriate velocity with the VLA for a good position/proper motion measurement. Apart from being tedious and expensive in observing time, single dishes are not nearly as sensitive as the VLA (both intrinsically, and due to ubiquitous absorption lines), and are undoubtedly missing many useful dynamical probes. Since the primary beams of the single dishes are much smaller than that of the VLA, those searches also tend to be biased towards 'expected' position/velocity pairings, which may lead to systematic errors in their interpretation.

In sum, with proper motions and radial velocities for 'unattached' ionized gas, H II regions, and masers associated with stars, the Ultrasensitive Array will provide a fully three-dimensional movie of gaseous and stellar motions around the nearest super-massive black hole.

Feeding the Monster

So far we have concentrated on the ionized gas as a probe of the gravitational potential, and of hydrodynamical effects; but the gas is also interesting in its own right. The mass loss from the young massive stars in the central 0.1pc has been suggested as one of the major sources of fuel for the central black hole. Radio observations can determine the stellar mass loss rates directly, as well as tracking the gas as it falls towards the black hole. These winds are also expected to arise from the large number of OB supergiants and WR-type stars which reside in the three dense stellar clusters located within the central 30 pc: (1) the Central cluster (within 0.1 pc of SgrA*), (2) the Quintuplet cluster, and (3) the Arches cluster, itself known to have more than 100 OB supergiants. Radio continuum emission from at least two stellar wind sources (IRS 7 and IRS 13) with mass loss rates of $\sim 10^{-4}\,M_\odot$/yr, together with a proper motion of 30 mas/yr for one of them (IRS13), have already been detected using the VLA (Yusef-Zadeh, Roberts, & Biretta 1998). With 30 times the sensitivity, the Ultrasensitive Array will detect mass loss rates as low as $\sim 10^{-6}\,M_\odot$/yr, giving a much more complete picture of mass loss in the very central regions of the Galaxy. The same observations will allow similar advances in the study of very compact H II regions and continuum emission from OH/IR stars. The result will be the most complete picture yet of the star formation environment in the central Galaxy.

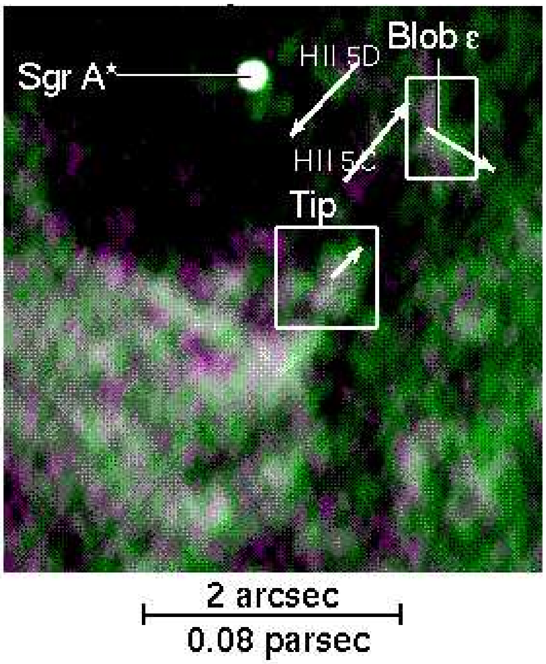

Figure 3.16: 22 GHz VLA proper motion measurements for the ionized gas near Sgr A* (courtesy J.H. Zhao 1999), as determined from cross-correlation of data taken between 1991 and 1998. The proper motion vectors are on a relative scale with the value for HII 5c= 1160 km/sec (31 mas/year).

3.2.5 Nearby Starburst Galaxies

The dense, central regions of starburst galaxies are almost by definition heavily enshrouded in dust, with $A_V \gtrsim 20$ not unusual. In such cases optical and even infrared imaging may give more insight into the topology of the dust than into the star formation process itself (*e.g.*, Sams *et al.* 1994). In these circumstances radio observations offer a unique dust-free window into the center of the star formation region. Radio continuum images of the nearest starburst galaxies reveal substantial numbers of compact radio sources, a mixture of supernova remnants (SNRs) and H II regions (*e.g.*, Ulvestad & Antonucci 1997), giving two independent determinations of the star-formation rate, as well as some indications as to the physical conditions in these unusually active regions. Radio recombination lines are also detected from a number of starburst galaxies (*e.g.*, Zhao *et al.* 1997), giving direct constraints on the number, size, and electron densities of the H II regions, as well as providing an unextincted dynamical probe of the central region. Finally, observations of more distant ultraluminous infrared galaxies (*e.g.*, Condon *et al.* 1991) have shown that many of these systems are optically thick even up to 8.4 GHz, requiring enormous emission measures, and suggesting that the central parts of these galaxies may best be thought of as hot, dense H II regions hundreds of parsecs across. Both continuum and line observations are now just at the limit of what is possible; the Ultrasensitive Array will realize the promise of these early detections, by providing (i) the sheer sensitivity needed to extend current samples; (ii) the frequency coverage and spatial resolution necessary to differentiate SNRs from H II regions, and to see into the optically-thick ULIRGs; and (iii) the bandwidths essential to covering the entirety of the $\sim 1000\,\mathrm{km/sec}$-broad radio recombination lines.

Continuum Observations

The interpretation of radio continuum observations of starburst galaxies rests primarily on spectral imaging, which alone allows one to differentiate between synchrotron emission from relativistic cosmic ray electrons, and optically-thick and optically-thin thermal emission from ionized gas. Knowing which is which, one can count SNRs and watch them decay, estimate the temperatures and emission measures ($\int n_e^2\, dl$) of H II regions, and generally gain a better understanding of the star-formation rate, the initial mass function, and the basic conditions of the interstellar medium out of which those stars are formed. Current VLA observations are hobbled by an inability to image the sources at multiple frequencies with sufficient sensivitity and resolution to undertake this decomposition cleanly.

For example, in NGC 253, one of the most nearby starbursts ($\sim 3\,\mathrm{Mpc}$), a very detailed study at 3 pc resolution gave accurate spectral indices (errors less than 0.2) for only 15 of the 50 or more known sources (Ulvestad & Antonucci 1997). The Ultrasensitive Array will allow pc-scale imaging of all the known sources (and presumably many more besides) from 15 to 50 GHz, cleanly separating the SNRs from the H II regions, mapping the spectral index (and possibly determining polarization fractions and rotation measures) across the individual SNRs, and determining directly both the brightness temperature and the turnover frequency (and hence the emission measure) of the compact H II regions. Such observations would incidently either detect or give much stricter limits to the decay of the SNRs (the known remnants have flux densities $\gtrsim 400\,\mu\mathrm{Jy}$, 400σ in 12 hours with the Ultrasensitive Array), giving a fairly direct handle on the supernova formation rate. The brightest of these sources could of course be imaged with the VLBA, but there the sensitivity is down by a factor of 30 or more.

Galaxy mergers are another fruitful area for study. The Antennae (NGC 4038/4039) at ~ 21 Mpc is among the nearest and most famous, and both of the galaxies involved are clearly undergoing massive bursts of star formation. Ultraviolet, optical, and infrared observations show a wealth of structures at resolutions of about 0.1 arcsec (10 pc). Once again however radio observations are the key to finding the most massive star clusters, which are probably buried in dust; a number of compact radio sources have already been detected (Neff *et al.*, *in prep.*), but imaging more than a handful would require microJy sensitivities at high frequencies. The Ultrasensitive Array, possibly in conjunction with the Pie Town VLBA antenna, would be ideal for this work, imaging at least 50 star clusters with $\lesssim 10\,\mathrm{pc}$ resolution.

Radio Recombination Lines

Radio recombination lines (RRLs) have been detected in at least 14 starburst galaxies (Phookun, Anantharamaiah, & Goss 1998; Zhao *et al.* 1997), providing unique constraints on the physical conditions of the gas and the gas dynamics on sub-arcsecond scales, at the very heart (few hundred parsecs) of the star formation region. Comparisons between these data and high-resolution observations of dense molecular gas, particularly HCN and HCO^+, will provide an unequalled view of the details of the star formation process in starburst systems. The Ultrasensitive Array is absolutely essential to this work. Currently the radio observations are difficult at best. Detection of a single line at 1 arcsec resolution in the most sensitive VLA band (8.4 GHz) takes 8 hours or more, and yields a spectrum covering only $\sim$ 900 km/sec at $\sim$ 60 km/sec resolution. Many galaxies (*e.g.*, Arp 220) are already known to have much broader lines, and this velocity resolution is clearly inadequate for any detailed dynamical studies. Further, while the detection of a single line does (in conjunction with the continuum measurement) place significant constraints on physical conditions, two or more lines would be vastly better, removing much of the confusion as to filling-factors and source sizes which currently dominate the literature.

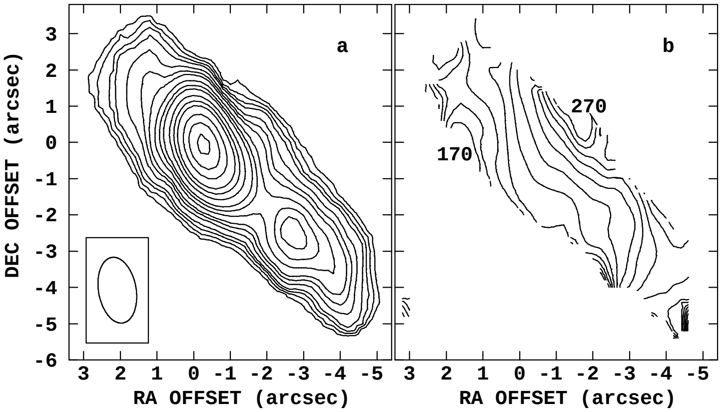

Figure 3.17: The radio recombination line H92α (8.4 GHz) in the central $\sim$ 150 pc nearby starburst galaxy NGC 253 (Anantharamaiah & Goss 1996). The *left* panel shows the integrated line emission; the *right* panel shows the velocity field from 170 to 270 in steps of 10 km/sec. The gas in this inner regions is rotating in a plane perpendicular to the main galactic disk. The Ultrasensitive Array will allow similar measurements at several times higher spatial and spectral resolution.

The Ultrasensitive Array will provide several important advances. With continuous frequency coverage and similar sensitivity from a few to 50 GHz, many more RRLs can be observed, implying much stricter constraints on the emitting material. This is particularly interesting at the high frequencies, since the lines grow stronger with frequency (to a certain point; beyond $\sim$ 50 GHz the lines may begin to mase, complicating the interpretation). A more flexible correlator, and the ability to tune all four IF pairs independently, will allow measuring several lines at once, with more than enough line-free channels and excellent (better than 10 km/sec) velocity resolution. Perhaps even more importantly, since even the broadest bandwidths will give a few hundred km/sec velocity resolution, the new correlator will allow searches for RRLs in *every* deep continuum observation;

and simultaneously provide multiple lines to check any putative detection. Since most RRLs are now just at the limit of detectability, the Ultrasensitive Array will almost undoubtedly lead to a vast increase in the number of known lines, and an equally impressive qualitative improvement in the science which can be done with them.

3.2.6 High Column Density QSO Absorption Line Systems

With the high spectral resolution over wide bandwidths provided by the Ultrasensitive Array, the VLA will for the first time be able to conduct unbiased spectral line surveys over a large range of redshifts. In this section we describe two possible surveys which together would determine the redshift evolution of the cosmic neutral baryon density from z=0 to 3, without the uncertainties due to dust obscuration inherent in optical studies.

Dust obscuration prevents optical studies of QSO absorption line systems from seeing the highest column density systems: $N(\mathrm{H\,I} + \mathrm{H_2}) \geq 10^{22}$ cm^{-2} corresponds to $A_v \geq 6$, assuming a Galactic dust-to-gas ratio. These high column density systems are thought to contain most of the neutral baryonic matter in the universe, and are the best tracers of the dense, (pre-) star-forming interstellar medium (ISM) in nascent galaxies. Radio telescopes are well suited to observing such systems, both in the H I 21cm line and in many molecular line transitions, thereby providing very detailed physical probes of the absorbing material. The major difficulty in studying these high column density absorption line systems is finding them, since optical selection is no longer applicable. To date, only four redshifted molecular absorption line systems are known, all seen toward 'red quasars', meaning flat spectrum radio sources with faint, or absent, optical counterparts (for references, see Carilli *et al.* 1999). The Ultrasensitive Array will be ideal both for finding and for studying these systems, due to the combination of excellent sensitivity, very wide field-of-view (45 arcmin at 1 GHz), high spectral resolution, and broad bandwidth.

Detecting H I 21cm and molecular absorption in and towards high-redshift galaxies opens up many new windows on the detailed physics of the dense ISM in high-redshift galaxies, including:

- Determining the redshift distribution of high column density absorption line systems (*i.e.*, 'damped Lyα systems'), and hence the evolution of the cosmic density of neutral baryonic material, without uncertainties due to dust obscuration.
- High resolution imaging of the cloud structure and dynamics on scales ranging from parsecs to kpc, including (i) imaging the circumnuclear gas in active galactic nuclei, (ii) imaging the gas in star forming disks in ultra-luminous infrared galaxies, and (iii) imaging the ISM and large-scale dynamics of gas in 'normal' galaxies at high z.
- Determining the evolution of the cosmic microwave background temperature by measuring the excitation temperature of the molecular gas (Wiklind & Combes 1996).
- Studying astrochemistry at high redshift, including: (i) determining the water and molecular oxygen abundances (these molecules cannot be studied in our own Galaxy with ground-based observations due to atmospheric absorption lines), and (ii) studying the evolution of the deuterium abundance in the molecular ISM.
- Determining the evolution of basic physical constants, such as the fine structure constant and the nucleon mass (Drinkwater *et al.* 1998).

- In the case of absorption by gravitational lenses, determining the dynamical mass of the lensing galaxy, hence providing a fundamental check on gravitational lens theory (Chengalur & de Bruyn 1999).

The Ultrasensitive Array will play a dominant role in such studies, due to its high sensitivity, high resolution, and wide field of view, and the natural interference rejection afforded by an interferometer.

Redshifted Molecular Absorption

Searches for molecular absorption line systems are impossible with the current VLA due to the correlator and the limited bandwidth: the VLA at the moment is limited to a 50 MHz bandwidth at 43 GHz with 8 spectral channels, implying a total velocity range covered of only 300 km/sec. The new VLA correlator will allow searches for molecular absorption line systems over a large range in redshift toward faint, flat spectrum radio sources. As an example, the Ultrasensitive Array could survey the frequency range 26 to 50 GHz with a velocity resolution of 50 km/sec to a noise level of 0.05 mJy/channel in under 24 hrs. This corresponds to the 5σ detection of 10% absorption towards 2.5 mJy sources, of which there are $\sim$ 7 per square degree. Possible lines include the first-order transition of CO at redshifts between 1.3 and 3.4, and HCN and HCO^+ at redshifts between 0.7 and 2.3.

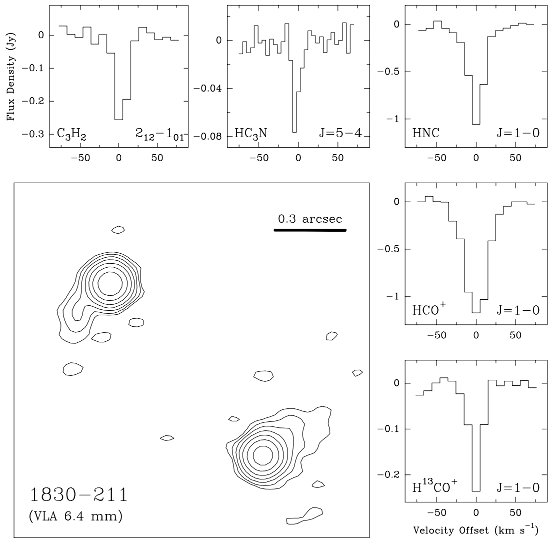

Figure 3.18: The contour plot shows an image of the 'Einstein ring' radio source PKS 1830-211 at 43 GHz with a resolution of 0.1″ made with the Very Large Array. The source redshift is 2.507. The spectra show molecular absorption by gas in the lensing galaxy, as observed with the Very Large Array toward the southwest radio component. Zero velocity corresponds to a heliocentric redshift of 0.88582 (Carilli, Menten, & Moore 1999).

Redshifted H I 21cm Absorption

Another, complementary experiment would be a search for H I 21cm absorption line systems toward high-redshift radio-loud quasars and radio galaxies. Ideally one would use a prime focus system (here proposed for design and development) to search in the redshift range 0 to 0.8; even with the new Cassegrain system one could observe from z=0 to 0.4. This could be done toward known high-redshift radio sources. However, the new VLA correlator allows the interesting possibility of blind surveys over a large area and redshift range. In 200 hours, the Ultrasensitive Array could survey the redshift range 0 to 0.4 (or 0.8 with a prime focus system) to a 4% optical depth limit (1σ) toward 1.5 mJy background continuum sources at 30 km/sec velocity resolution, corresponding to an $N(\mathrm{H\,I})$ limit of 2×10^{20} cm^{-2} assuming a spin temperature of 100 K. Source counts imply about 55 background radio sources with flux densities of 1.5 mJy or more at 1 GHz in a VLA primary beam (45 arcmin FWHM), most of which will be at z$\geq$0.5. Ultraviolet studies with HST indicate about one high column density absorption system ($N \geq 10^{21}$ cm^{-2}) per unit redshift in this range. Hence we expect at least 43 systems to be detected at $\geq 5\sigma$ in such a survey. Note that this is a *lower limit* to the number of expected systems, due to the dust bias inherent in optical studies. Moreover, given that all the sources surveyed are within 45 arcmin of each other, these data could also be used to study large-scale structure in the universe by studying the correlation between absorption systems as a function of redshift and source angular separation. After phase two of the VLA Expansion Project, the 0.1 arcsec resolution of the A+ configuration will also allow detailed imaging of any detected gas toward the (typically) extended background continuum radio source.

3.3 The Transient Universe

Radio telescopes are in many ways ideal for observations of transient (highly-variable) sources. Observations at centimeter wavelengths are naturally sensitive to non-thermal processes and relativistic particles, and hence to jets, shocks, and particle acceleration associated with transient phenomena and compact sources. Since they can observe over many decades in frequency, radio instruments can characterize both absorption and emission processes in exquisite detail, both at a given epoch and as a function of time. A radio telescope can also observe the entire sky visible from its location, day or night, 365 days a year, providing accurate and consistent flux densities and astrometry; this allows uniform observations of variability and proper motions, on time scales from milliseconds (*e.g.*, pulsars) to decades (*e.g.*, H II regions and supernova remnants). The VLA in particular has provided multi-frequency radio light curves of such diverse sources as solar flares, novae, and gamma-ray bursts, and monitored the expansion of supernova remnants and extragalactic jets; these data have been used to derive sizes, distances, velocities, and magnetic field strengths, as well as the mass and clumpiness of both ejecta and surrounding gas. Almost every important variable source found at other wavelengths has been observed with the VLA, from X-ray transients to optical novae to gamma-ray bursts.

The Ultrasensitive Array will provide even more impressive capabilities. The enhanced *instantaneous* sensitivity is particularly important, because long integrations are generally not an option for variable sources. With improved sensitivity, detailed observations can be made of more typical and more distant objects; these larger samples will yield a much better determination of the luminosity function, particularly important for transient sources as they often differ enormously from event to event. For individual sources, going fainter means observing both earlier (while the source is still optically thick) and longer (as the flux density fades): the former gives important information on particle acceleration and the absorbing material, while the latter connects the initial event to its environment (through deceleration, growing instabilities, or simply abrupt changes in flux signaling sudden changes in a shock front). The enhanced sensitivity also allows observations over a wider range of frequencies, important again for absorption, but also for resolution – the Ultrasensitive Array will be able to detect at 45 GHz any source bright enough to be seen now by the VLA at any frequency, giving spatial resolutions as high as 50 mas. Multi-frequency synthesis will also allow better imaging in the limited time which can be allocated at the last minute, as well as opening the possibility of producing high-fidelity images using only a subarray of the full VLA (which may make scheduling much easier). Continuous frequency coverage from 1 to 50 GHz will allow one to 'zoom in' on the right frequency for any particular phenomenon (*e.g.*, refractive scintillation), while the availability of high spectral resolution over wide bands will allow line searches 'for free' towards any transient event, giving instant H I kinematic distances within the Galaxy, permitting extragalactic sources to be used as wide-band absorption line probes, and providing limits on radio recombination lines towards thermal sources like novae. Finally, an observational point which may be the most important of all, the shift to dynamic scheduling, coupled with the enormous increase in sensitivity (which makes even very short observations useful), will lead to much faster reaction times and much more detailed light curves. Currently, unless one is incredibly lucky (the transient is found during business hours, both the local scheduler and the first observer contacted are available and willing, and act quickly and decisively), there is an inevitable delay of at least a day, and often a week, in getting onto the source. Since the initial rise is often critical to the interpretation (*e.g.*, was the source beamed?), and since some sources at least turn on and decay very rapidly (*e.g.*, the prompt radio emission from SN 1987A, and the optical outburst of GRB 990123), this delay means the loss of important and irreplaceable information.

The rest of this section enlarges on these themes, as applied to a few specific types of transient sources; but the key point is that the Ultrasensitive Array will mark a major advance in the study of *all* such sources, from local scattering events to the most energetic explosions in the universe.

3.3.1 Coronal Heating

One of the fundamental questions in solar physics is how the solar corona maintains its high temperature of several million Kelvin above a surface with a temperature of 6000 K. The power needed to maintain the corona above an active region against radiation and conduction losses is $> 10^{28}$ erg s^{-1}. The leading theories for coronal heating involve either some form of resonant wave heating or a superposition of many tiny flare-like events ("nanoflares").

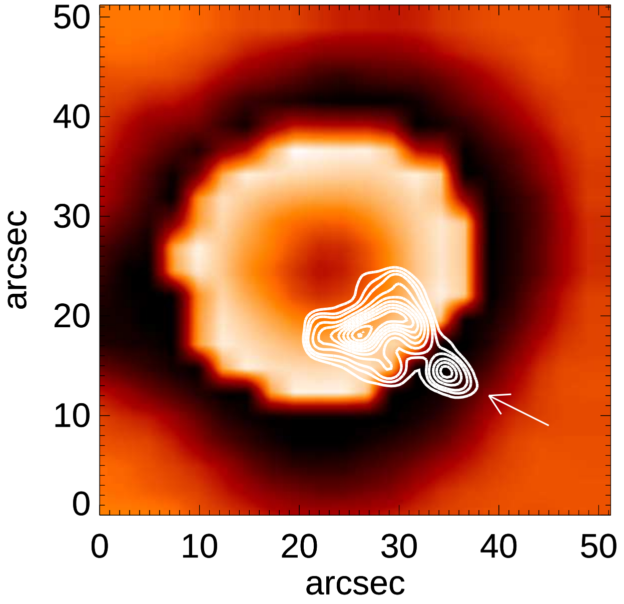

Figure 3.19: Example of radio emission from a transient microwave brightening (Gopalswamy *et al.* 1994). The contours represent 15 GHz emission observed by the VLA. The greyscale shows the umbra of a sunspot seen in white light. The total energy liberated by the event was $\sim 10^{24}$ ergs.

Wave Heating

Wave heating models make specific predictions of where and on what time scales energy deposition occurs in coronal magnetic loops. The Ultrasensitive Array will provide a detailed history of the temperature, density, and magnetic field in coronal loops in active regions, from which the rate of energy deposition can be calculated as a function of position and time.

Nanoflares

The role of "nanoflares" – tiny, flare-like releases of energy from small magnetic reconnection events – depends critically on the rate at which they occur. Numerous studies have shown that X-ray events ranging over as much as five orders of magnitude in energy, from 10^{27} to 10^{32} erg, form a single power-law with slope 1.5–1.6. Smaller events cannot be energetically significant relative to the larger events unless the rate distribution at lower energies becomes significantly steeper.

Microwave observations are the *only* means available for probing these tiny energy release events. Even events near the limit of visibility for the Yohkoh Soft X-Ray Telescope (SXT) are easily detectable in total power by small non-imaging radio telescopes. Interferometric observations are vastly more sensitive, as demonstrated by VLA detections of events over the penumbra of a large sunspot (Figure 3.19) which are two orders of magnitude weaker in energy content than those detected in soft X-rays: the inferred energy release rates are as low as 3×10^{22} erg/sec, and total energies are not much above Parker's canonical nanoflare value of 10^{24} ergs. Recently observations using multi-band VLA and SoHO[2] EIT[3] and MDI[4] data have show that even tiny transient events in the quiet chromospheric network are, in fact, flare-like (Figure 3.20). Attempts to characterize the distribution function of these small events have so far given mixed results. The Ultrasensitive Array will significantly improve on the state-of-the-art by wide, continuous frequency coverage with vastly improved continuum sensitivity. The resulting observations will extend and quantify the flare/microflare/nanoflare distribution function at the smallest energies, and show definitively whether nanoflares heat the solar corona.

3.3.2 Radio Stars

Prior to the VLA's completion, only a few stars were confirmed radio sources, and those comprised an oddball collection of extreme objects. Thanks primarily to its great sensitivity, the VLA has completely revolutionized the field of stellar radio astronomy, with detections across almost the whole Hertzsprung-Russell diagram, and the opening of entire new fields of research (see Figure 3.21). The Ultrasensitive Array will permit similarly impressive advances in this field, including the study of time variability in sources which can now barely be detected, and the characterization of the radio properties of stars over a much wider range of stellar activity. One major milestone will be the detection for the first time of solar-level activity on other stars.

Solar Analogs & Ordinary Stars

The stars detected as radio sources so far are all very luminous compared to the Sun; these are the same active stars which show strong variability activity at other wavelengths, notably in optical flaring and in X–rays. This gap between solar and stellar activity makes it difficult to fit the Sun into the general picture of stellar radio emission – we do not for instance know whether the Sun is a typical G star in its magnetic field strength and flaring activity, nor do we have any information on changes in the solar radio emission on timescales longer than the historical record. The Ultrasensitive Array will make a fundamental contribution, by detecting for the first time other stars with radio emission as weak as the Sun, and more generally by investigating the radio properties of *ordinary* stars, not just the very active minority we can currently study. For example,

---

[2] Solar and Heliospheric Observatory

[3] Extreme-Ultraviolet Imaging Telescope

[4] Michelson Doppler Imager

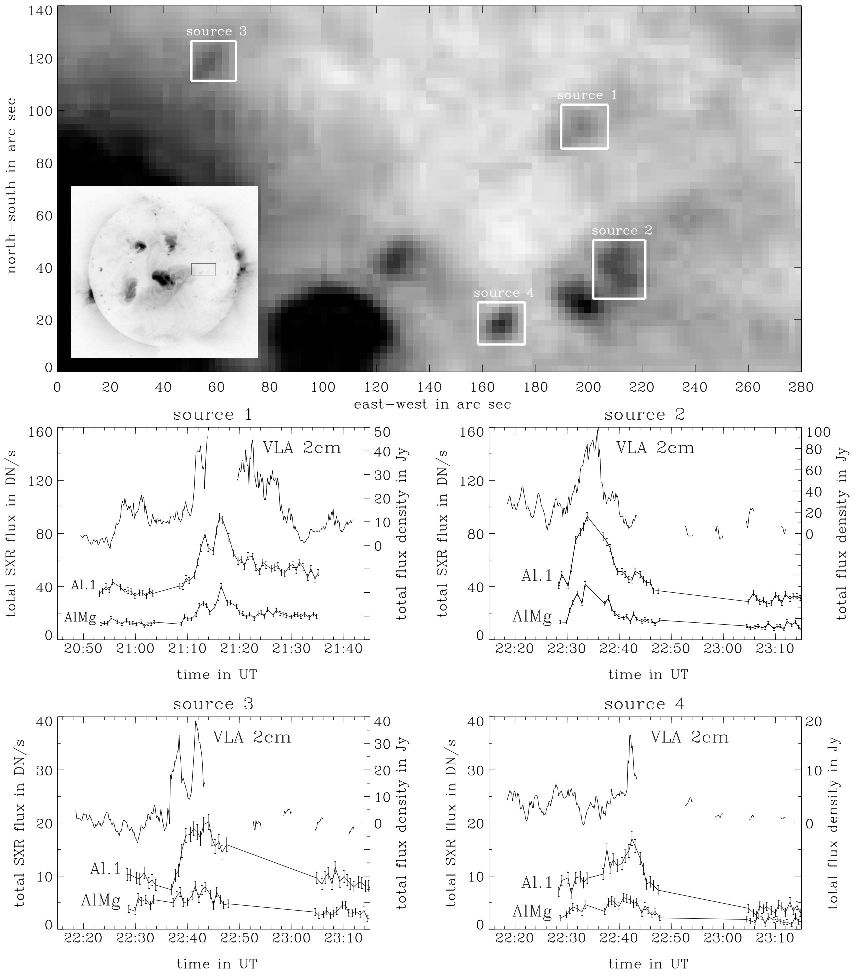

Figure 3.20: Temporal evolution of network flares observed in soft X-ray (SXR) and radio emission on 20 Feb 1995 (Krucker *et al.* 1997). The image at the top shows the region observed in SXRs; the inset shows its location on the solar disk. Enhanced emission is dark. The locations of network flares are indicated by boxes. The plots below show the temporal variations of the SXR flux in the Al.1 and AlMg filters, and the 2 cm radio emission for the different network flares.

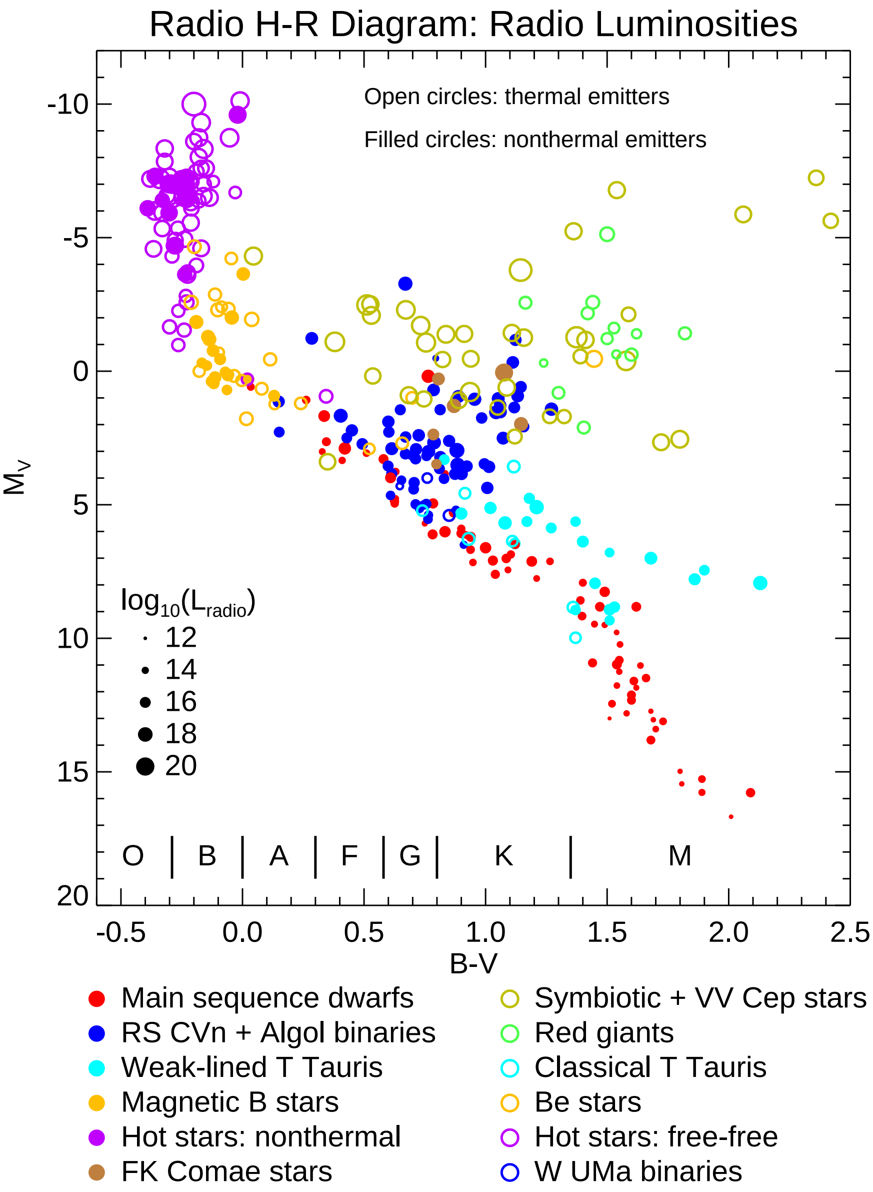

Figure 3.21: An HR diagram for stars detected as radio emitters. For hot stars corrections for extinction have been applied where available. The size of the symbol reflects the radio luminosity of the star as labelled (in ergs s^{-1} Hz^{-1}). The Sun's radio luminosity is of order 10^{11} ergs s^{-1} Hz^{-1} at 8 GHz. The diagram is restricted to stars for which distances are available, and therefore is an incomplete but reasonably representative sample of all the stars detected by the VLA. Stars believed to be nonthermal emitters are represented by filled symbols, while thermal emitters are shown by open symbols.

of the several thousand stars within 25 parsec of the Sun, only about 100 have been detected by the VLA – the Ultrasensitive Array should detect almost all of them.

Young Stars

The VLA has shown that stars $\sim 10^6$ years old tend to be very luminous radio sources, detecting them as far away as the Orion nebula at 500 pc; but by 10^7 years, they have faded enormously. Currently there are too few detections (tens of stars at $\sim 10^6$ years, none at $\sim 10^7$) to understand the cause of this abrupt decline: we need to correlate luminosity levels with other stellar parameters such as rotation rate and age in order to understand what generates the radio activity. Only the factor-10 improvement in sensitivity provided by the Ultrasensitive Array will give us the required sample of older stars.

Interday Variability in Cool Stars

The radio variability of cool stars on timescales of days is analogous to the Sun's slowly–varying emission, which results jointly from intrinsic changes in active regions on the surface, and from the rotation of those regions on and off the visible hemisphere. Nonthermal emission from electrons accelerated in the atmospheres of very active stars is detected, but the thermal emission from hot gas in strong magnetic fields, which is how the Sun's slowly–varying emission is produced, is just below detectability. Observations of this form of emission (its spectral and polarization behaviour and time variability) can be used to infer the magnetic structure of the stellar atmospheres, which is crucial for our understanding of the solar–stellar connection. The Ultrasensitive Array will make it possible to detect this emission on hundreds of nearby stars.

Radio Flares in Pre-Main-Sequence Stars

The VLA has detected radio flares from 50–100 pre-main-sequence stars in the Taurus, Ophiuchus, Chameleon and Orion molecular clouds, but typically at flux levels of order 1 mJy, making polarization and variability studies very difficult. The Ultrasensitive Array will detect many more, perhaps thousands of these stars, and permit detailed studies of their radio properties. This is particularly exciting because the role of magnetic fields in these very young stars is at best poorly understood; we do not know whether their activity arises from the same process as occurs in the Sun (a stellar dynamo at the base of the convection zone), or whether an entirely distinct physical mechanism is operating. Many of these stars are believed to be fully convective, in which case the generation of magnetic fields in the stellar interior may take on a completely different form.

Physical Processes in Stellar Atmospheres

The large instantaneous bandwidths and broadband spectral processing capabilities of the Ultrasensitive Array will allow the first detailed spectroscopic observations of coherent bursts in dMe and RS CVn stars. The basic properties are clear – highly circularly polarized coherent radiation, a rich variety of structure in both time and frequency, brightness temperatures which can exceed 10^{16} K – but the basic emission mechanisms have not yet been identified. Early radio observations of the Sun identified the role of particle beams and of shocks in the solar corona; more detailed observations of these coherent radio bursts on other stars may similarly open up completely new areas of astrophysical research. The extremely high brightness temperatures of certain coherent bursts may also drive phenomena which are impossible to study in other astrophysical objects, *e.g.*, stimulated Compton or Raman scattering.

3.3.3 Galactic Novae: Light Curves, Masses, and 3D Imaging

Galactic novae are the closest natural thermonuclear explosions to the Sun. Some tens of times each year a white dwarf in a binary star system in the Galaxy accumulates enough matter on its electron-degenerate surface to ignite a thermonuclear runaway explosion; the resulting blast produces substantial radio, infrared, optical, and ultraviolet radiation, which, unless obscured by dust, can be visible for weeks or months. The Ultrasensitive Array will provide excellent radio light curves and images of every nova found in the Galaxy, measuring shell masses, showing directly the varying physical conditions within the shell, and (through radio recombination lines) measuring the kinematics throughout the source as well.

Radio emissions are uniquely valuable in providing a direct look at the entirety of the ejected mass; optical lines by contrast pick out regions of specific densities or temperatures. The potential of radio observations is best illustrated by the two novae which have been imaged in some detail at radio wavelengths, Nova QU Vul 1984 (Taylor *et al.* 1988) and V1974 Cyg 1992 (Pavelin *et al.* 1993; Hjellming 1996a,b). Both confirmed the tentative conclusion from radio light curve fitting: nova explosions eject five to ten times more mass ($4.8 \times 10^{-4}\,M_\odot$ for QU Vul, $3.1 \times 10^{-4}\,M_\odot$ for V1974 Cyg) than predicted by theoretical models of the explosion process. By contrast, optical mass estimates are typically a factor 10 lower but are derived mainly from spectral line observations that measure the mass only of the inner regions. The radio results imply either that white dwarfs are significantly more massive than usually supposed, or that the explosion models themselves are wrong. This is a severe problem, because most known biases (*e.g.* unmodeled opacities) work in the opposite sense, and because the physics is believed to be simple enough that there is little room for more fundamental disagreements.

Apart from simple mass estimates, sequences of radio images can show directly the *three-dimensional* distribution of both temperature and density within the source: the decreasing optical depth effectively 'peels the onion,' allowing one to see deeper and deeper into the source. The imaging sequence of V1974 Cyg (Figure 3.22), for instance, revealed high temperatures (10^5 K) in the nova shell even 80–100 days after the outburst. The images also show clear morphological changes as the emission becomes optically thin, revealing the distribution of the gas as a clumpy ellipsoid with a 90-degree change in orientation between the outer and inner shell. Rather surprisingly, a detailed fit to these images also reproduces the shapes of the optical lines quite well (Hjellming 1996a,b).

The combination of detailed, multi-frequency radio light curves and radio imaging covering both the optically thick and optically thin stages thus provides an excellent observational probe of the *entire* gaseous content of ejected nova shells. The source elongation, shell thickness, and ejecta clumpiness derived from these images can then be combined with ultraviolet, infrared, and optical data to yield very detailed and amazingly accurate models. The Ultrasensitive Array will make these observations routine, as well as adding important new capabilities. For the first time, we will

- *detect and follow the light curves of not just a few, but all novae that are found in our Galaxy.* The brightest novae are some 10s of mJy at a few kpc; even the most distant and faintest will therefore peak at some 10s of microJy, easily detectable in an hour with the post-expansion VLA. Detailed radio light curves can be used to derive good estimates of the shell velocity and total shell mass, but these data exist so far for only nine sources. The Ultrasensitive Array would provide multi-frequency monitoring of even the faintest sources (potentially several every year) over their entire lifetimes, from the faint radio rise to the optically-thin decay.

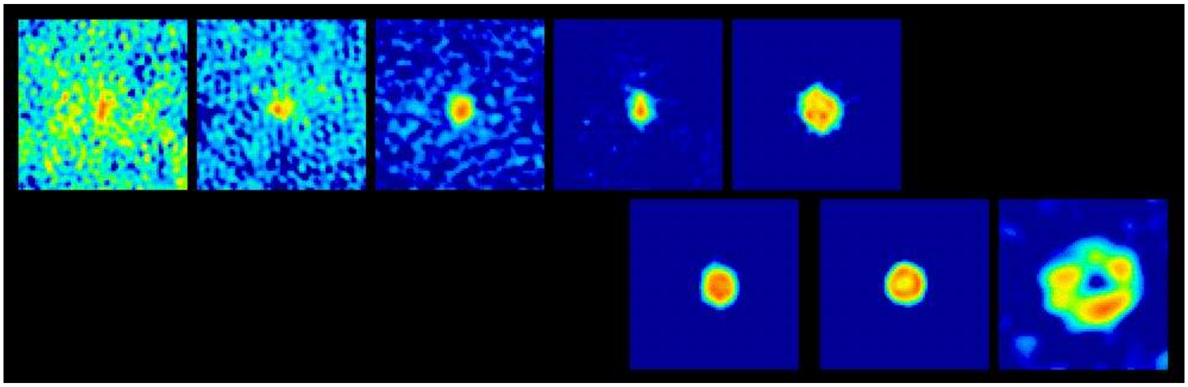

Figure 3.22: Merlin (*upper*) and VLA (*lower*) images of Nova V1974 Cyg 1992 (Pavelin *et al.* 1993; Hjellming 1996a,b). The 5 GHz Merlin data were taken 81, 106, 155, 173, and 271 days after outburst; the 22.5 GHz VLA data were taken 255, 313, and 769 days after outburst. Note the evolution from a centered-filled source highly elongated north-south, to a shell slightly elongated east-west. This corresponds to the change from optically thick to optically thin emission, with the later images 'peeling away' the outer skin to reveal the three-dimensional structure.

- *resolve and image most nova shells to determine brightness temperatures, temperatures during optically thick phases, and the evolution of both radial and clumping mass distributions.* The inner and outer velocities of nova shells range from 500 to 5,000 km/sec, with 1000–3000 being most common. The angular size is therefore

  $$\theta = 210\,\mathrm{mas} \cdot \frac{v}{1000\ \mathrm{km/sec}} \cdot \frac{t_{\mathrm{year}}}{d_{\mathrm{kpc}}} \tag{3.1}$$

  By providing excellent sensitivity at 33 and 45 GHz, the Ultrasensitive Array will produce excellent images at $\sim$ 50 mas resolution, resolving novae from a few months to many years after the outburst. The A+ configuration would give a factor 9 higher resolution at these frequencies, resolving the sources within a few *days* of the explosion; the longer baselines would also allow high-resolution observations over a significant range of frequencies, giving direct spectral index maps.

- *measure the velocity profiles of radio recombination lines in some cases, allowing fits to the 3-D spatial and clumping distribution of the gas.* This cannot be done with the current VLA, because the lines are both very weak (a few μJy) and very broad (1000s of km/sec); only the broad bandwidths and excellent high-frequency sensitivity of the Ultrasensitive Array will make these observations possible. Because the line-to-continuum ratio rises as $\nu^{1.1}$, while the linewidths (in MHz) increase as ν, 33 and 45 GHz are the optimal observing frequencies. Assuming a 2000 km/sec line, one could achieve 5σ detections in 40 km/sec channels in 12 hours, even for 10 mJy sources. In brighter novae the VLA will be able to image the clumps and structure directly in three dimensions, with no strong density or temperature selection of the regions being detected.

- *address the major mismatch between the observed shell masses and those predicted from* *current theoretical modeling.* With only a handful of novae imaged at the moment, and those the brightest, best-studied, and hence known to be the most unusual, it is not clear whether this disagreement is fundamental or idiosyncratic. The observation of more and more typical novae will pin this down, and possibly aid the interpretation by suggesting links between the severity of the shortfall and other physical parameters.

Recurrent Novae

The rarer class of recurrent novae occur in binary systems with longer orbital periods than those of classical novae. Indeed, in the best-studied members of this class, the mass-donating star is a red giant and outbursts probably occur via thermonuclear runaway on the surface of its mass-accreting white dwarf companion. Unlike classical novae, where the inter-outburst period is thought to be 10^4 to 10^5 years, recurrent nova outbursts occur on timescales of decades.

The best-studied outburst of any recurrent nova was that of RS Oph in 1985 (*e.g.*, Bode 1987). It turned out to be a bright and rapidly evolving object from the radio to the X-ray. Models of the outburst involve the interaction of the high-velocity ejecta with the slower wind of the red giant, built up since the last outburst. In many ways, what then follows is comparable to the evolution of a supernova remnant, but on timescales of months rather than millennia. Unfortunately, although the light curve coverage of RS Oph was very detailed, only two images were obtained in the radio, and then at the margins of detection. Real tests of these models await the next recurrent nova; the Ultrasensitive Array will ensure that even a weak one will be detected, and allow for excellent imaging (if it is anything like RS Oph) for many hundreds of days.

3.3.4 X-ray Transients: Relativistic Jets in the Milky Way

The advent of all-sky X-ray monitoring satellites like Ginga, CGRO BATSE, and RXTE ASM has given new impetus to the study of X-ray transients, primarily X-ray binaries powered by Roche lobe overflow or wind accretion onto a neutron star or black hole. Radio follow-up observations have led to some spectacular results, including the first clear correlations between X-ray and radio emission, tying accretion disk instabilities to relativistic particle ejection; the discovery of the first Galactic superluminal jet sources (GRS 1915+105 [Mirabel & Rodríguez 1994], GRO J1655-40 [Hjellming & Rupen 1995; Figure 3.23], & 1748-288 [Hjellming *et al.*, *in prep.*); and the rapid imaging of the radio emission from a large number of these sources, showing that relativistic jets are typical byproducts of accretion onto massive, compact objects. Radio monitoring is now used as a standard trigger on virtually all target-of-opportunity X-ray observations. Despite these impressive results, there are a great many outstanding questions:

- Do disk instabilities (as seen in X-rays) always trigger relativistic particle acceleration (as seen in the radio)?
- Does the speed of the jet really reflect the mass or rotation rate of the compact object?
- Do relativistic jets really obey the extragalactic lore built up over the past decades? For example, does a one-sided jet always indicate strong Doppler boosting, and are jets always emitted perpendicular to the originating accretion disks?
- How do individual jet ejecta decay over time?
- Do all jets precess? What determines their precession periods? How is this related to warping and precession of the accretion disk?

- Do quiescent accretion disks also produce radio emission (as predicted by ADAF and other models)? What are the implied accretion rates?

All of these questions are answerable, given sensitive and reliable monitoring and imaging of a substantial number of sources. The Ultrasensitive Array will make this possible.

Imaging

Although the rewards are great, imaging relativistic jets in the Galaxy is a challenging business, first because long-lasting, high-flux events are so rare (perhaps one a year), and second because the sources evolve so rapidly. A characteristic angular size is

$$\theta = 170\,\mathrm{mas}\,\beta_{app}\,t\,[\mathrm{days}]/d\,[\mathrm{kpc}]$$

where $0.1 \lesssim \beta_{app} \lesssim 2$, and $1 \lesssim d\,[\mathrm{kpc}] \lesssim 15$. 10 days therefore corresponds to 60 mas (about the size of the 45 GHz beam in A configuration) for a $0.3c$ source at the Galactic Center. The actual time-scale is set by the decay of the ejecta, which in exceptional cases might be weeks or months, but is more usually a few days to a week. Such sources rapidly expand beyond the size-scales sampled by the VLBA (see Figure 3.23), but only the most long-lived can be imaged with the current VLA, observing in A configuration at the highest frequencies. Even then the sensitivity of the current 22 GHz system leaves much to be desired for such steep-spectrum sources (45 GHz is basically hopeless), and the weak, extended features which are most interesting are seldom detectable. Spectral index maps are of course out of the question.

The Ultrasensitive Array will vastly improve the situation, permitting many more sources to be observed, over a much longer time, at higher resolution, with much greater sensitivity. Many source are too faint, fade too rapidly, or simply go off at the wrong time (not during A configuration) to be imaged. The Expansion Project will provide a factor 30 improvement in sensitivity at high frequencies; since typical sources fade as $\sim t^{-1}$ to $t^{-1.5}$, this corresponds to tracking a source 10 to 30 times longer. Many sources currently fade beyond observability in a week. If those could be followed instead for 70 or more days, they would be half an arcsecond or more across, and could be imaged even in C configuration, using the new high-sensitivity 45 GHz system. The VLA could thus perform useful imaging in three (rather than one) of its four configurations, effectively tripling the number of targets. Those sources which happen to go off in A configuration could be imaged for several months, the bright or long-lasting ones for years, yielding invaluable information on the flux decay of individual ejecta. Accurate spectral indices would be obtained at the same time (given the wide bandwidths allowed by the new correlator), while the use of fainter calibrators would cut down on uncertainties due to self-calibration. A+ configuration would of course be ideal, bridging the gap in coverage between the A configuration and the VLBA, providing excellent imaging capability at all times, and allowing even the smallest features to be imaged without worrying about missing flux density or large-scale structure.

Monitoring

The Ultrasensitive Array is even more important for monitoring programs. Current monitoring projects are granted at most an hour every week or two, enough to monitor a few sources at the 0.5 mJy level. While this provides useful and unique information, most often the results are non-detections, or a poorly-sampled decaying light curve at one or two frequencies. It's not clear whether this is fundamental – the sources simply aren't emitting radio waves most of the time –

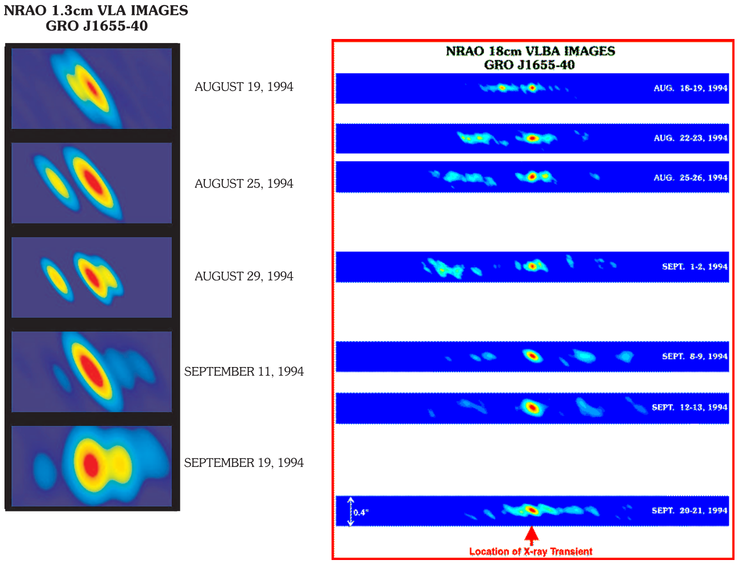

Figure 3.23: VLA 22 GHz (*left*) and VLBA 1.6 GHz (*right*) images of GRO J1655-40, a Galactic superluminal jet source (Hjellming & Rupen 1995). Note the time-scale. By the second epoch the source was so extended that the VLBA missed more than half the flux density, picking out only the smallest and narrowest features. Resolutions are 20-40 mas for the VLBA, 200-400 mas for the VLA.

or the result of poor sensitivity, although long-term monitoring of a few very bright sources by the Green Bank Interferometer (SS433, Cygnus X-3, GRS 1915+105) suggests that some binaries at least remain radio-active at a low level most of the time, with occasional flares to very high levels.

For the same commitment of observing time, the Ultrasensitive Array will provide continuous, sensitive, multi-frequency (5 or more) radio light curves for months, for any transient as strong as those which have so far been detected. Such detailed light curves constrain theoretical models infinitely more tightly than the current 3-5σ sprinkling of possible detections. Even without imaging we can learn the time offset between the radio ejection and the X-ray flare, whether there was a single or multiple outbursts, and whether the jets (assuming they are jets) are expanding freely. Several sources have slowed their decays significantly after an initial sharp decline; this opens the possibility of imaging long after the initial outburst, and learning something about both the 'old age' of the ejecta, and the medium into which they expand. Currently we only know about the brightest of these long-lived sources, the others having faded beyond detection before reaching this stage.

The detection of weak 'quiescent' emission is potentially even more exciting, because we may be seeing deep into the accretion disk. In GRS 1915+105 (Figure 3.24) the radio tracks the X-ray flux density almost exactly, on time-scales of minutes, implying that even moderate instability in the accretion disk can produce relativistic particles. The radio micro-flares appear to be tied to the 20-30 minute cycles which are now believed to be tied to the "disappearance" (into the black hole?) of the inner portions of the accretion disk. We have no idea whether this behavior is common to all sources (or just black hole systems), or whether the correlation holds on even finer time-scales

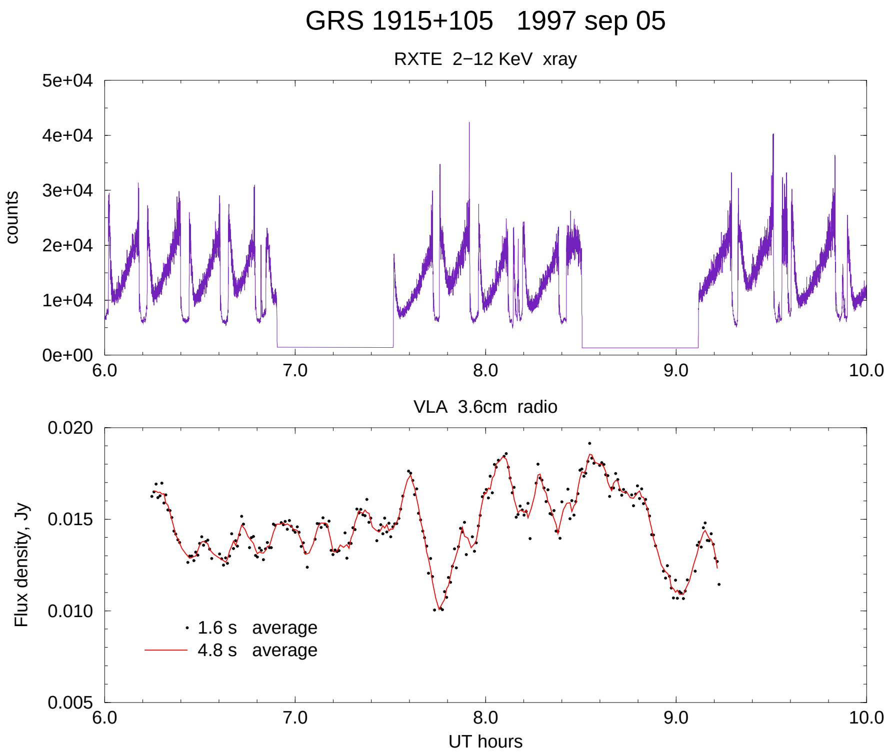

Figure 3.24: X-ray (*top*) and radio (*bottom*) light curves of GRS 1915+105 (Mirabel *et al.* 1998), the first Galactic superluminal jet source to be discovered. The periodicities in the two bands are correlated, as are the length of the X-ray minimum and the strength of the radio oscillation. The current interpretation associates both the X-ray flares and the radio emission with the violent expulsion of material from the inner parts of the accretion disk; the radio peaks grow as the period lengthens, because more of the disk is being expelled, creating more violent flares. The offset between X-ray and radio peaks is caused by light-travel time effects for the optically-thick synchrotron emission. This same source shows quasi-periodic oscillations in X-rays down to time-scales shorter than a second; the Ultrasensitive Array will allow searches for similarly rapid variability at radio frequencies.

in GRS 1915+105. The Ultrasensitive Array could detect GRS 1915+105 in 1 millisecond (5-7σ), allowing an unprecedented comparison between the radio flux and the incredible small-scale structure seen at X-rays.

Even more fundamental is the general question of quiescent radio emission — do accretion disks create winds of relativistic particles? This is part of the standard model for high-energy X-rays, and some models at least (ADAFs) predict a core which might give off observable radio emission. One source, V404 Cyg, has already been detected at the 0.2–0.4 mJy level (Hjellming, Rupen, & Narayan, *in prep.*), but there is no prospect of determining any sort of detailed light curve. The Ultrasensitive Array could provide $> 10\sigma$ detections at five frequencies every 10 minutes, giving basic information on the nature of the emission (is this a series of flares, or a slowly-varying continuous level of emission? is there any connection to the X-rays? etc.), either within a single many-hour run, or over the course of many weeks. Such observations would also yield good polarization measurements or upper limits. Flaring and other rapidly-variable emission is very difficult to model, and theorists instead concentrate on relatively simple quasi-equilibrium models like ADAFs; high-sensitivity detections of steady low-level radio emission from X-ray binaries would help enormously in tying down those models.

3.3.5 Radio Supernovae

After several decades of study, the radio emission from supernovae remains something of a mystery. All agree that the emission is synchrotron, in most cases due to relativistic particles accelerated in the shock front between the supernova ejecta and the surrounding circumstellar material, presumably ejected earlier by the progenitor star or its companion. Beyond this the controversies arise (see Figure 3.25):

- Why are so few supernovae strong radio sources, even in cases where optical data suggest significant circumstellar material?
- Do type Ia supernovae produce radio emission, or is this really confined to the explosions of massive stars?
- What sets the peak radio flux density?
- What causes the opacity at early times (free-free, synchrotron self-absorption, Razin-Tsytovich effect), and what determines its decay?
- Why have we not seen evidence for a pulsar in any extragalactic supernova, even decades after the explosion?
- How are radio supernovae related to radio supernova remnants?

The Ultrasensitive Array will address all of these questions, by observing many more sources, over a wider range in frequency, for a much longer time. With some 10s of radio supernovae detected each year (compared to the current one or two), we will at last be able to compare optical, infrared, and radio properties for a real sample, and learn for instance whether the narrow lines seen in some supernovae do indeed imply significant circumstellar material, with associated radio emission. Such a sample would also show conclusively whether radio supernovae can be used as distance indicators (Weiler *et al.* 1998), and more fundamentally, determine the real radio luminosity function of these explosions. We know already from SN 1987A that some supernovae are thousands of times weaker than the strong ones the VLA can see now; there is no hope of seeing such extragalactic sources at the moment (SN 1987A as seen in M81 would peak at $\sim 20\,\mu$Jy), but with the Ultrasensitive Array this would be the work of a few hours. Easy and quick spectral studies, extending to high frequencies, are equally important, giving a much clearer picture of the nature and evolution of the absorption: the high frequencies 'see through' the absorbing material, allowing a direct determination of the absorption at lower frequencies. This is of great interest because that absorption, if well understood, may give direct information on the source size (Chevalier 1998), the distribution of the surrounding material, the deceleration of the shock front (Chevalier 1982; Weiler *et al.* 1989), and the clumpiness of the CSM. The high frequencies are also critical for models of particle acceleration: one wants to watch the 'raw' flux density evolve from the earliest possible moment, just when absorption obscures most of the low-frequency flux and all of the intrinsic flux information.

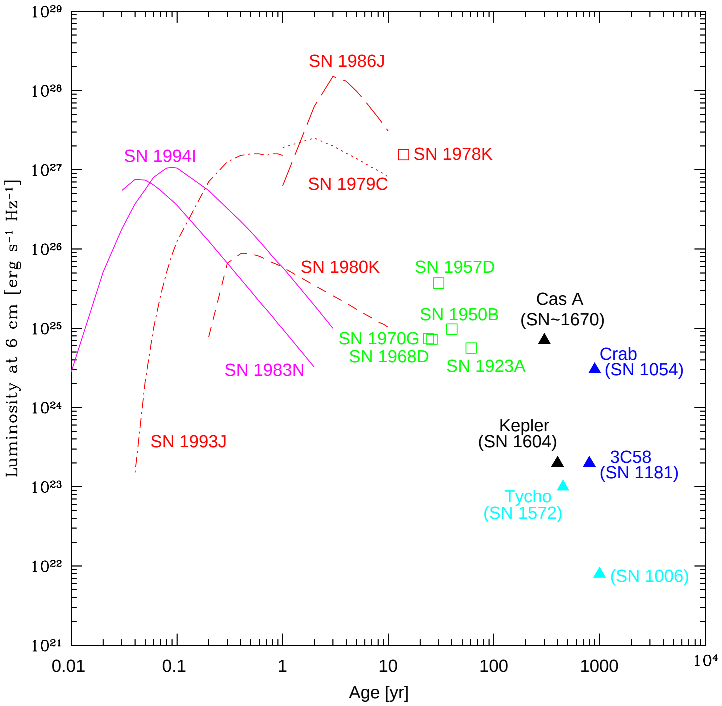

Figure 3.25: The radio luminosity vs. age for a number of young radio supernovae (*curves*), older "historical" supernovae which have been detected (*squares*), and the youngest known galactic SNRs (*triangles*). The prompt burst of SN 1987A peaked at a luminosity about an order of magnitude below the bottom of this plot; the Ultrasensitive Array could detect such a source in a few hours out to >5 Mpc. Courtesy S. D. Van Dyk, K. W. Weiler, R. A. Sramek, M. J. Montes, & N. Panagia (1999).

The improved sensitivity will stretch radio light-curves out to much greater ages, decades to centuries in fact (since most radio supernovae follow power-law decays). As well as looking for upturns (as in SN 1987A), indicating renewed particle acceleration, and downturns (as in SN 1980K), indicating abrupt changes in the shock conditions, one can hope at last to tie supernovae (where we see the explosion) to supernova remnants (where we see the final stages of interaction with the general ISM). More speculatively, one could hope to do a deep survey for radio remnants surrounding known optical supernovae, from back to the 1880s; the resulting general and complete statistics would provide a unique probe into supernova particle acceleration and ISM interaction, with attached time-scales, initial velocities, and ejecta masses (from the original optical spectra).

Finally, there is the question of 'missing' sources, most obviously, young pulsars and supernova Ia's. Even a single detection of either population would have enormous implications; a significantly larger number of non-detections would also be very important, placing limits both on pulsar nebulae, and on the mass-loss rates of type Ia progenitors. In the same vein, it is becoming embarrassing that searches in starburst galaxies have yet to turn up a single new supernova. Radio observations are the best way to look for these, since (1) heavy dust obscuration makes optical and near infrared searches impossible, (2) poor resolution, copious dust emission, and the expected steep spectral index make far infrared searches unattractive, and (3) if the radio flux does indeed grow with the local density, such enshrouded supernovae should be very impressive radio sources. The Ultrasensitive Array will both make these searches far easier (by detecting 'standard' radio supernovae in a minute or less), and extend them to more distant (and hence more active) star forming systems (to $z \sim 1$ for the most luminous known radio supernovae).

3.3.6 Gravitational Lenses and H_0

Gravitational lenses are excellent tools for studying cosmology; in particular, individual lens systems can be used to determine H_0, independent of the cosmic 'distance ladder' (*e.g.*, Blandford & Narayan 1992). This requires the accurate measurement of the time delays between lensed images, which in turn rests on continuous, well-sampled light-curves for the individual lens components (*e.g.*, Biggs *et al.* 1999). Radio observations are in principle ideal for these studies, since they may be made day or night, any time of the year, and since radio interferometers can easily provide sub-arcsecond images in almost any weather. However, there are currently several practical difficulties. First, the VLA spends half its time in the compact C and D configurations, which cannot provide sub-arcsecond images at frequencies below 45 GHz; the resulting gaps in the light-curves may miss the sharp changes in intensity which are needed to accurately measure the time delay (*e.g.*, Figure 3.26). Second, the VLA is currently limited by sensitivity to observing such systems at low frequencies. This has several unfortunate side effects: poorer resolution, making it difficult to distinguish different lens components; confusion with more extended emission, which tends to be stronger at lower frequencies; and relatively weak intrinsic variability (typically 5–10%). Third, the VLA simply does not have the sensitivity to effectively monitor any but the brightest handful of lenses. Finally, the uncertainties in current radio light curves are dominated by systematic errors in the flux scale; these are alleviated considerably by comparison with flux densities of background sources in the field, but these sources are generally weak and such comparisons are themselves limited by sensitivity.

The Ultrasensitive Array will address all of these problems, by providing over a factor 30 improvement in sensivity at the high frequencies, allowing any currently-detectable lens to be monitored at 30–50 GHz, and providing a much larger sample of higher-signal-to-noise-ratio detections of background sources. The sensitivity will allow many more lenses to be monitored. This monitoring could be carried out at high frequencies. where the spatial resolution is highest, allowing effective imaging in all but D configuration. Smaller lenses could be monitored as well, since at 45 GHz the VLA's resolution is $\sim$ 60 mas in A configuration. Even better, since most radio

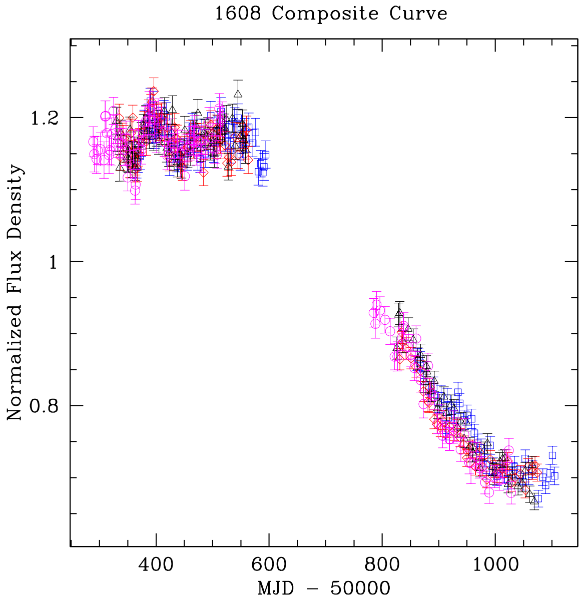

Figure 3.26: Composite radio light curve for the CLASS B1608+656 lens system. The curve is constructed from the four individual light curves associated with the four lensed images in this system. These component light curves have been shifted by the best estimates for the system time delays, and scaled by their relative magnifications (Fassnacht *et al.*, *in prep.*). The change from a constant flux to a monotonic decay occurs in the gap in the light curve associated with the VLA being in its C and D configurations.

sources are more variable at higher frequencies, it will be much easier to align the light curves of the different components, even with a relatively short series of observations.

3.3.7 Gamma-ray Bursts

The study of gamma-ray bursts (GRBs) has undergone a renaissance since the launch of the Italian-Dutch satellite BeppoSAX and the subsequent discovery of long-lived "afterglows" at X-ray (Costa *et al.* 1997), optical (van Paradijs *et al.* 1997) and radio (Frail *et al.* 1997) wavelengths. In short, we now know that GRBs are the most violent explosions (10^{52}-10^{54} erg) in the cosmos, driving relativistic shocks into their surroundings with bulk Lorentz factors $\Gamma_\circ \simeq 300$. The progenitor object(s) of GRBs remain unknown but there is mounting evidence that GRBs announce the births of black holes.

The VLA has been at the forefront of this emerging field, making the first discovery of a radio afterglow from GRB 970508 (Figure 3.27) and making all subsequent radio afterglow discoveries in the northern hemisphere. Despite this impressive beginning, the potential of radio observations has barely been touched. The Ultrasensitive Array will find and follow the evolution of, not one or two, but as many as a hundred GRBs a year, in greater detail, over a wider range of frequencies, and for longer times than any current afterglows. Here the excellent sensitivity and responsiveness

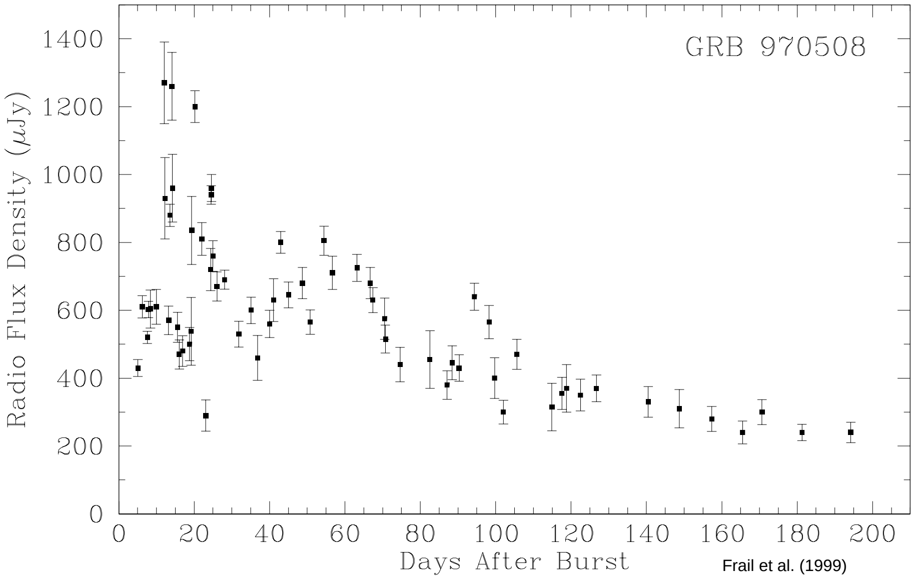

Figure 3.27: 8.46 GHz light curve of the radio afterglow from GRB 970508 (Frail *et al.*, *in prep.*). The flux density fluctuations at early times are the result of refractive interstellar scintillation (RISS), an interference effect produced by the intervening ionized gas along the line of sight. This scintillation provides a direct measurement of the angular size of the expanding fireball (see text for details). At late times (>100 days) the radio light curve undergoes the same power-law decay seen at X-ray and optical wavelengths.

of the Ultrasensitive Array is the key, since even the brightest radio afterglows peak at around 1 mJy. These data will make fundamental contributions in several areas:

- *Complete spectral energy distributions:*
  Combining VLA data with those from optical (Keck, Gemini, HST), submillimeter (JCMT, ALMA), infrared (UKIRT, SIRTF), and X-ray (XMM, Chandra, Astro-E) observatories gives the instantaneous spectrum of the afterglow over 10 orders of magnitude. This can be used to derive the total GRB energy and the ambient density of the surroundings, and to probe the physics of particle accleration in relativistic shocks (*e.g.*, Sari, Piran, & Narayan 1998; Wijers & Galama 1999). Radio observations are particularly important in constraining theoretical models, because the radio emission is observable throughout all the major phases in the light curve For instance, the most robust estimates of the total energy and the geometry come from radio observations at late times, when the blastwave has slowed to sub-relativistic speeds and the entire radiating surface is visible. In providing detailed and long-lasting light curves of many dozens of GRBs each year, the Ultrasensitive Array will make a major contribution to

our physical understanding of these sources.

- *Sizes and expansion rates:*
  GRB afterglows are only a few micro-arcseconds in diameter; surprisingly, such diameters can actually be measured by radio telescopes, thanks to refractive interstellar scintillation (RISS). The propagation of radio waves through the turbulent ionized gas of our Galaxy introduces a modulation of the received signal; the strength and character of these modulations depends on the size and shape of the background source. Well-sampled data taken at the right frequency (which depends *e.g.* on the Galactic latitude) can measure GRB sizes and expansion rates, and have already provided the only *direct* demonstration that GRBs and their afterglows originate from relativistic shocks (Figure 3.27). Such measurements are currently limited to a few of the brighter radio afterglows; the Ultrasensitive Array will extend this to provide sizes and expansion velocities for dozens of GRBs every year.

- *Jets, rings, or spheres:*
  RISS can in principle determine not only the size but also the geometry of the radio afterglow, at least to the extent of settling one of the major outstanding questions: are GRBs jets or spherical outflows? Obviously this requires very well-sampled and low-noise radio light curves, and the Ultrasensitive Array is ideally suited to providing them. Additional constraints on the geometry come from the intrinsic linear polarization, which can in principle be followed for much longer times at radio wavelengths; the evolution of the polarization fraction and orientation should then reflect the shift from highly beamed to more isotropic radiation. Current instruments are simply not sensitive enough to measure radio polarizations. The Ultrasensitive Array by contrast could detect (5σ) 10% polarization in the $\sim 500\,\mu$Jy afterglows seen now, in under 10 minutes.

- *Dust-free samples:*
  There are now several afterglows which have only been detected at radio frequencies, and several others where there are clear signs of reddening (Taylor *et al.* 1998). This raises the possibility that optical studies may miss a substantial fraction of the afterglow population, and particularly those GRBs born in dense, star-forming regions. Radio afterglows can be detected regardless of dust extinction, and the Ultrasensitive Array will provide a large enough sample that such biases can be rigorously checked.

In addition to providing unique data on the bursts themselves, the Ultrasensitive Array will image radio emission from the host galaxies. Any model of GRBs must be consistent both with the positions of the GRB within their host galaxies, and with the properties of the host galaxies themselves; for instance, models based on the explosions of massive stars ("hypernovae") predict an association with the disks of actively star-forming galaxies. Currently this work is the domain of optical studies, and is limited by the small number of optical afterglows and the possibility of optical obscuration. The Ultrasensitive Array will be able to detect the radio emission from host galaxies out to z=1 or beyond, giving extinction-free estimates of the host galaxy's star formation rate, and providing sub-arcsecond measurements of the position of the GRB within the galaxy. The A+ configuration would of course be ideal, improving this relative astrometry by another factor of ten, and hence allowing even more stringent tests of progenitor models.

3.4 The Evolving Universe

What was the early solar system like? How are stars born? When and how were galaxies formed? What role does their environment play in their births, their lives, their deaths? These are among the most basic questions of modern astronomy. Like most basic questions, their answers are far from obvious, and likely to be both subtle and complex. Star formation obviously requires accretion, but exactly how this works in the presence of angular momentum and magnetic fields is still a mystery. Galaxies are basically defined as conglomerations of stars, which presumably were themselves made out of primordial gas; but when, how quickly, and how efficiently this occurred, is still hotly debated. The situation is made more difficult observationally by the penchant of stars to be born out of dusty, dense gas, and by the obvious fact that galaxies were young a long time ago, a time now to be glimpsed only by looking back to the most distant parts of the universe. Much of what is most interesting occurs behind clouds of dust, or on size-scales requiring the utmost in angular resolution; at the same time the complex interaction of physical processes, and the redshifting of distant light into different bands, require observations over a huge range of the electromagnetic spectrum. For these reasons multi-wavelength studies are more important in this than in any other area of astronomy. One needs optical instruments like HST and Keck to observe the stars, and (sub-)millimeter telescopes like IRAM, JCMT, SIRTF, and the ALMA, to see the dust which re-radiates most of the luminosity, and to map the molecular gas out of which stars are formed. High-energy satellites like ROSAT, BATSE, AXAF, and Constellation-X offer another, orthogonal view, probing the final stages of stars, the hot thermal gas in which galaxies live, and both massive stellar explosions and the neutron stars and black holes which they create.

Radio observatories too offer unique information, and unique possibilities. Stellar cores are surrounded by dust too dense to penetrate even at submillimeter wavelengths; here radio waves offer the only hope of seeing directly into these regions where planets may be formed. Luminous young stars also ionize their surroundings, and radio observations of free-free emission can be used to measure both the amount and the distribution of this material, on scales ranging from ultra-compact H II regions in Orion, to giant star-forming regions in galaxies 10s of Mpc away. The resulting star-formation rates are independent of extinction and allow much higher resolution than current submillimeter telescopes. Finally, at lower frequencies synchrotron radiation dominates, providing a unique probe of cosmic ray generation and evolution. Cosmic rays are generated in high-velocity shocks, and so act as useful tracers of such activity near young stellar objects, black holes, & neutron stars, as well as in supernova remnants. This latter connection makes synchrotron emission another valuable, extinction-free indicator of massive star-formation, as dramatically evidenced by the far-infrared/radio correlation. Finally, cosmic rays are an important heat source in dense molecular clouds, closing the circle between dying stars and stellar nurseries. Of course, relativistic particles are also accelerated in active galactic nuclei (AGNs), somewhat confusing this simple picture; but this confusion also allows interesting tests of the relative importance of star formation and nuclear activity in shaping galaxy evolution, since the two can be distinguished both by imaging the radio source in question, and by sampling the spectral energy distribution at both radio and far infrared wavelengths. Assuming one understands the operative physical mechanisms, one can even use such broad-band millimeter and centimeter photometry to derive rough redshifts for sources which may be too faint (or too extincted) to see optically.

In addition to these continuum considerations, radio telescopes are sensitive to a number of very interesting spectral lines, including the lowest energy transition of neutral hydrogen, an enormous number of radio recombination lines, several very useful maser transitions, and important lines of such simple molecules as ammonia and formaldehyde. While the ALMA will be the premier telescope for most molecular observations, the cold neutral gas is best studied at radio wavelengths; and radio telescopes also offer important data on low-order transitions of molecules like CO, which rapidly redshift into the centimeter regime. Evolutionary studies demand observations across the entire electromagnetic spectrum, and the radio band makes its unique contributions as much as the submillimeter or optical.

Unfortunately, these studies are severely restricted currently by the limitations of the VLA. The sensitivity (especially at the high frequencies) allows observations of only the brightest and nearest objects; the limited frequency coverage, together with uneven sensitivity, makes it difficult to measure the full spectral energy distributions (SEDs); the narrow bandwidths and poor spectral resolution prevent spectral line searches, restricting us to low-resolution follow-up spectroscopy of sources with known redshifts. The VLA Expansion Project will change all this. The Ultrasensitive Array will permit the observation of intrinsically-faint young stellar objects (YSOs) over the entire range from 1 to 50 GHz, imaging both synchrotron and thermal jets, and (especially in combination with ALMA data) allowing a reliable decomposition of their SEDs. Similar observations will be possible for star-forming galaxies over a wide range in redshift; continuum observations will provide unextincted estimates of the star-formation rate, rough 'photometric' redshifts, images of the star formation regions and the structure of the magnetic fields, and reveal as directly as possible the role of active galactic nuclei in galaxy evolution. For spectral lines, the new correlator will for the first time allow efficient surveys with the VLA, with a single frequency setting covering hundreds of thousands of km/sec in H I, checking for redshifted absorption irrespective of dust against hundreds of background sources, looking for CO emission at redshifts of several to 10 or beyond. In our own Galaxy the VLA will finally be able to observe multiple transitions at once, take advantage of maser lines to calibrate weak continuum signals, and observe with fine enough velocity resolution to see signatures of infall and rotation at $\lesssim 0.1\,\mathrm{km/sec}$. The improved sensitivity will also provide numerous high-redshift targets for absorption and rotation measure studies, giving a unique probe both of the intervening gas, and of the magnetic fields both at large redshifts and in local star formation regions. Some of these observations have been discussed in the preceding sections; here we concentrate directly on a few experiments of special relevance to understanding evolution, the birth, aging, and death of objects ranging from asteroids to galaxies.

3.4.1 Minor Bodies of the Solar System

The minor bodies (comets, asteroids, and satellites) provide very important information about the formation and evolution of the solar system. Radio observations in principle offer unique information, particularly about the surfaces and near-subsurfaces of these bodies, because they are cold enough that thermal emission is expected at relatively low frequencies, and because radio photons probe depths roughly equal to their wavelength, *i.e.* a few to some 10s of millimeters. In addition, OH provides a useful indicator of out-gassing. But radio studies have so far been quite limited, primarily because of limited sensitivity. The Ultrasensitive Array will make a huge difference, allowing the detection of many 10s of sources from a few to 50 GHz, giving a unique look into and beneath the surfaces of a wide variety of the smaller denizens of the solar system.

Comets

- *OH imaging:*
  The outgassing of water drives most of the observable phenomena of comets; unfortunately interference by terrestrial H_2O has prevented its direct observation in all but one comet. The primary photo-dissociation product, OH, has both UV and radio transitions, but only

the radio lines can be observed with velocity resolution finer than the outflow velocity. The VLA has successfully imaged the 1667 MHz transition in a few comets, providing the only cometary images which are resolved both spatially and in velocity (*e.g.*, Palmer, de Pater, & Snyder 1989). However, the VLA resolves out as much as 2/3 of the total flux, even in D configuration; nor is it possible currently to image multiple transitions with adequate frequency resolution and sensitivity. The wide bandwidths, high spectral resolution, and improved RFI excision provided by the Ultrasensitive Array will allow simultaneous imaging of all four 18cm lines of OH, in both senses of polarization; this should lead to a much better understanding of the state of this molecule in cometary comae. Recovering the full flux would require simultaneous total power measurements, preferably combined with a more compact arrangement of the antennas (the E configuration) to maximize surface-brightness sensitivity. This would unambiguously resolve long-standing uncertainties about the degree of symmetry in outgassing of comets (Bockelée-Morvan & Gérard 1984; de Pater, Palmer, & Snyder 1986; Combi 1987). Current plans call for these improvements to be studied during the first phase of the VLA Expansion Project, and implemented during phase two.

- *Thermal emission from cometary nuclei:* Only a single cometary nucleus has been detected thus far at radio wavelengths – that of comet Hale-Bopp (Fernandez *et al.* 1997). The Ultrasensitive Array will not only detect also but obtain full spectral information from 15 to 50 GHz on nearly all short period comets with diameters more than a few kilometers, and on all newly-discovered long-period comets which come within ~ 2 A.U. of the Earth. Apart from spacecraft encounters, these data offer the only means to place constraints on the actual physical structure of cometary nuclei surfaces and sub-surfaces.

Kuiper Belt Objects

Kuiper Belt Objects (KBOs) are relatively small icy bodies in the outer parts of the solar system which may hold a record of the very earliest stages of the formation of our solar system. As for cometary nuclei, observations of KBOs at radio wavelengths are important because they offer a unique probe into the sub-surfaces of these bodies, and hence constrain surface and subsurface temperatures and physical characteristics. For example, the distribution of temperature with depth in an icy body in the outer solar system might be used to help determine the nature and distribution of ices on the surface of that body, and hence give indirect information on the chemical composition of the upper part of its surface. Having this type of information on all of the small icy objects in the outer solar system will help in determining the cause for their variation in properties (*e.g.*, their spectral diversity). Unfortunately, no current radio telescope is sensitive enough to detect these objects at $\lambda \gtrsim 350\,\mu$m.

The Ultrasensitive Array will extend this down to almost 5cm for the brightest objects. At the shorter wavelengths ($\lambda \lesssim 2$ cm), more than half of all currently known KBOs could be detected in 12 hours or less (Figure 3.28). Sub-arcsecond astrometry would of course also be obtained for these detections. These data could then be used in conjunction with higher-frequency measurements by the ALMA to give a full three-dimensional view of the temperature structure in the outer few to 10cm of these bodies.

Asteroids

- *Main-belt asteroids:*
  Thermal emission has been detected from the four largest asteroids (Ceres, Pallas, Vesta,

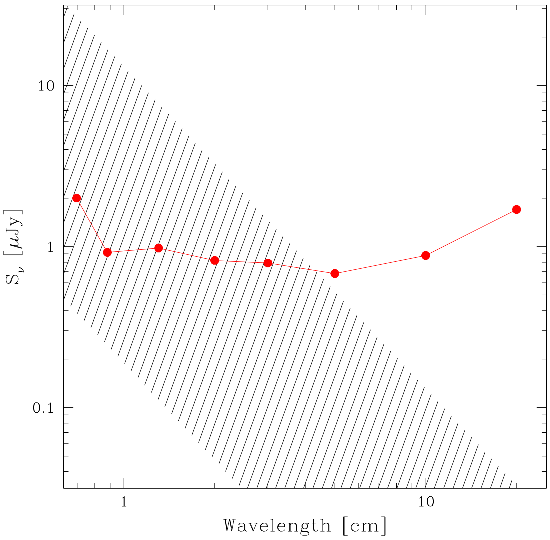

Figure 3.28: The estimated sensitivity of the upgraded VLA in a 12 hour observation (connected dots) and the estimated range of thermal emission from all currently known KBOs as of July 1998 (hatched area).

& Hygiea) at wavelengths from 1mm to 20cm (Webster and Johnston 1989, and references therein), and from a few smaller asteroids at 2cm. Such measurements place constraints on the thermal and electrical properties of those objects' surface layers. The existing observations indicate that the asteroids studied so far are covered with fine-grained regoliths, which are thought to result from meteoroid bombardment ("sand blasting") of the surfaces over hundreds of millions of years. Differences in the microwave spectra of Ceres, Pallas, Vesta, and Hygiea suggest variations in the dielectric properties of those regoliths and/or variations in the regolith thickness. However, those few objects represent just a tiny fraction of the thousands of main-belt asteroids, most of which cannot be detected with the current VLA: a 100km object at a distance of 1 AU has a flux density of only ~ 0.4 mJy at 15 GHz, and ~ 0.1 mJy at 8 GHz. In addition, there is an important gap in the wavelength coverage between 1mm and 1cm. Over this range, the spectra show a distinct drop in brightness temperature. The Ultrasensitive Array's improved sensitivity and wavelength coverage will lead to detections of large numbers of these objects at several wavelengths. Of particular importance is the 7mm (45 GHz) band, which fills the 0.1−1.0cm wavelength gap.

- *Near Earth Asteroids:*
  NEAs are of especial interest, since one will eventually crash into the Earth. The Ultrasensitive Array will be able to detect all NEAs more than about 100m across at the shorter wavelengths ($\lesssim 2$ cm) with 5σ confidence in a single track (6 hours on-source). Here the ability to observe during daytime and obtain accurate astrometry is particularly important.

3.4.2 Distinguishing Dust and Free-Free Emission, Disks and Jets in Local Star Formation Regions

As discussed in §3.2.3, disks and jets around young stellar objects are part of the early evolution of solar-type stars. The current paradigm for the formation of single stars leads naturally into the formation of disks that may then evolve into a planetary system. Thus the study of such disks and accompanying jet/outflow systems are required to understand the origin of our own solar system.

The spectral energy distribution of an embedded young stellar object from optical to radio wavelengths shows that, at wavelengths shorter than about 7mm, dust emission dominates the spectrum. Longward of about 7mm, free-free emission from ionized gas, presumably from the jets/outflows begins to be important. Finally, in at least one source, non-thermal synchrotron emission, apparently from a double-sided jet has been discovered (W3(OH): Reid *et al.* 1995). So in order to understand both the gas and the dust and their interaction, imaging observations at several wavelengths from long-wavelength centimeter the sub-millimeter are required. Complementary, similar-resolution observations from the Ultrasensitive Array and ALMA will be necessary to disentangle the emission from these competing mechanisms.

Radio observations are also essential for the innermost regions of dense dust cores, which are probably opaque at millimeter wavelengths. Here the high sensitivity of the Ultrasensitive Array will allow the high-resolution observations at $\sim 1\,\mathrm{cm}$ which are required to see into the regions where solar systems might form.

3.4.3 Spectral Imaging of Nearby Galaxies

The Ultrasensitive Array will be the perfect instrument for spectral studies of radio emission from nearby galaxies, mapping the aging of cosmic ray electrons, showing directly the origin of the far infrared/radio correlation, detecting and imaging complete samples of individual supernova remnants in other galaxies, and giving dust-free measurements of the flux of ionizing photons – and hence the star formation rate – throughout nearby galactic disks. The key improvement is the availability of excellent sensitivity over several decades of frequency, from 75 to 50000 MHz.

The radio emission from normal galaxies is dominated by synchrotron emission from relativistic cosmic ray electrons (CRE) and thermal free-free emission from ionized gas at $\sim 10^4$ K. Both are intimately related to the star formation process: cosmic rays are produced by supernovae and supernova remnants, and provide an important heat and ionization source for molecular clouds and dust; while thermal emission from H II regions is a dust-free tracer of luminous young stars. The two processes are distinguishable primarily by their spectra, with synchrotron emission generally much brighter at low frequencies ($S_\nu \propto \nu^\alpha$, with $\alpha \sim -0.5$ to -3), while thermal emission either gently falls (optically thin, $\alpha = -0.1$) or sharply rises (optically thick) with frequency. Disentangling the two requires sensitive imaging at the same resolution over as wide a range of frequencies as possible. High spatial resolution is also important, to separate the different emission regions as cleanly as possible; at the same time, since the spectral decomposition is based on the change in the *total* flux density with frequency, it is essential to retain sensitivity to large-scale structures. This makes wide-field spectral imaging a particularly demanding problem in terms of sensitivity and *uv*-coverage. The Ultrasensitive Array will be ideal for this work, combining high sensitivity and scaled-array capability across a huge frequency range with the ability to image a large range of spatial scales with excellent fidelity. A few of the more obvious scientific advances which will result are expounded below.

Low-Frequency Halos

Because the energy loss rate for synchrotron-emitting particles varies as E^2, regions with little on-going particle re-supply/acceleration have steeper spectra; the range from $\nu^{-0.5}$ to ν^{-3} has been observed in nearby galaxies. The sites and length scales of this spectral evolution, both in and out of the disk, therefore give direct information on where CRE are accelerated, and about the diffusion and convection processes which determine their subsequent movement. These effects are seen most clearly in the steep-spectrum radio 'halos' ($\sim \nu^{-2}$ to ν^{-3}) which have been observed kiloparsecs above the disks of a number of edge-on galaxies (*e.g.*, Allen, Baldwin, & Sancisi 1978; Carilli *et al.* 1992 [Figure 3.29]). These halos are difficult to detect, let alone image, because they are easiest to see at low frequencies where the resolution is poorest and the confusion with disk emission most serious. The improved sensitivity of the Ultrasensitive Array will allow imaging both at higher frequencies and with a factor 3–4 higher spatial resolution. With much more accurate spectral information as well (cf. Figure 3.30) it will be much easier to see the detailed changes in spectra with height above the disk, and so to place direct constraints on models for cosmic ray diffusion/convection, as well as on theories about the origin of chimneys, bubbles, and other phenomena connecting disk to halo. The eventual goal is to match individual supernova remnants and H II regions to individual outflows above the disk, and track the aging of the electrons as they escape from the plane.

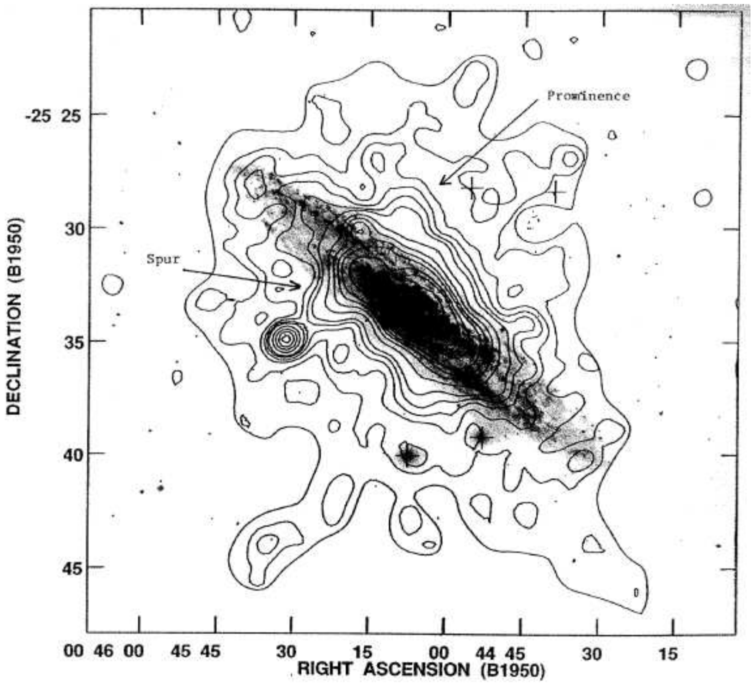

Figure 3.29: The radio halo of NGC 253 (contours), as seen by the VLA at 330 MHz (Carilli *et al.* 1992), superposed on an optical image (greyscale. The halo rises to a height of at least 9 kpc.

The Far-Infrared/Radio Correlation

The primary difficulty in disentangling synchrotron emission with varying spectral index from thermal emission is the limited spectral range now available. This is where the real strength of the Ultrasensitive Array is apparent, making available the full range of frequencies from 75 to 50000 MHz. With so many measurements of the radio spectrum available as a function of position in a galaxy (Figure 3.30), one can finally hope to image the thermal and non-thermal emission *separately*, following the spectral aging of the synchrotron component with good spectral index sensitivity over a wide range of spatial scales. The combination of high- and low-resolution observations will allow both the identification of SNRs and H II regions, and their removal from the low-resolution images needed to trace more diffuse structures. This is essential to any detailed understanding of galaxies in general and the interstellar medium in particular. To take a single example: one of the great puzzles found by the Infrared Astronomical Satellite (IRAS) was the FIR-radio correlation, which shows an incredibly tight relation between FIR and radio emission over many orders of magnitude. The origin of this relationship, and the heat sources for the dust which emits the FIR radiation, remain controversial. While the dust must be heated by stars, whether those stars are mostly the very bright ones in H II regions, or the more diffuse population of A and B stars, is still debated. On the radio end, the synchrotron emission can presumably be traced eventually to SNRs, but the details of this are not at all clear. The Infrared Space Observatory (ISO), new NASA missions like SOFIA and SIRTF, ground-based instruments like SCUBA on JCMT, and most especially the ALMA, will provide high-resolution probes of the FIR emission. The Ultrasensitive Array will make similarly-detailed images available at radio wavelengths, and more importantly, show whether the FIR-radio correlation is tighter when done with pure thermal/non-thermal emission (either or both might be expected). Assuming we do understand this correlation, various authors (especially Helou) have used the details of the relative FIR/radio distribution to constrain cosmic ray diffusion lengths; these models can only be tested and refined through high-resolution, multi-wavelength studies.

Supernova Remnants

Supernova remnants (SNRs) are the last signposts of the deaths of stars. They reflect both the star(s) that exploded, and the medium with which the ejecta or pulsar nebulae are interacting; they are also thought to be a major source of high-energy cosmic rays in galaxies. SNRs are rather difficult to study in our own Galaxy, primarily due to a combination of distance uncertainties and extinction. Extragalactic studies can provide a large sample of SNRs at known (or at least common!) distances, with (generally) much lower opacities, and with unambiguous locations with respect to the various ISM and stellar components. Radio observations in particular provide very valuable information. Many SNRs (*e.g.*, the Crab Nebula) are much more prominent at radio than at optical wavelengths. Radio waves can penetrate extensive dust layers with ease, allowing one to see SNRs even in starburst systems where A_V may be 20 or more. And most importantly, the radio emission is the direct result of the energetic particles which the SNRs create, interacting with the magnetic fields which both accelerate and confine them.

Currently observations of extragalactic SNRs are limited by sensitivity and resolution. The state-of-the art for normal (non-starburst) galaxies is illustrated by recent VLA observations of M33 (Gordon *et al.* 1999), in which flux densities and spectral indices were measured for some 53 SNRs — by far the largest extragalactic radio sample to date. Unfortunately the interpretation was hampered by relatively poor spatial resolution (7 arcsec $\sim$ 30pc at 840 kpc), which made it impossible to resolve the SNRs, and led to confusion with thermal emission from associated H II

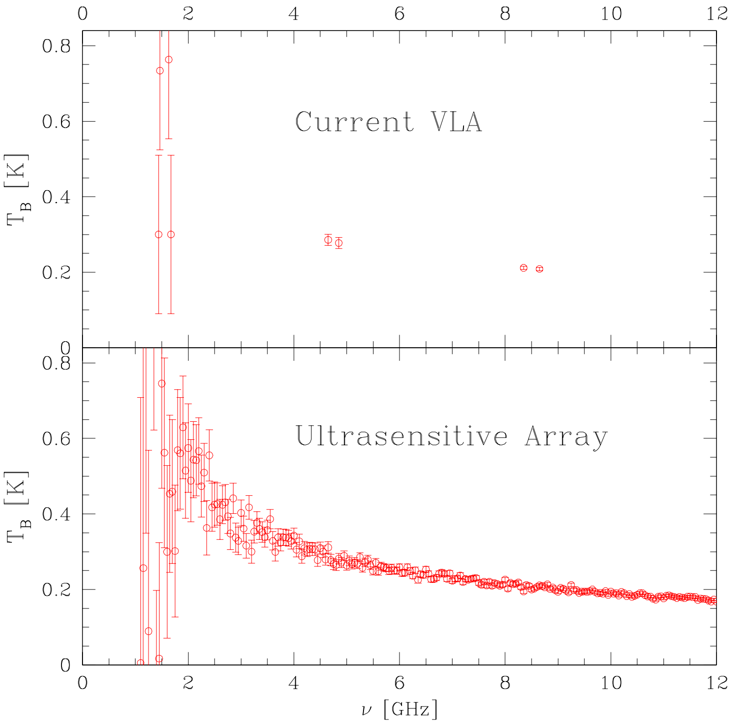

Figure 3.30: Spectral index mapping of local galaxies now, and after the first phase of the Expansion Project. The red points illustrate the data obtained for identical total integration times (12 hours at each of 3 bands for the current VLA; 9 hours for each of 4 bands for the Ultrasensitive Array; both assume 50 MHz channels, and 6 arcsec resolution [100pc at M81, or 22pc at M33]). The underlying spectrum is that of a random location in a typical spiral galaxy, which emits ten times more synchrotron ($\propto \nu^{-0.7}$) than free-free ($\propto \nu^{-0.1}$) emission at 1 GHz (Condon 1992), and has a mean brightness temperature at that frequency of ~ 0.75 K (Hummel 1981).

regions. Clearly more distant systems would be even more challenging.

The improved sensitivity and frequency flexibility of the Ultrasensitive Array will truly revolutionize this field. A simple extrapolation of Gordon *et al.*'s source counts implies that a *one hour* observation at 1.5 or 3.0 GHz would yield 1100 SNRs ($\sim 5\sigma$) – five times the number known in our own Galaxy (Green 1998). Of course, if there aren't any such faint SNRs, we will instead have the only complete sample of radio SNRs in any galaxy, which might be even more interesting in understanding the origin and diffusion of cosmic rays. Spectral indices would come along 'for free,' given the 2:1 bandwidth ratio and excellent spectral resolution afforded by the new correlator and feeds. Observing in A configuration would give a 0.8 arcsec (3.3pc) beam, sufficient to resolve any of the famous SNRs in the Milky Way; the sensitivity for these relatively-bright (0.7 mJy) sources would easily allow mapping polarizations like those seen in Galactic remnants, tracing the magnetic field orientation directly for the first time in extragalactic SNRs. For even higher resolution, a 12-hour observation at 33 GHz would provide 0.3pc (0.08 arcsec) imaging with sufficient sensitivity to provide more than 20 beams (in each dimension) across sources like Tycho or Kepler; the previous observations show there are about 40 such sources in M33.

One could also extend these studies to more distant systems, and a wider variety of galaxies. The M81 group for instance offers a nice example of strongly interacting galaxies (Figure 3.31, including perhaps the most famous starburst galaxy (M82). A 6-hour observation with the Ultrasensitive Array would give similar sensitivity to the current M33 measurements, at twice the spatial resolution. Such observations would give unbiased samples of significant numbers of equidistant SNRs in a variety of galaxy environments, showing directly the influence of interactions, central starbursts, and galaxy morphology on the end products of star formation – and the generation and retention of cosmic rays.

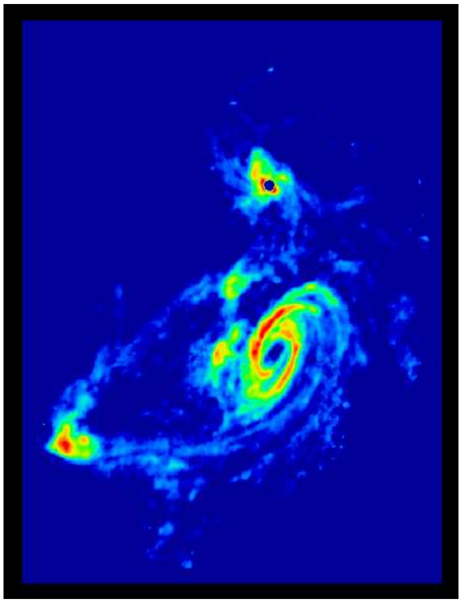

Figure 3.31: VLA H I mosaic of the M81 group. M81 is the large spiral; M82 inhabits the concentration of gas to the north. The entire field is roughly 2° across, and the resolution is about 1 arcmin. Courtesy M. S. Yun (see Yun, Ho, & Lo 1994).

H II Regions

These same observations would give, 'for free,' the most sensitive radio surveys yet obtained for free-free emission from H II regions. Extragalactic H II regions, direct tracers of luminous young stars, are traditionally studied in Hα, Hβ, and other optical lines characteristic of gas at 10^4 K. Radio observations, though difficult, offer the key advantage of seeing through the dust associated with star-forming clouds, allowing both a dust-free measure of the (luminous) star-formation rate, and (by comparison with optical measurements) a direct determination of the optical extinction. This is particularly important in observations of the most actively star-forming galaxies; the H II regions seen in radio surveys of local starbursts (*e.g.*, NGC 253, Ulvestad & Antonnuci 1997) very seldom have UV, optical, or even infrared counterparts. Radio observations offer a uniquely reliable probe of the details of star formation in such systems.

The Ultrasensitive Array will at last allow observers to fully exploit these advantages. A 10 minute observation could detect the H II region created by a single 05 star, out to the distance of M81 (3.63 Mpc). For nearby galaxies this means picking up many more of the optically-detected H II regions, allowing the determination of extinctions, and the direct measurement of temperatures and densities (useful for example in abundance work). Such observations would give the ages and (high end) initial mass functions for star-forming regions across entire galactic disks, in unprecedented detail, with no worries about extinction. This simply cannot be done now. On larger scales, another 10 minute observation would reveal individual optically-thick regions like those in NGC 253 out to Virgo, allowing one to easily search for 'mini-starbursts' throughout the entire galaxy cluster. Giant and supergiant H II regions could be imaged in Coma in a few hours, and starburst galaxies as a whole detected to $z \sim 1$ or beyond.

Table 3.4.3. H II Regions with the Ultrasensitive Array

	Diameter	10^7 E.M.		5σ in		Resolved to
H II Region	[pc]	[cm^{-6} pc]	1hr	6hrs	12hrs	[Mpc]
Ultracompact	0.1	1	0.8 Mpc	1.3 Mpc	1.5 Mpc	0.25 Mpc
Compact	0.5	1	4.0	6.3	7.8	1.3
NGC 253	1.0	20	30	47	56	2.6
Orion	5.0	0.16	16	26	30	13
Giant	100.	0.05	180	290	340	260
Supergiant	100.	0.01	82	130	150	150
ULIRG	100.	30	$z \sim 0.6$	$z \sim 0.9$	$z \sim 1$	340

How far can the VLA detect an H II region, after the first phase of the Expansion Project? Most entries are taken as representative of typical Galactic values; starburst galaxies are observed to have much higher densities, both locally (as in the individual pc-scale H II regions in NGC 253) and over large regions (as in the starburst cores observed by Condon *et al.* 1991). Detection limits assume 5σ at the optimal frequency, usually 6 GHz. The *Resolved to* column shows the distance at which the source would begin to be resolved at 33 or 45 GHz (depending on sensitivity).

3.4.4 Redshifted Molecular Lines

The Ultrasensitive Array will allow efficient spectral line searches with the VLA for the first time, through a combination of continuous frequency coverage, wide bandwidths, and excellent spectral resolution. Carbon monoxide (CO), with rest frequencies at 115, 230, 345, ...GHz, is among the most interesting molecules to look for. A major coolant of dense molecular gas in actively star-forming regions, the CO luminosity is a robust tracer of total molecular gas mass, and the gas temperature can be inferred directly from the peak line brightness. Despite the initial concern that CO may not be present in the early universe due to low metallicity, secure detections of luminous

CO-emitting galaxies have now been made out to $z = 4.7$ (Ohta *et al.* 1996, Omont *et al.* 1996), including the first two dusty SCUBA galaxies which have been looked at in CO (Frayer *et al.* 1998, 1999). This is presumably due to local enrichment in actively star-forming systems (cf. Yun *et al.* 1997), and suggests that it is reasonable to expect luminous CO emission in gas-rich starburst galaxies and proto-ellipticals even in the early epochs when the mean cosmic metallicity was very low. The study of redshifted CO rotational transitions in actively star-forming galaxies is one of the key science drivers for the ALMA. Spectral energy distributions for the recent submillimeter-detected sources suggest dust (and presumably gas) temperatures of about 50−100 K, implying that the best CO transitions to study are $J = 6 \rightarrow 5$ ($E_J = 155$ K) and lower.

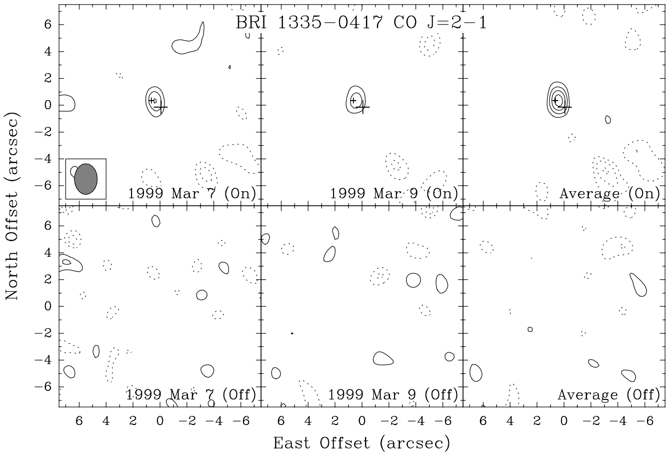

Figure 3.32: CO (2−1) emission at $z = 4.4$, as seen with the VLA in BRI 1335−0417 near 43 GHz (Carilli, Menten, & Yun 1999). The implied molecular gas mass is $M(\mathrm{H}_2) \sim 10^{11}\, M_\odot$. Millimeter observations gave a line-width of 420±60 km/sec (Guilloteau *et al.* 1997), but the maximum bandwidth available with the VLA currently is 50 MHz, corresponding to 350 km/sec at 43 GHz. The authors were therefore forced to use two independent tunings in continuum mode, on (*top*) and off (*bottom*) the line, and correct the observed flux density difference upwards for the missing velocities. The Ultrasensitive Array will give 8 GHz bandwidth – 56,000 km/sec – with a velocity resolition of $\sim 50\,$km/sec.

The Ultrasensitive Array will provide information in this area which is both unique and complementary to the ALMA. The improved sensitivity, frequency coverage, bandwidth, and spectral resolution of the Ultrasensitive Array will be ideally suited for studies of the CO emission at $z \geq 10$, as the key CO transitions redshift into the VLA receiver bands. The contraction of the redshifted spectrum (*i.e.*, $\nu_{obs} = \nu_o/(1+z)$) also means that the VLA receiver bands cover a much broader redshift range for each CO transition, and several rotational transitions can be observed simultaneously (e.g. J = 2, 3, & 4 for $z = 10$). Observing multiple transitions both confirms the individual detections and gives a direct indication of the excitation conditions. This last is especially interesting since the cosmic microwave background temperature ($T_{CMB} = 2.7\ (1+z)$) becomes high enough to affect the population of the lower J levels at redshifts of only a few. In this

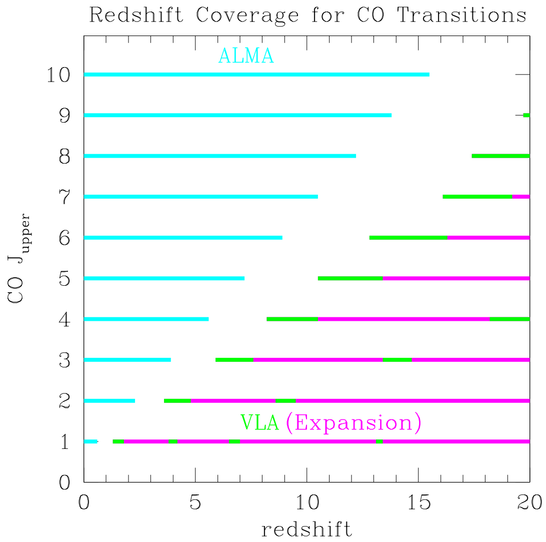

Figure 3.33: Redshift coverage of different CO rotational transitions covered by the ALMA (magenta) and the Ultrasensitive Array (cyan). The Ultrasensitive Array will give a continuous redshift coverage, unlike the current VLA (green), and the new IF system and new correlator will provide 160 times the spectral bandwidth – large enough even for a redshift search. Note that it is not yet clear whether the ALMA will have 30–70 GHz capability; this plot assumes *not*.

respect, the Ultrasensitive Array will complement the ALMA very nicely by observing the lower J transitions (Figure 3.33). The expected detection limits are shown in Figure 3.34.

3.4.5 Studying Star Forming Galaxies at High Redshift

The presence of dust at high redshift leads to a bias in optical studies against the dense, dusty stages of star formation in high-z galaxies. Current optical estimates of the cosmic star formation rate may under-estimate the total at z>1 by a factor three or more due to this dust bias, based on submillimeter source counts, sub-mJy radio source counts, and ISO source counts (Flores *et al.* 1999; Hughes *et al.* 1998; Cram *et al.* 1998; Blain *et al.* 1999a). Much of this star formation may take place in massive starbursts driven by galaxy mergers during the formation epoch of the spheroidal components of galaxies at redshifts between 2 and 5, as predicted by cosmic structure formation models (Tan, Silk, & Blanard 1999). The situation is analogous to studies of Galactic star forming regions, in which the early stages of the star formation process can be studied only by the radio through far IR observations.

Studying dusty, star forming galaxies at high redshift is one of the main science drivers for NGST, SIRTF, SKA, and the ALMA. The Ultrasensitive Array, working in concert with the

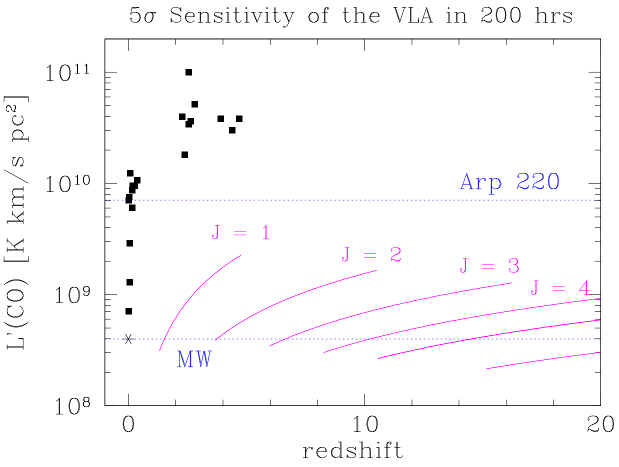

Figure 3.34: 5σ sensitivity of the VLA for detected CO emission from high-redshift galaxies after 200 hrs of integration. Filled squares represent the measured CO luminosity of local and high-redshift gas-rich galaxies. Gas-rich galaxies like Arp 220 (thus most SCUBA-detected submillimeter sources) should be easily detected at all redshifts. Galaxies with CO luminosity comparable to the present day Milky Way may be detectable at $z \geq 8$.

ALMA, will provide samples of high-redshift galaxy candidates, which can then be studied with the NGST. The Ultrasensitive Array will provide critical, complementary information on high-redshift star-forming galaxies out to z≈6, including:

- Estimates of the massive star formation rate in high z galaxies, unbiased by dust extinction. The Ultrasensitive Array will allow the study of non-thermal synchrotron radio continuum emission from 'normal' galaxies (star formation rates of 10 $M_\odot$/year) to z=3, and ULIRGs ($\geq$ 100 $M_\odot$/year) to z=5 (Figure 3.35). This will complement the work of near IR and optical telescopes, which study the starlight from such galaxies, and of the ALMA, which will delineate the thermal continuum emission from warm dust and the molecular line emission.

- Study of the non-thermal radio continuum associated with star formation, including estimates of the ISM pressure, and the magnetic field strength and geometry.

- Identification of a possible AGN component, from the radio spectral index and/or morphology.

- Sub-arcsecond astrometry, thereby facilitating source identification and follow-up at other wavelengths.

- Imaging with sub-arcsecond resolution, tracing the distribution of star formation in high-redshift galaxies.

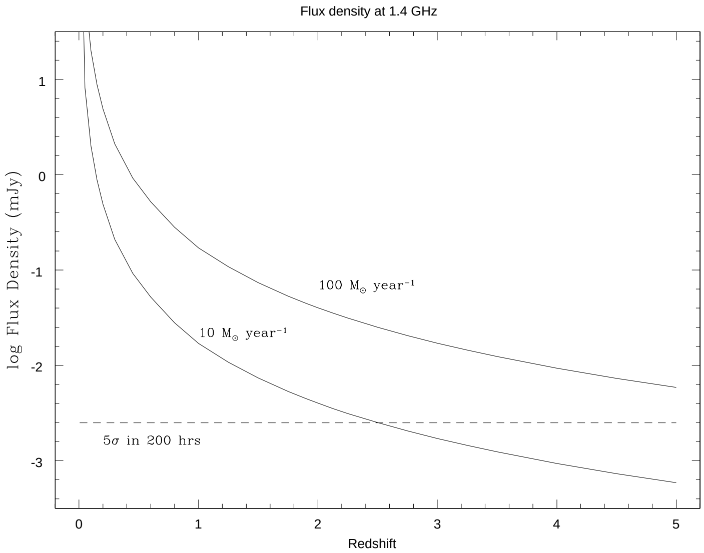

Figure 3.35: The solid lines show the expected 1.4 GHz flux density of star-forming galaxies as a function of redshift; the dashed line represents the 5σ limit of the Ultrasensitive Array in 200 hrs. Note that the in-beam source confusion in the A and B arrays is more than an order of magnitude below this limit.

- Source redshift estimates, from comparisons of the radio and submillimeter flux densities (Carilli & Yun 1999). The sharp rise in the Rayleigh-Jeans portion of the thermal dust spectrum shifts into the submillimeter bands with increasing redshift, implying a strong evolution in the relative strengths of the radio and submillimeter emission.

- Imaging free-free emission from high-z star-forming galaxies, thereby constraining the temperature and density of the ISM. The spectra of star-forming galaxies is dominated by free-free emission between 40 GHz and 120 GHz (*e.g.*, Condon 1992). The 5σ sensitivity of the Ultrasensitive Array is 2μJy at 33 GHz in 200 hrs; the expected free-free emission from galaxies with star formation rates of 100 $M_\odot$/year is about 5μJy at z=2 at this frequency.

On a final speculative note, the next generation of near IR space- and ground-based telescopes have set a goal of studying galaxies to z=10, and perhaps beyond. The Ultrasensitive Array could play a fundamental role in such studies by imaging the thermal dust emission. The 5σ sensitivity of the Ultrasensitive Array in 200 hrs is 3μJy at 43 GHz. At this observing frequency the 'negative K-correction' for the dust emission spectrum more than offsets the distance losses in the redshift range of $4 \lesssim z \lesssim 30$, so that a galaxy with a star formation rate of 100 $M_\odot$/year will have a flux density of only 0.5μJy at z=4, rising to 3μJy at z=10, and 10μJy at z=20. The Ultrasensitive Array could thus detect dust emission from rapidly star-forming galaxies at redshifts of 10 or beyond.

3.4.6 H I Surveys

The VLA Expansion Project will open up two major new research areas in H I studies, in addition to enhancing all current work. With the new correlator, the VLA will become the premiere instrument for optically unbiased searches in the H I line; while the new prime focus feeds will open a new window for studies of H I at redshifts from z=0.2–1.0. The 25m diameter antennas already provide an impressive field of view at cm wavelengths (30 arcmin FWHM at 1400 MHz, 1 degree at 700 MHz), making the VLA ideally suited for continuum surveys. For H I searches a third dimension comes into play, the instantaneous velocity range that can be probed. The new correlator and back-end transmission system will improve the instantaneous velocity coverage and increase the number of channels available by several orders of magnitude: 8192 channels at 13 km/sec resolution, vs. the current 63 channels at 20 km/s resolution. This will make the VLA the instrument of choice for surveys of general environments (*e.g.*, clusters, intra-cluster filaments, intermediate redshift Lyα forest lines); in addition, every observation of an individual galaxy will automatically cover an additional 10,000−100,000 km/sec. In this sense, every H I observation will provide an optically unbiased view of the local universe. A particularly interesting possibility would be to make a complete inventory of all the H I in a group or cluster down to a million solar masses of H I, while simultaneously probing the sightline in front and behind such an object over z=0 to 0.25, tracing deviations from the Hubble flow in these regions. Large numbers of low-redshift Lyα forest systems can be targeted in a single observation, allowing an inventory of the gaseous environment of such systems. The proposed E configuration would allow one to reach H I column densities of order 10^{15} cm^{-2} in about 100 hours, approaching the sensitivities of optical absorption lines.

The VLA H I Deep Field

In the last decade tremendous strides have been made in observational cosmology. Galaxy evolution is probed directly by deep optical, infrared and submillimeter imaging of sources out to redshifts larger than 5. Major questions currently being addressed are: what is the star-formation history of the Universe? What is the origin of the Hubble morphological sequence? What kind of galaxies form, and at what time? The refurbished HST and surveys with ground based large telescopes are pointing to a recent era of galaxy formation, with strong evolutionary effects in the galaxy population even at redshifts less than 1. The Hubble Deep Field, arguably the single most important observation for our understanding of galaxy evolution to date, shows that a majority of the fainter sources is at a redshift less than 1, and that there is a strong increase out to z=1 of a population of star forming galaxies with blue colors, intense emission lines and irregular morphology. Early ground based work and recent HST imaging show that the density morphology relation changes dramatically at intermediate redshifts. The number of star-forming galaxies in rich clusters increases rapidly with z and by z=0.5 spirals are almost as frequent in cluster cores as in the field.

The one ingredient that is missing from these observations is the evolution of the neutral hydrogen content of galaxies, the component out of which stars and galaxies form. The VLA Expansion Project will provide just that information, particularly with the design & development of the new prime focus UHF systems. It could make the equivalent of a 3-dimensional Hubble Deep Field, but over an area that is 350 times larger. An area of 50 by 50 arcmin and a redshift interval $z = 0.2 - 1$ could be probed in a single pointing using a prime focus UHF system. This survey would have an angular resolution of $\sim$ 7 arcsec and velocity resolution of 20 km/sec. In a 2700 hour observation, the expected number of H I detections (assuming no evolution) is several thousand, with about 30% of those galaxies at redshifts larger than 0.6 (Figure 3.36). Mild evolution would triple the expected number of detections.

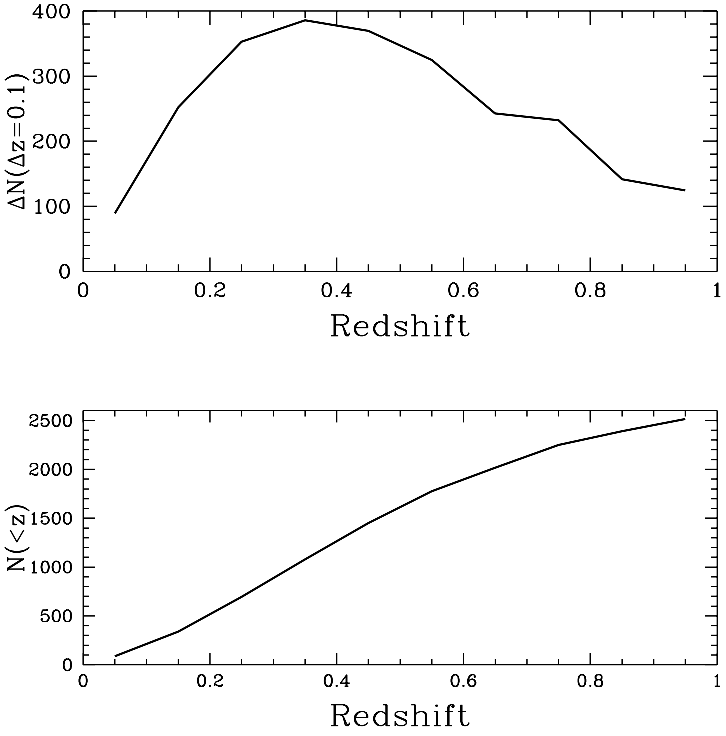

Figure 3.36: The VLA H I Deep Field: expected differential (*top*) and integral (*bottom*) counts of galaxies detected (5σ) in H I in 2700 hours using the proposed prime focus UHF system. Assumes no evolution, based on the H I mass function of Zwaan *et al.* (1997); these numbers are independent of cosmology.

Such a deep H I observation will make it possible to probe the large scale structure defined by the gas-rich population out to a redshift of 1. It will provide a census of gas-rich systems independent of stellar content or star formation rate. As an added benefit, it will not only show how the gas content of galaxies evolves with redshift, but also provide detailed kinematics for all its detections. As such, this survey will give critical information on the dynamical nature of the large population of faint blue galaxies and peculiar/irregular galaxies which are found to dominate the galaxy number counts at these redshifts. If this population is due to an increased frequency of interactions and mergers, the tidally extended outer regions can be mapped, both spatially and kinematically, out to redshifts of $z \sim 0.5$ (Figure 3.37).

Combined with the optical data, this H I Deep Field will reveal the dynamical state and star formation history of the faint blue galaxies, probe the evolution of the Tully-Fisher relation with redshift, and image almost uniquely the assembly of galaxies at intermediate redshifts. The very existence of completed and planned optical surveys will make this project particularly exciting:

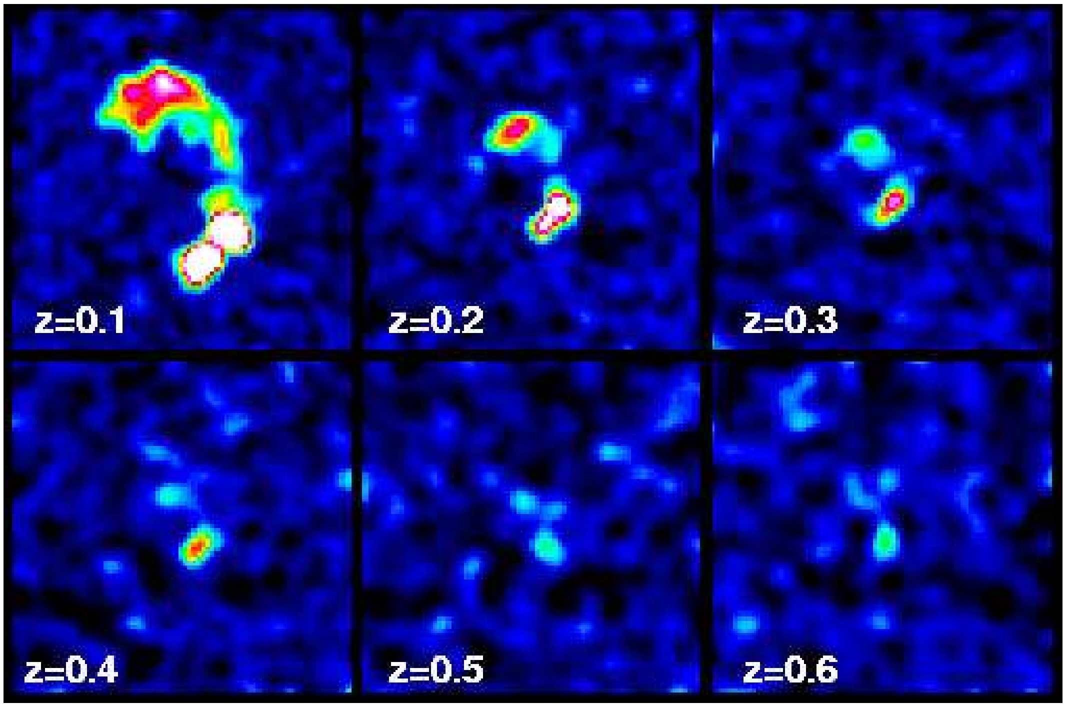

Figure 3.37: The VLA H I Deep Field: the nearby IR luminous merger Arp 299 as a function of redshift ($H_0 = 75\,\mathrm{km/sec/Mpc}$, $q_0 = 1$). The system remains recognizable as a merger out to at $z \gtrsim 0.5$.

knowing the size of gas reservoirs, current and past star formation rates, and, perhaps most importantly, where the gas is with respect to the galaxies, will tell about galaxy formation and evolution in unprecedented ways. This survey will also be sensitive to OH megamaser emission from ultraluminous IR mergers out to redshifts of 1.6, providing the evolution of the merging rate over the last half of the age of the universe. Finally, the H I deep field will simultaneously provide the deepest radio continuum observation to date. Such an observation is expected to detect over 40,000 sources down to $0.5\,\mu$Jy, including ultraluminous starbursts out to redshifts of 10 as well as the star formation from normal disk galaxies such as the Milky Way to redshifts of 1–2.

3.4.7 The Radio Continuum Deep Field

The improved sensitivity and lower systematic errors available with the Ultrasensitive Array will revolutionize studies of faint radio sources. The deepest radio images made thus far reach rms noise levels of about $7.5\,\mu$Jy/beam at $\sim 1\,$GHz (Richards 1999); such projects will take *under an hour* with the Ultrasensitive Array. An observation of similar length to the H I Deep Field ($\sim 2700\,$hours) could detect over 40,000 sources down to 500 nanoJy (see Figure 3.38). This would give an unobscured view of cosmic star formation history and the formation and evolution of active galactic nuclei (AGNs) at redshifts from 0 to 10 or more. Over 90% of the detected radio sources are expected to be normal late-type star forming galaxies (Yun, Reddy, & Condon, *in prep.*), and an unevolved Milky Way or Arp 220 could be detected out to z=1 and z=10, respectively (see

Figure 3.39). Already some evidence for a strong source evolution exists (*e.g.*, Condon 1984; Lilly *et al.* 1995; Madau *et al.* 1996; Madau, Pozzetti, & Dickinson 1998; Blain *et al.* 1999b), and pushing the faint radio source counts to the nanoJy level will provide a much stronger constraint on the extinction-free cosmic star formation history. Recently, studies of submillimeter sources have received much attention as a new way of probing dust-obscured starburst systems at high redshifts. However, the strong positive K-correction in the dust spectrum wins over the distance effects only at $z > 1$, and a strong bias against star-forming galaxies in the intermediate redshift ranges is inherent in the submillimeter studies. In comparison, simple models suggest that the radio continuum study offers the best overall sensitivity at $z < 2$ (see Figure 3.40). The point here is not that these models are likely to predict the true number counts – we simply do not know enough about the faintest sources yet, to make such a claim – but clearly the combination of deep radio and submillimeter observations is a powerful one in constructing a complete cosmic star formation history. The combined data may also provide photometric redshifts for the optically-faint submillimeter sources at cosmological distances (see Carilli & Yun 1999). This of course assumes that the local far infrared/radio correlation holds at arbitrary redshift, but that assumption may itself be tested using these and related data. Finally, note that the synthesized beam of the VLA's A configuration at 30cm matches that of the ALMA at 850μm; but a single pointing with the VLA at 30cm would cover an area on the sky some 30,000 times larger. The combination of the Ultrasensitive Array with the ALMA will be much more powerful than either alone, yielding an unbiased view of star formation throughout the universe.

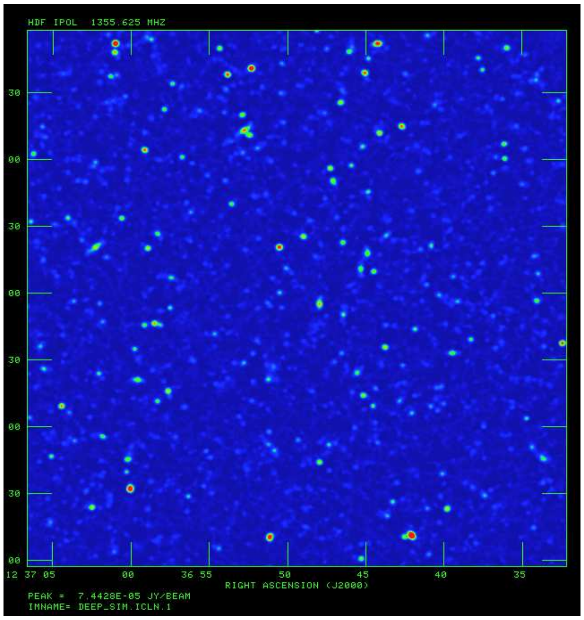

Figure 3.38: A small section of the (simulated) Radio Continuum Deep Field image, covering a $4' \times 4'$ region (out of $\sim 45' \times 45'$ total) at $2''$ resolution. In this sub-field about 400 sources with flux density 1 μJy are expected to be detected (S/N>5).

The Radio Continuum Deep Field would also offer valuable insights into the evolutionary history of AGNs. There is already clear evidence for a strong luminosity evolution among the luminous

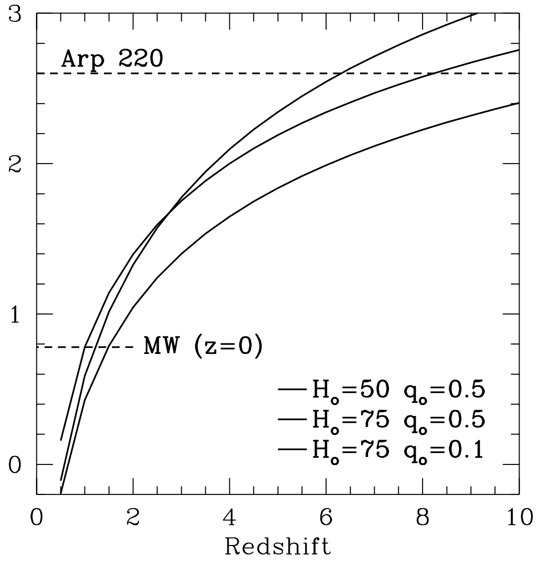

Figure 3.39: The Radio Continuum Deep Field: 5σ detection limits in terms of the star formation rate, log SFR ($M_\odot$ per year), assuming the local relationship between star formation rate and radio continuum flux density (Condon 1992).

AGNs (Hughes, Dunlop, & Rawlings 1997, Willott *et al.* 1999), but little is known about the evolution of weak AGNs which are ubiquitous among field and cluster galaxies. Existing faint radio source studies suggest that radio AGNs may be far more abundant than expected from the local radio luminosity function (*e.g.*, Gruppioni, Mignoli, & Zamorani 1999) and may be able to account for the cosmic X-ray background (Fabian & Rees 1995). Weak AGNs can be identified by their radio spectral indices as well as by follow-up spectroscopy, and their formation and evolution history may be derived from the redshift distribution. As an added benefit, such a deep survey would also provide a unique study of radio variability on timescales from days to months for the brightest ~ 1000 sources, down to flux levels of order 10 μJy.

The VLA Deep Field observation would also provide an important additional constraint on the large scale structure which cannot be obtained in any other way. With high sensitivity, wide frequency coverage, and high spectral resolution, ~ 1000 radio continuum sources can be used to derive unbiased rotation measures across the 45 arcmin field-of-view. This unique information on large-scale magnetic field structures is simply impossible to obtain with current instruments.

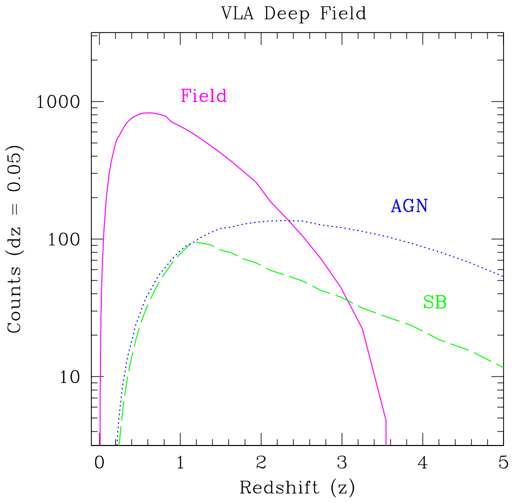

Figure 3.40: The VLA Radio Continuum Deep Field: redshift distribution of expected detections, based on one current model. The *"field"* galaxies, representing an unevolving population of late type galaxies, based on the local radio luminosity function, dominates the number counts out to $z \leq 2.5$ ($q_0 = 0.5$). The *starburst* population ("SB"; see Yun, Reddy, & Condon, *in prep.*) represents IR luminous objects with $L_{IR} \geq 10^{11} L_{\odot}$; this allows for strong evolution as required by the SCUBA submillimeter source counts (the "Peak-5" model of Blain *et al.* 1999b). The *AGN* population is modeled using the luminosity function for "Monster" by Condon (1989), and also evolved using the "Peak-5" model. The break in the redshift distribution for the field and SB population is due to a strong K-correction with a spectral index of -0.75. A flat spectrum is assumed for the AGN population.

3.5 Summary

The Very Large Array is the most powerful and flexible radio telescope in the world, conducting observations for more than 500 scientific programs each year, in fields ranging from solar physics to cosmology. Even so, the VLA has not come close to fulfilling its potential. Tied to a correlator which provides neither bandwidth nor spectral resolution, held back by receivers which limit the sensitivity and cover only a fraction of the available frequency space, the VLA is a superb observatory shackled to 20-year-old instrumentation. The Ultrasensitive Array will unleash the full power of the basic instrument, increasing the bandwidth by a factor of eighty, improving the spectral resolution at a given bandwidth by more than a factor of sixteen hundred, and providing continuous frequency coverage, with comparable sensitivity, from 1 to 50 GHz. This will only enhance the true strength of the VLA: its ability to make essential contributions across the entire breadth of modern astronomy. Radio observations can map out magnetic fields, and peer into the cores of proto-stars and galaxies from which optical and even IR photons cannot escape. By indicating and mapping both star formation and nuclear activity, radio observations directly trace two of the most important processes in the evolution of the universe. From the solar wind to galaxy clusters, from stellar jets to QSO absorption line systems, the Ultrasensitive Array will make a unique and fundamental contribution to our understanding of the universe.

References

Allen, R. J., Baldwin, J. E., & Sancisi, R. 1978, A&A, 62, 397-409.

Anantharamaiah, K. R. & Goss, W. M. 1996, ApJ, 466, L13-L16.

Anantharamaiah, K. R., Pedlar, A., Ekers, R. D., & Goss, W. M. 1991, MNRAS, 249, 262-281.

Athreya, R. M., Kapahi, V. K., McCarthy, P. J., & van Breugel, W. 1997, MNRAS, 289, 525-534.

Beck, R., Brandenburg, A., Moss, D., Shukurov, A., & Sokoloff, D. 1996, ARA&A, 34, 155-206.

Benson, P. J., Caselli, P., & Myers, P. C. 1998, ApJ, 506, 743-757.

Biggs, A. D., Browne, I. W. A., Herbig, P., Koopmans, L. V. E., Wilkinson, P. N., & Perley, R. A. 1999, MNRAS, 304, 349-358.

Blain, A. W., Kneib, J.-P., Ivison, R. J., & Smail, I. 1999a, ApJ, 512, L87-L90.

Blain, A. W., Smail, I., Ivison, R. J., Kneib, J.-P. 1999b, MNRAS, 302, 632-648.

Blandford, R. D., & Narayan, R. 1992, ARA&A, 30, 311-358.

Bockelée - Morvan, D. & Gérard, E. 1984, A&A, 131, 111-122.

Bode, M. F. (ed.) 1987, *RS Ophiuchi (1985) and the recurrent nova phenomenon* (Utrecht: VNU Science Press).

Boss, A. P. 1997, Science, 276, 1836-1839.

Buczilowski, U. R., & Beck, R. 1991, A&A, 241, 47-56.

Butler, B. J., Muhleman, D. O., & Slade, M. A. 1993, JGR, 98, no. E8, 15,003-15,023.

Carilli, C. L., Harris, D. E., Pentericci, L., Röttgering, H. J. A., Miley, G. K., & Bremer, M. N. 1998, ApJ, 494, L143-L146.

Carilli, C. L., Holdaway, M. A., Ho, P. T. P., & De Pree, C. G. 1992, ApJ, 399, L59-L62.

Carilli, C. L., Menten, K. M., & Moore, C. P. 1999, in *Highly Redshifted Radio Lines*, eds. C. Carilli, S. Radford, K. Menten, & G. Langston (San Francisco: PASP), 171-182.

Carilli, C. L., Menten, K. M., & Yun, M. S. 1999, ApJ, *in press* (astro-ph/9906135).

Carilli, C. L., Owen, F. N., & Harris, D. 1994, AJ, 107, 480-493 (see also erratum: AJ, 107, 2299).

Carilli, C. L., Radford, S., Menten, K., & Langston, G. (eds) 1999, *Highly Redshifted Radio Lines* (San Francisco: PASP).

Carilli, C. L., Perley, R. A., Röttgering, H. J. A., & Miley, G. K. 1996, in *IAU Symposium 175: Extragalactic Radio Sources*, eds. R. D. Ekers, C. Fanti, & L. Padrielli (Dordrecht: Kluwer), 159-162.

Carilli, C. L., Röttgering, H. J. A., van Ojik, R., Miley, G. K., & van Breugel, W. J. M. 1997, ApJS, 109, 1-44.

Carilli, C. L., & Yun, M. S. 1999, ApJ, 513, L13-L16.

Chegalur, J. & de Bruyn, G. 1999, A&A, *in press.*

Chevalier, R. A. 1982, ApJ, 259, 302-310.

Chevalier, R. A. 1998, ApJ, 499, 810-819.

Clarke, T. E. 1999, *Combined Radio & X-ray Analysis of Magnetic Fields in Clusters of Galaxies* (Ph.D. Thesis: University of Toronto).

Combi, M. R. 1987, Icarus, 71, 178-191.

Condon, J.J. 1984, ApJ, 287, 461-474.

Condon, J.J. 1989, ApJ, 338, 13-23.

Condon, J. J. 1992, ARA&A, 30, 576-611.

Condon, J. J., Huang, Z.-P., Yin, Q. F., & Thuan, T. X. 1991, ApJ, 378, 65-76.

Costa, E. *et al.* 1997, Nature, 387, 783-785.

Cram, L., Hopkins, A., Mobasher, B., & Rowan-Robinson, M. 1998, ApJ, 507, 155-160.

Dreher, J. W., Carilli, C. L., & Perley, R. A. 1987, ApJ, 315, 611-625.

Drinkwater, M. J., Webb, J. K., Barrow, J. D., & Flambaum, V. V. 1998, MNRAS, 295, 457-462.

Eckart, A. & Genzel, R. 1997, MNRAS, 284, 576-598.

Fabian, A. C. 1994, ARA&A, 32, 277-318.

Fabian, A. C. & Rees, M. J. 1995, MNRAS, L55-L58.

Feretti, L., Dallacasa, D., Govoni, F., Giovannini, G., Taylor, G. B., & Klein, U. 1999, A&A, 344, 472-482.

Feretti, L., & Giovannini, G. 1996, in *Extragalactic Radio Sources, IAU Symposium 175*, eds. R. D. Ekers, C. Fanti, & L. Padrielli (Kluwer Academic Publishers: Amsterdam), 333-338.

Fernandez, Y. R., Kundu, A., Lisse, C. M., & A'Hearn, M. F. 1997, Plan. & Spac. Sci., 45, 735-739.

Flores, H. *et al.* 1999, ApJ, 517, 148-167.

Frail, D. A., Diamond, P. J., Cordes, J. M., & Langavelde, H. J. V. 1994, ApJ, 427, L43-L46.

Frail, D. A., Kulkarni, S. R., Nicastro, S. R., Feroci, M., & Taylor, G. B. 1997, Nature, 389, 261-263.

Frayer, D. T. *et al.* 1998, ApJ, 506, L7-L10.

Frayer, D. T. *et al.* 1999, ApJ, 514, L13-L16.

Fusco-Femiano, R., Dal Fiume, D., Feretti, L., Giovannini, G., Grandi, P., Matt, G., Molendi, S., & Santagelo, A. 1999, ApJ, 513, L21-L24.

Ghez, A. M., Klein, B. L., Morris, M., & Becklin, E. E. 1998, ApJ, 509, 678-686.

Giovannini, G., Feretti, L., Venturi, T., Kim, K.-T., & Kronberg, P. P. 1993, ApJ, 406, 399-406.

Gopalswamy, N., Payne, T. E. W., Schmahl, E. J., Kundu, M. R., Lemen, J. R., Strong, K. T., Canfield, R. C., & de La Beaujardiere, J. 1994, ApJ, 437, 522-528.

Gordon, S. M., Duric, N., Kirshner, R. P., Goss, W. M., & Viallefond, F. 1999, ApJS, 120, 247-264.

Gray, A., Nicholls, J., Ekers, R. D., & Cram, L. 1995, ApJ, 448, 164-178.

Green, D. A. 1998, *A Catalogue of Galactic Supernova Remnants (1998 September version)*, Mullard Radio Astronomy Observatory, Cambridge, United Kingdom (available on the World-Wide-Web at `"http://www.mrao.cam.ac.uk/surveys/snrs/"`).

Gruppioni, C., Mignoli, M., & Zamorani, G. 1999, MNRAS, 304, 199-217.

Guilloteau, S., Omont, A., McMahon, R. G., Cox, P., & Petitjean, P. 1997, A&A, 328, L1-L4.

Hjellming, R. M. 1996a, in *Radio Emission from the Stars and the Sun*, eds. A. R. Taylor, & J. M. Paredes, ASP Conf. Series, Vol. 95, 174-181.

Hjellming, R. M. 1996b, in *Cataclysmic Vartiables and Related Objects*, eds. A. Evans & J. H. Wood (Kluwer Academic Publishers: Amsterdam), 317-320.

Hjellming, R. M. & Rupen, M. P. 1995, Nature, 375, 464-468.

Horrelou, C., Beck, R., Berkhuijsen, E. M., Krause, M., & Klein, U. 1992, A&A, 265, 417-428.

Hughes, D. H., Dunlop, J. S., & Rawlings, S. 1997, MNRAS, 289, 766-782.

Hughes, D. H. *et al.* 1998, Nature, 394, 241-247.

Hummel, E. 1981, A&A, 93, 93-105.

Jackson, B. V., Hick, P. L., Kojima, M., & Yokobe, A. 1998, JGR, 103, no. A6, 12,049.

Killeen, N. E. B, Lo, K. Y., & Crutcher, R. 1992, ApJ, 385, 585-603.

Kim, K.-T., Kronberg, P. P., & Tribble, P. C. 1991, ApJ, 379, 80-88.

Krucker, S., Benz, A. O., Bastian, T. S., & Acton, L. W. 1997, ApJ, 488, 499-505.

Lang, C. C., Morris, M., & Enchevarria, L. 1999, ApJ, *submitted.*

Lilly, S. J., Tresse, L., Hammer, M., Crampton, D., & Le Fèvre, O. 1995, ApJ, 455, 108-124.

Liszt, H. & Spiker, R. 1995, ApJS, 98, 259-270.

Looney, L. W., Mundy, L. G., & Welch, W. J. 1997, ApJ, 484, L157-L160.

Madau, P., Ferguson, H. C., Dickinson, M. E., Giavalisco, M., Steidel, C. C., & Fruchter, A. 1996, MNRAS, 283, 1388-1404.

Madau, P., Pozzetti, L., & Dickinson, M. 1998, ApJ, 498, 106-116.

Mangum, J. G. 1990, *The Throes of Star Formation: A Study of the Orion-KL and DR21(OH) Molecular Clouds* (Ph.D. Thesis: University of Virginia, Charlottesville).

Mangum, J. G. & Wootten, A. 1993, ApJS, 89, 123-153.

Martí, J., Rodìguez, L. F., & Reipurth, B. 1998, ApJ, 502, 337-341.

Mirabel, I. F., Dhawan, V., Chaty, S., Rodríguez, L. F., Martí, J., Robinson, C. R., Swank, J., & Geballe, T. 1998, A&A, 330, L9-L12.

Mirabel, I. F. & Rodríguez, L. F. 1994, Nature, 371, 46-48.

Morris, M. & Yusef-Zadeh, F. 1985, AJ, 90, 2511-2513.

Muhleman, D. O., Grossman, A. W., & Butler, B. J. 1995, Ann. Rev. Earth & Planet. Sci., 23, 337-374.

Muhleman, D. O., Grossman, A. W., Butler, B. J., & Slade, M. A. 1990, Science, 248, 975-980.

Myers, P. C. & Benson, P. J. 1983, ApJ, 266, 309-320.

Ohta, K., Yamada, T., Nakanishi, K., Kohno, K., Akiyama, M., & Kawabe, R. 1996, Nature, 382, 426-428.

Omont, A., Petitjean, P., Guilloteau, S., McMahon, R. G., Solomon, P. M., & Pecontal, E. 1996, Nature, 382, 428-431.

Palmer, P., de Pater, I., & Snyder, L. E. 1989, AJ, 97, 1791-1797.

van Paradijs *et al.* 1997, Nature, 386, 686-689.

de Pater, I., Palmer, P., Mitchell, D. L., Ostro, S. J., Yeomans, D. K., & Snyder, L. E. 1994, Icarus, 111, 489-502.

de Pater, I., Palmer, P., & Snyder, L. E. 1986, ApJ, 304, L33-L36.

Pavelin, P. E., Davis, R. J., Morrison, L. V., Bode, M. F., & Ivison, R. J. 1993, Nature, 363, 424-426.

Pentericci, L., Röttgering, H. J. A., Miley, G. K., Carilli, C. L., & McCarthy, P. 1997, A&A, 326, 580-596.

Pentericci, L., Röttgering, H. J. A., Miley, G. K., Spinrad, H., McCarthy, P. J., van Breugel, W. J. M., & Maccheto, F. 1998, ApJ, 504, 139-146.

Phookun, B., Anantharamaiah, K. R., & Goss, W. M. 1998, MNRAS, 295, 156-166.

Plante, R. L., Lo, K. Y., & Crutcher, R. M. 1995, ApJ, 445, L113-L116.

Reid, M. J., Argon, A. L., Masson, C. R., Menten, K. M., & Moran, J. M. 1995, ApJ, 443, 238-244.

Roberts, D. A., Yusef-Zadeh, F., & Goss, W. M. 1996, ApJ, 459, 627-631.

Richards, E. A. 1999, ApJ, *in press.*

Roberts, D.A., & Goss, W.M. 1993, ApJS, 86, 133-152.

Rodríguez, L. F. *et al.* 1998, Nature, 395, 355-357.

Sams, B. J., Genzel, R., Eckart, A., Tacconi-Garman, L., & Hoffman, R. 1994, ApJ, 430, L33-L36.

Serabyn, E. & Morris, M. 1994, ApJ, 424, L91-L94.

Serabyn, E. & Morris, M. 1996, ARA&A, 34, 645-701.

Sari, R., Piran, T., & Narayan, R. 1998, ApJ, 497, L17-L20.

Stahler, S. W., Palla, F., & Ho, P. T. P. 2000, in *Protostars and Planets IV*, eds. V. Mannings, A. P. Boss & S. S. Russell (Tucson: University of Arizona Press), *in press.*

Tan, J., Silk, J., & Blanard, C. 1999, ApJ, *in press.*

Taylor, A. R., Hjellming, R. M., Seaquist, E. R., & Gehrz, R. D. 1988, Nature, 335, 235-238.

Taylor, G. B., Barton, E. J., & Ge, J.-P. 1994, AJ, 107, 1942-1952.

Taylor, G. B., Frail, D. A., Kulkarni, S. R., Shepherd, D. S., Feroci, M. & Frontera, F. 1998, ApJ, 502, L115-L118.

Taylor, G. B. & Perley, R. A. 1993, ApJ, 416, 554-562.

Ulvestad, J. S. & Antonucci, R. J. 1997, ApJ, 488, 621-641.

Webster, W. J. & Johnston, K. J. 1989, in *Asteroids II*, eds. R. P. Binzel, T. Gehrels, & M. S. Matthews (Tucson: Univ. of Arizona Press), 213-227.

Weiler, K. W., Panagia, N., Sramek, R. A., van der Hulst, J. M., Roberts, M. S., & Nguyen, L. 1989, ApJ, 336, 421-428.

Weiler, K. W., Van Dyk, S. D., Montes, M. J., Panagia, N., & Sramek, R. A. 1998, ApJ, 500, 51-58.

Wijers, R. A. M. J. & Galama, T. J. 1999, ApJ, *in press* (astro-ph/9805341).

Wiklind, T. & Combes, F. 1996, Nature, 379, 139-141.

Willott, C. J., Rawlings, S., Blundell, K. M., & Lacy, M. 1999, MNRAS, *submitted.*

Wilner, D. J., Reid, M. J., & Menten, K. M. 1999, ApJ, 513, 775-779.

Wiseman, J. J. & Ho, P. T. P. 1998, ApJ, 502, 676-694.

Yun, M. S., Ho, P. T. P., & Lo, K. Y. 1994, Nature, 372, 530-532.

Yun, M. S., Scoville, N. Z., Carrasco, J. J., & Blandford, R. D. 1997, ApJ, 479, L9-L13.

Yusef-Zadeh, F., Morris, M., & Chance, D. 1984, Nature, 310, 557-561.

Yusef-Zadeh, F., Roberts, D. A., & Biretta, J. 1998, ApJ, 499, L159-L162.

Yusef-Zadeh, F., Roberts, D. A, Goss, W. M., Frail, D. A., & Green, A. J 1999, ApJ, 512, 230-236.

Yusef-Zadeh, F., Wardle, M., & Parastaran, P. 1997, ApJ, 475, L119-L122.

Zhao, J.-H., Anantharamaiah, K. R., Goss, W. M., & Viallefond, F. 1997, ApJ, 482, 186-202.

Zhao, J.-H. & Goss, W. M. 1998, in *Galactic Center Workshop 98: The Central Parsecs*, eds. H. Falke, A. Cotera, W.